

TEST AND EVALUATION OF A
VTPR RETRIEVAL SYSTEM FROM
CLEAR-COLUMN NOAA 2 RADIANCES

Harry Milton Dyck

DUDLEY KNOX LIBRARY
MONTENAPPEL HIGH SCHOOL
MONTENAPPEL, CALIFORNIA 93940

NAVAL POSTGRADUATE SCHOOL

Monterey, California



THESIS

TEST AND EVALUATION OF A
VTPR RETRIEVAL SYSTEM FROM
CLEAR-COLUMN NOAA 2 RADIANCES

by

Harry Milton Dyck Jr.

March 1975

Thesis Advisor:

F.L. Martin

Approved for public release; distribution unlimited.

T165947

REPORT DOCUMENTATION PAGE		READ INSTRUCTIONS BEFORE COMPLETING FORM
1. REPORT NUMBER	2. GOVT ACCESSION NO.	3. RECIPIENT'S CATALOG NUMBER
4. TITLE (and Subtitle) Test and Evaluation of a VTPR Retrieval System from Clear-Column NOAA 2 Radiances		5. TYPE OF REPORT & PERIOD COVERED Master's Thesis; March 1975
7. AUTHOR(s) Harry Milton Dyck Jr.		6. PERFORMING ORG. REPORT NUMBER
9. PERFORMING ORGANIZATION NAME AND ADDRESS Naval Postgraduate School Monterey, California 93940		8. CONTRACT OR GRANT NUMBER(s)
11. CONTROLLING OFFICE NAME AND ADDRESS Naval Postgraduate School Monterey, California 93940		10. PROGRAM ELEMENT, PROJECT, TASK AREA & WORK UNIT NUMBERS
14. MONITORING AGENCY NAME & ADDRESS (if different from Controlling Office)		12. REPORT DATE March 1975
		13. NUMBER OF PAGES 123
		15. SECURITY CLASS. (of this report) Unclassified
		15a. DECLASSIFICATION/DOWNGRADING SCHEDULE
16. DISTRIBUTION STATEMENT (of this Report) Approved for public release; distribution unlimited.		
17. DISTRIBUTION STATEMENT (of the abstract entered in Block 20, if different from Report)		
18. SUPPLEMENTARY NOTES		
19. KEY WORDS (Continue on reverse side if necessary and identify by block number) Clear-Column VTPR Radiance Temperature Retrieval Satellite Transmittance		
20. ABSTRACT (Continue on reverse side if necessary and identify by block number) An iterative technique for the retrieval of temperatures at each of 100 levels ranging from 1000 mb to 0.01 mb is evaluated. Clear-column radiance data in the carbon dioxide channels of the VTPR of NOAA 2 are used in inverting the radiative transfer equations to deduce the T(P) profile. The retrieval technique includes the computation of atmospheric transmittances due to three atmospheric absorber masses (carbon dioxide, water vapor,		

(20. ABSTRACT Continued)

and ozone) and non-homogeneous temperature-pressure effects along the vertical. The program also corrects these transmittances for zenith path differences between the satellite and the retrieval site when the site is not directly below the sensor. A normalized wave number, close to 700 cm^{-1} , but decreasing with decreasing values of pressure, was used in solving the Planck function for temperature, level-by-level. The retrieved temperatures were then compared with matching radiosondes at 15 key atmospheric levels and the resulting errors analyzed on a globally averaged and latitude band basis at each of the 15 levels.

Test and Evaluation of a
VTPR Retrieval System from
Clear-Column NOAA 2 Radiances

by

Harry Milton Dyck Jr.
Lieutenant Commander, United States Navy
B.S., California State University, Fresno, 1964

Submitted in partial fulfillment of the
requirements for the degree of

MASTER OF SCIENCE IN METEOROLOGY

from the
NAVAL POSTGRADUATE SCHOOL
March 1975

ABSTRACT

An iterative technique for the retrieval of temperatures at each of 100 levels ranging from 1000 mb to 0.01 mb is evaluated. Clear-column radiance data in the carbon dioxide channels of the VTPR of NOAA 2 are used in inverting the radiative transfer equations to deduce the T(P) profile. The retrieval technique includes the computation of atmospheric transmittances due to three atmospheric absorber masses (carbon dioxide, water vapor, and ozone) and non-homogeneous temperature-pressure effects along the vertical. The program also corrects these transmittances for zenith path differences between the satellite and the retrieval site when the site is not directly below the sensor. A normalized wave number, close to 700 cm^{-1} , but decreasing with decreasing values of pressure, was used in solving the Planck function for temperature, level-by-level. The retrieved temperatures were then compared with matching radiosondes at 15 key atmospheric levels and the resulting errors analyzed on a globally averaged and latitude band basis at each of the 15 levels.

TABLE OF CONTENTS

I.	INTRODUCTION -----	12
II.	SATELLITE DATA -----	17
	A. NOAA 2 VTPR DESCRIPTION -----	17
	B. CLEAR-COLUMN PROCEDURE -----	19
III.	TRANSMITTANCE MODELS IN THE VTPR CHANNELS -----	26
	A. ATMOSPHERIC TRANSMITTANCE COMPUTATIONS: GENERAL CONSIDERATIONS -----	26
	B. WATER VAPOR - MIXING RATIO ESTIMATION PROCEDURE -----	28
	C. ADJUSTMENT OF WATER VAPOR AMOUNTS FOR NON-HOMOGENEOUS ATMOSPHERES -----	31
	D. WATER VAPOR TRANSMITTANCE MODEL -----	35
	E. CARBON DIOXIDE TRANSMITTANCE MODEL -----	38
	F. TRANSMISSIVITY ADJUSTMENT FOR ZENITH ANGLE -	40
IV.	RETRIEVAL OF TEMPERATURE PROFILES -----	43
	A. INPUT DATA USED FOR TEMPERATURE RETRIEVAL --	43
	1. First Guess Temperatures -----	43
	2. Other Input Data -----	45
	B. MATHEMATICAL DEVELOPMENT OF THE TEMPERATURE RETRIEVAL -----	45
	C. STEPWISE TEMPERATURE RETRIEVAL -----	52
	D. PROGRAM OUTPUT -----	55
V.	RESULTS OF THE VTPR TEMPERATURE RETRIEVAL -----	58
	A. GLOBALLY AVERAGED RESULTS -----	58
	B. LATITUDE BAND RESULTS -----	60
VI.	CONCLUSIONS -----	64

APPENDIX A-1, A-2, ..., A-15. Histograms of the Globally Averaged Errors in Temperature, T(P), as Retrieved at the Levels P = 1000, 850, 700, 500, 400, 300, 250, 200, 150, 100, 70, 50, 30, 20, 10 mb -----	66
APPENDIX B Ozone Transmittances for the Six VTPR Clear-Column Channels -----	81
APPENDIX C U. S. Standard Atmosphere Supplements -----	84
COMPUTER PROGRAM -----	86
A. MAIN PROGRAM -----	86
B. SUBROUTINES -----	100
SAMPLE COMPUTER PROGRAM OUTPUTS -----	109
A. CARBON DIOXIDE TRANSMITTANCES -----	109
B. WATER VAPOR TRANSMITTANCES -----	112
C. TOTAL ATMOSPHERIC TRANSMITTANCES -----	115
D. SAMPLE OUTPUT FROM STATION 1 -----	118
LIST OF REFERENCES -----	119
INITIAL DISTRIBUTION LIST -----	122

LIST OF TABLES

1.	VTPR channel designators and centroid wave numbers for filter set number four of NOAA 2 VTPR instrument number 1 (used in March 1973) -----	19
2.	Eleven levels used for predictor levels in water vapor retrieval -----	30
3.	56 level atmosphere with merged climatology and 15 level first guess field for sample sounding --	44
4.	Normalized wave numbers and corresponding pressure levels used in inverting the Planck function for temperature retrieval -----	51
5.	Latitude bands used for error analysis of the VTPR retrieved temperatures -----	57
6.	Retrieved temperature error on a global basis -----	59
7.	Retrieved temperature error on a latitude band basis -----	61

LIST OF FIGURES

1.	Derivative of transmittance with respect to (pressure) ^{2/7} for the SIRS-B radiometer channels ----	13
2.	Satellite tracks for NOAA 2 VTPR coverage -----	18
3.	VTPR scan pattern and data analysis array -----	21
4.	NOAA 2 VTPR lateral scan geometry at raw radiance spots -----	22
5.	Scanning patterns used by the National Environmental Satellite Service (NESS) for pair comparison in determining VTPR clear-column radiance -----	24
6.	Multi-level atmosphere showing P(J), T(J), U(J) -----	32
7.	Transmittance curves for atmospheric layers 1 and 2 illustrating modification to effective U(J) in a non-homogeneous atmosphere -----	34
8.	Thirty three K-layer atmosphere model used for the integration of the radiative transfer equation -----	47
9.	Carbon dioxide transmittances in channels 1 through 6 -----	50
10.	Weighting functions used in determining a weighted mean Planck function -----	51

TABLE OF SYMBOLS AND ABBREVIATIONS

$B_i [T(P)]$	Planck radiance function for temperature T at pressure level p and channel i
$\bar{B}_i (K)$	Layer mean Planck function for layer K, in channel i
$B^{(n)} [\bar{\nu}, T(J)]$	Weighted mean Planck function at iteration n and for level J, using the normalized wave number $\bar{\nu}$
CLRAD	National Environmental Satellite Service (NESS) program for obtaining clear-column radiances
ITPR	Infrared Temperature Profile Radiometer
J	The subscript used to denote the levels in a 100 level atmosphere where
$J = 1 + 99 \left[\frac{P^{2/7} - (0.01)^{2/7}}{(1000)^{2/7} - (0.01)^{2/7}} \right]$	
K	The subscript used to denote the layers in a 33 layer atmosphere
mb	millibar
NASA	National Aeronautics and Space Administration
NESS	National Environmental Satellite Service
NMC	National Meteorological Center
NOAA	National Oceanic and Atmospheric Administration
NTP	Normal Temperature and Pressure conditions
ν_i	Wave number at the center of channel i
$\bar{\nu}$	Normalized wave number, $\bar{\nu} \doteq 700 \text{ cm}^{-1}$ and is a decreasing function of pressure
$P(J)$	Pressure at level J
P_s	Pressure at the surface of the earth (1000 mb)
RTE	Radiative transfer equation

SIRS	Satellite Infrared Spectrometer
SR	Scanning Radiometer
$T[P(J)]$	Temperature of the atmosphere at the pressure level $P(J)$
$\tau_i(J)$	Atmospheric transmittance at level J , in channel i
$\tau[X(J)]$	Atmospheric transmittance at level J from constituent X
μm	micrometers = 10^{-6} meters
VTPR	Vertical Temperature Profile Radiometer
*	Fortran symbol for multiplication used, if necessary, for clarification

ACKNOWLEDGEMENTS

The author wishes to express his appreciation to Professor Frank L. Martin for his generous assistance, infinite patience and guidance in the research and development of this paper.

Grateful acknowledgements are also extended to Dr. D. Q. Wark and Dr. H. E. Fleming of NESS for making available the archival tapes of the select data of March 1973, which made this paper possible.

It is appropriate here to recognize the generous support of Dr. L. M. McMillin and Dr. M. P. Weinreb who provided not only operational programs which were consistent with the instrument in use, but also, when requested, explained the physical rationale of such programs in connection with retrieval procedures at NESS.

I. INTRODUCTION

The quantitative measurement of temperatures at known pressure levels in the atmosphere is fundamental to present day weather analysis and forecasting. Until the launch of the Nimbus 3 satellite with its Satellite Infrared Spectrometer (SIRS) in April 1969, free air temperature soundings were obtained entirely from balloons, aircraft, and rockets. Since these sources were readily available only from populous land areas and a few ships, large areas of the world were without any reports. World-wide distribution of temperature sounding data was made possible by the use of satellites. The retrieval of a temperature profile by remote-sensing satellite measurements was first suggested by Kaplan (1959), and has been the object of numerous research studies.

The Nimbus 3 and Nimbus 4 satellites were equipped with SIRS-A and SIRS-B respectively. These first generation SIRS instruments, SIRS-A with a vertical scan, and SIRS-B with an additional side scan, measured monochromatic radiances in seven narrow regions or channels of the $15\ \mu\text{m}$ band of carbon dioxide, and one in the window region of water vapor centered at $899\ \text{cm}^{-1}$. Figure 1 (from Gelman et al. 1972) shows the weighting functions $d\tau_i/d(\ln P)$, after Smith et al. (1972), of the radiometric emitting channels of the SIRS-B instruments. A peak in $d\tau_i/dx$ relative to the $\ln P$ axis depicts the layer in the vertical contributing the maximum radiance to the

satellite channel sensor. These radiances could then be related to temperature profiles through the Radiative Transfer Equation (RTE)

$$I_i = B_i[T(P_s)] \tau_i(P_s) + \int_{P_s}^{P_o} B_i[T(P)] \frac{d\tau_i}{dP} dP . \quad (1)$$

Here, I_i is the spectral radiance in channel i ($i=1,2,\dots,8$), $B_i[T(P)]$ is the well-known Planck function for wave number ν_i and at temperature $T(P)$, $\tau_i(P)$ is the atmospheric transmittance averaged over wave number i (where i signifies the channel number centered at ν_i), and P is the pressure-level for which $\tau_i(P)$ has been computed.

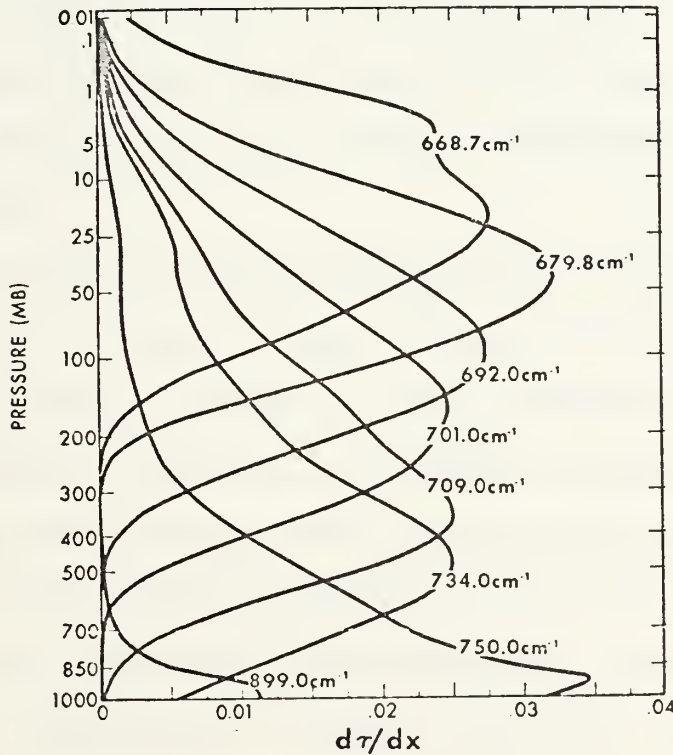


FIGURE 1. Derivative of transmittance (τ) with respect to $x(P) = P^{2/7}$ for SIRS-B (after Gelman et al. 1972)

Retrieval of temperature profiles from the SIRS-B radiometer was continued in systematic fashion by the National Environmental Satellite Service (NESS) until the radiometer output was considered non-usable on 8 April 1971. The number of retrievable satellite soundings collected during 1969-71 was insufficient to make a marked impact on the analysis problem over the oceans.

Anticipating an increased demand for quantitative weather observations from orbiting satellites, the National Oceanic and Atmospheric Administration (NOAA) in conjunction with the National Aeronautics and Space Administration (NASA), developed a second generation set of remote-sensing radiometers, improved over the SIRS-type, that would provide twice daily coverage of most of the globe and a higher resolution at individual scan spots.

As a result of these developments, the first of the new instruments was the Infrared Temperature Profile Radiometer (ITPR) as used on Nimbus 5. This radiometer carried four carbon dioxide channels, two window channels at 4.3 μm and 11.5 μm , respectively, and a water vapor channel near 20 μm . In 1972, NASA launched the NOAA-2 satellite, which carried aloft a new remote-sounding radiometer for which the ITPR had been a prototype. The new instrument, the Vertical Temperature Profile Radiometer (VTPR), had been still further improved over the ITPR in its angular-array scanning technique. The VTPR carried six carbon dioxide channels, a window channel,

and a water vapor channel. Observations made at scan spot arrays in channels 1,2,...,8 made it possible to systematically retrieve clear-column radiances at a higher resolution than before. The new instrument was designed to provide two temperature profiles per grid point per day on a 400 kilometer spacing over the oceans, or a global total of 6000 temperature profiles per day. An actual yield of 72%, or about 4000 profiles per day has been realized [Jastrow and Halem (1973)]. The use of these VTPR clear-column radiances from the NOAA 2 satellite and the temperature retrieval system described by McMillan et al. (1973) was the basis for a thesis by Moran (1974). The basic differences between the Moran study and previous work by Smith et al. (1972) was the use, by Moran, of standard atmospheric carbon dioxide transmittances with no interactive effects on the channel 1,2,...,6 transmittances from the other atmospheric constituents. Moran also computed radiances by the use of a 17-layer quadrature scheme for integration of Eq. 1 rather than by means of the more usual 100-level atmosphere. This was done in order to attempt to reduce the truncation error involved with uncertainties in the integration of the function $B_i[T(P)]d\tau_i/dp$ when a relatively crude model for $\tau_i(P)$ was utilized.

The first objective of the present thesis was to improve upon the Moran retrieval technique by incorporating recently updated state-of-the-art methods [Fritz et al (1972)] for computing atmospheric transmittances, including the combined

effects of water vapor, ozone, and carbon dioxide in each channel, as well as their vertical path dependencies on pressure and temperature. It was also necessary to correct these transmittances in each channel for the applicable zenith angles of the clear-column spot. For this purpose, a special data set for March 1973, including the tuned transmittance coefficients for the period, coupled with the first-guess temperature and humidity profiles, was acquired from NESS.

A second and equally important objective was to test the final temperature retrievals by comparison with radiosondes at island and coastal stations matching the VTPR scan spots in both time and spatial location. The retrieved profiles were compared at each of the 15 standard pressure levels (Table 3) with the matching radiosondes and were analyzed both by latitude and by pressure level.

The retrieval system used here has the feature of integrating Eq. 1 over 33 atmospheric layers at each clear-column radiance scan spot. This system was incorporated in order to minimize the truncation error in the quadrature scheme applied to the function $B_i d\tau_i / dp$ which appears in the RTE (Eq. 1). The improved accuracy in the determination of the temperature profile using this method is one of the main thrusts of this thesis.

II. SATELLITE DATA

The NOAA series of satellites are modifications of the earlier Environmental Science Service Administration (ESSA) satellites. The major change was the elimination of all vidicon camera systems in favor of radiation-sensing instruments, and in particular the inclusion of the vertical temperature profile radiometer (VTPR).

A. NOAA 2 DESCRIPTION

The NOAA 2 satellite orbits the earth at an altitude of 1464 kilometers once during each 115 minutes. Figure 2 illustrates the projection of seven orbits onto the earth. The solid lines indicate the north-to-south or "descending" portions of the orbits, which occur over the sunlit hemisphere; dashed lines are nighttime "ascending" portions of the same orbits. Equatorial crossings occur at 0900 (descending) and 2100 (ascending) local solar time.

The VTPR instrument scans perpendicularly relative to the subsatellite track from left to right, when viewed downtrack, in 23 individual non-overlapping steps covering ± 30.3 degrees from local nadir. The instrument observes each spot in eight spectral intervals or channels through the use of the automatic optical filter selector equipment of the VTPR. Six of the channels are located in the $15\text{ }\mu\text{m}$ band of carbon dioxide, one in the $19\text{ }\mu\text{m}$ region of the rotational band of water vapor, and

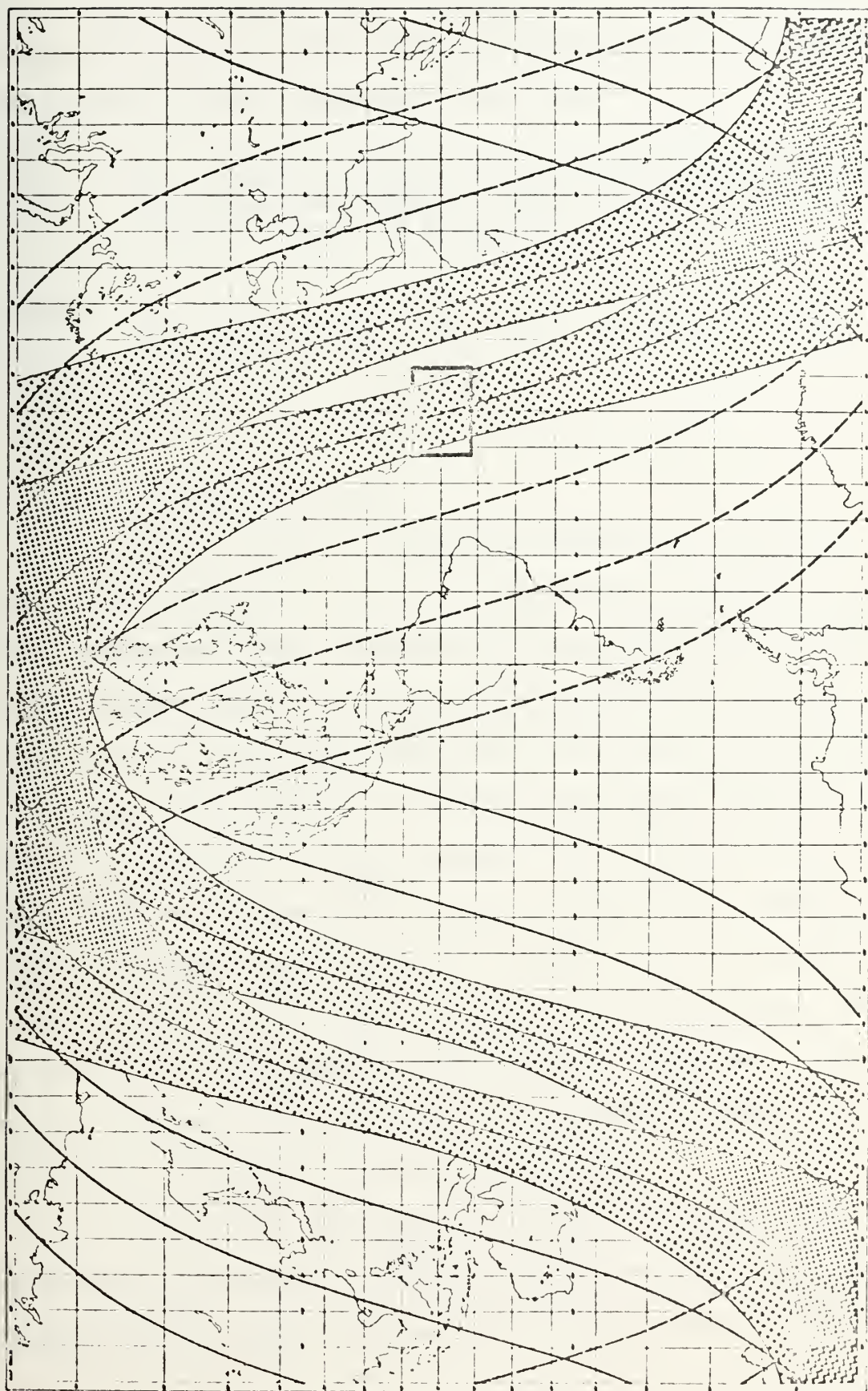


Figure 2 - Satellite tracks for NOAA 2 VTPR coverage

one in the 12 μm atmospheric window (see Table 1). After the entire set of 8 spectral measurements has been obtained, the scanning mirror rotates to the next spot.

Table 1. VTPR channel designators and centroid wave numbers for filter set four of NOAA 2 VTPR instrument number 1 (used in March 1973).

CHANNEL	1	2	3	4	5	6	7	8
WAVE NO. (cm^{-1})	668.5	677.5	695.7	707.2	724.7	747.5	534.5	835.1

B. CLEAR-COLUMN PROCEDURE

In order to obtain an accurate temperature retrieval, the "raw" radiances, that is the radiances measured at the VTPR instrument, must be adjusted to eliminate the effects of any clouds that may be located in the field of view. Smith (1970) and others introduced cloud layer models wherein the extent and thickness of cloud layers which would give the radiance as sensed at the satellite are mathematically introduced into the temperature profile calculation. However, the results in the neighborhood of a single scan spot tend to result in non-unique cloud heights and amounts which causes uncertainty in the deduced clear-column radiances. The method described below was later developed by Smith (1971) in order to eliminate these uncertainties.

The National Environmental Satellite Service (NESS) eliminates cloud contamination through the use of a conversion program called CLRAD, applied to a large array of contiguous

raw radiance spots. Sets of eight scan lines, containing 23 scan spots are divided into 3 subarrays or boxes of 8 by 8, 8 by 7, and 8 by 8 scan spots as shown in Figure 3. Observations of raw VTPR radiances are made in each of the eight channels and at each scan spot. Figure 4 shows the lateral scan geometry along each scan line, where spot 5, spot 12, and spot 19 in line 4, are the center of box left, box center and box right, respectively. Each box-center is denoted by an X in Figure 3. At these locations it is necessary to determine the exact zenith angles to the sensor aboard the satellite using the following relationship

$$\sin(Z_n) = \sin(N_n) \frac{a+H}{2} \quad (2)$$

Here Z_n is the zenith angle at scan spot n ($n = 5, 12, 19$). N_n is the nadir angle at the same spots, a is the constant 6370 km (earth's radius), and H is the altitude of the satellite (mean value of 1460 km). The mean zenith angle at spot 12 is 0° , while at spots 5 and 19 it is $23^\circ 47'$ left and right of center respectively.

In addition to the VTPR radiances, measurements in a Window-channel Scanning Radiometer (SR), sensing in 10.5 to 12.5 μm , permits determination of the sea surface temperatures at each of the scan spots. McMillin et al. (p 25-33, 1973) outline a process of extrapolation of raw-radiance to clear column radiance within localized sub-areas about the scan

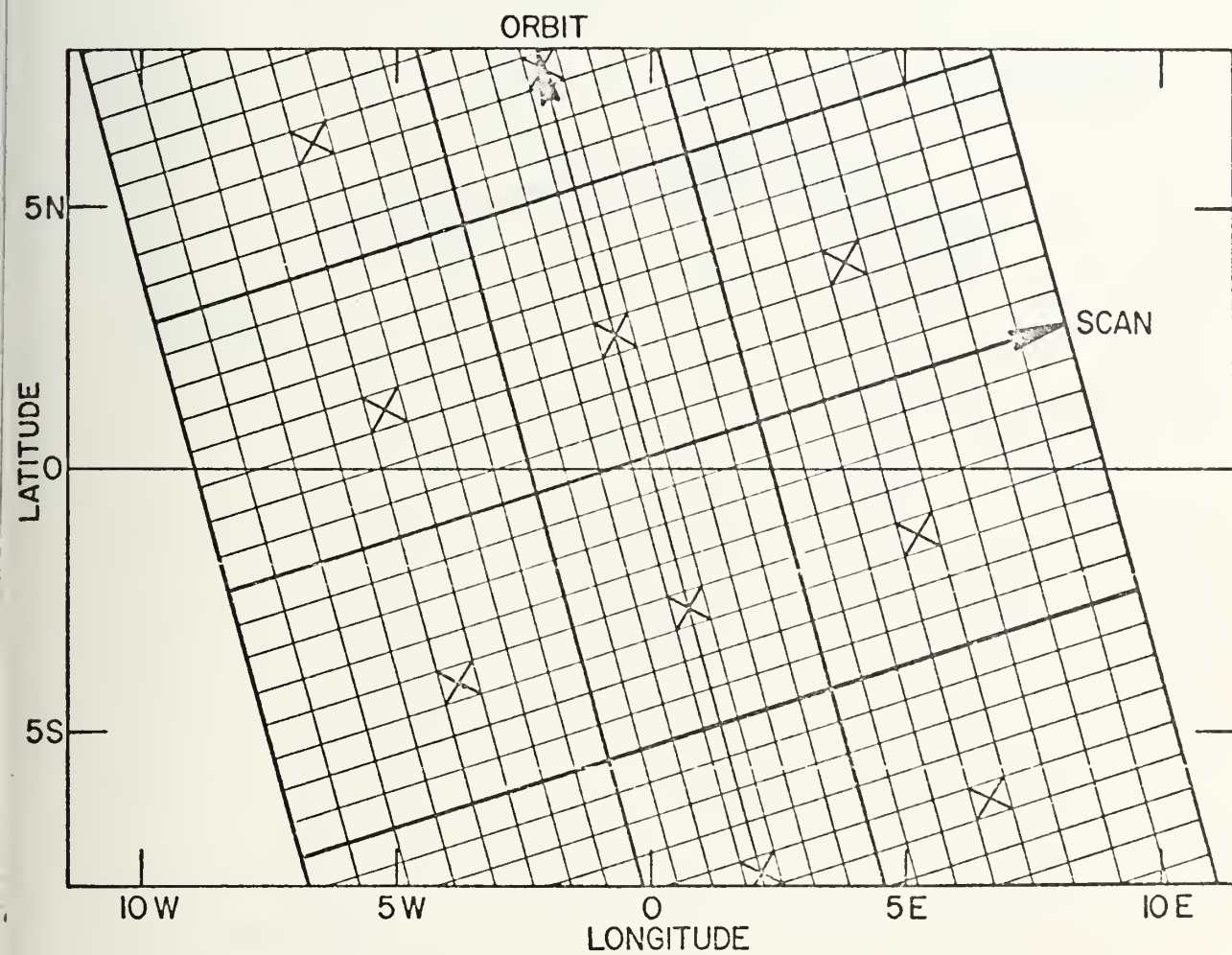
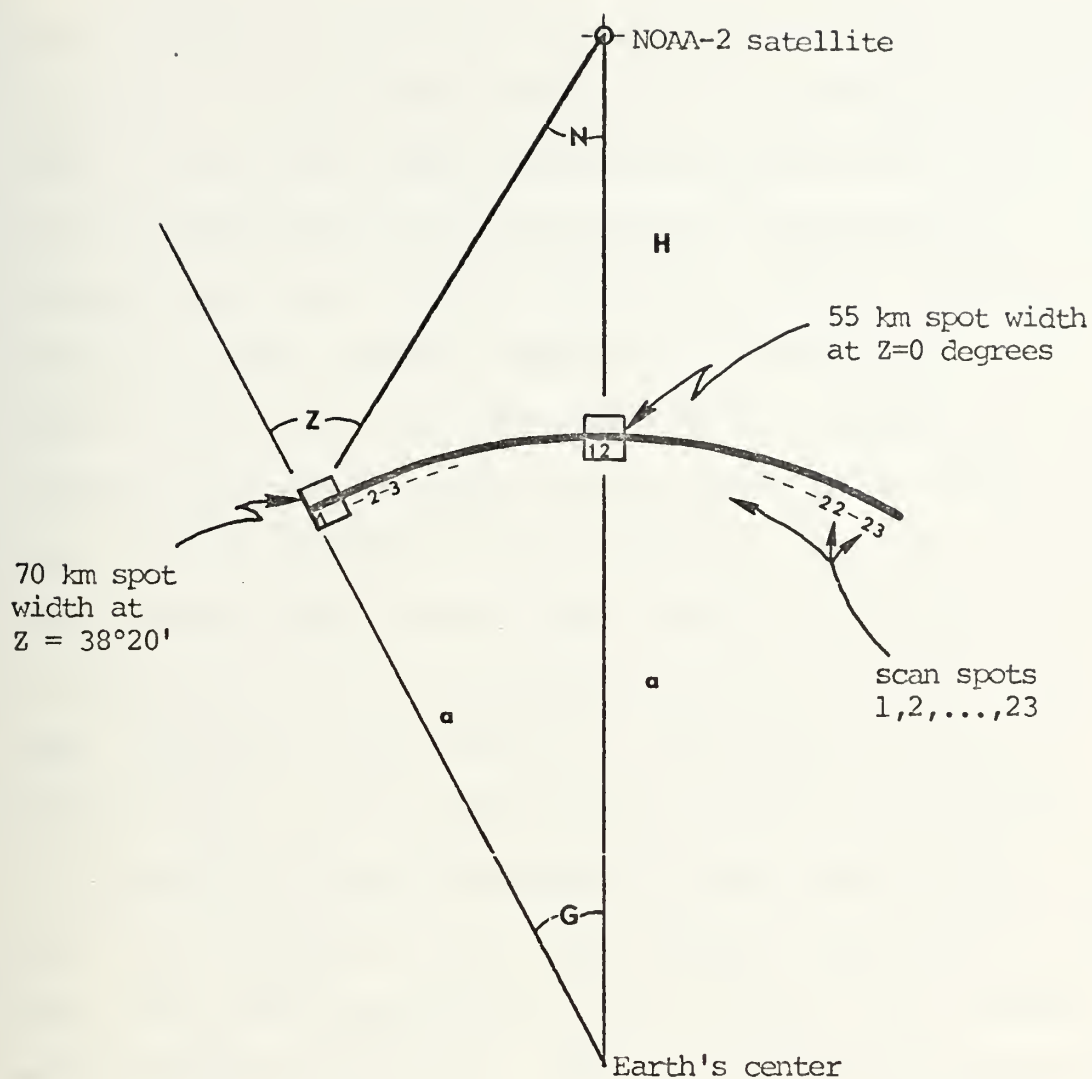


Figure 3 - VTPR scan pattern and data analysis array



N = Nadir angle

Z = Zenith angle

G = Geocentric angle

a = Earth's radius (6370 km)

H = Satellite altitude (mean = 1460 km)

Figure 4. NOAA-2 VTPR lateral scan geometry at raw radiance spots

spots. The specifics of the clear radiance conversion method involves: (1) the specifications of a reasonably accurate value of the first guess temperature profile $T(P)$ to 10 mb, (2) an estimation of the water vapor transmittances in the window channel derived from the $T(P)$, and (3) the determination of the sea surface temperature derived from the SR. The value of the clear-column window channel radiance can then be computed and compared with the observed window channel radiance. If the observed "raw" radiance is equal to or greater than the computed radiance, the sounding is considered to be cloud free. If the computed radiance is greater than the "raw" radiance, the sounding is considered to be cloud contaminated and the extrapolation process is necessary.

To facilitate the extraction of the clear-column radiance set, "raw" radiance values from adjacent spot pairs (spots 1 and 2 with their associated $I_1(v)$ and $I_2(v)$ for example) are extrapolated to $I_{\text{clear}}(v)$. This can be done if the cloud amounts vary linearly in the field of view and share approximately the same cloud top level. Figure 5 shows the patterns used by NESS for pair comparisons. Each 8 by 8 box, so analyzed, will contain 49 scan spots, which can be compared with four adjacent spots for a total possible yield of 196 values of clear-column radiance $I_{\text{clear}}(v_i)$. Here i denotes all channels other than the window channel since the window channel gives rise only to a possible 49 clear-column estimates. A proportionately smaller number of both radiance sets are found in the 8 by 7 box. If a suitable number of

the scan spots are capable of giving four adjacent clear-column values without excessive variances, all resulting values are usable in obtaining the weighted clear-column radiance in the respective channels.

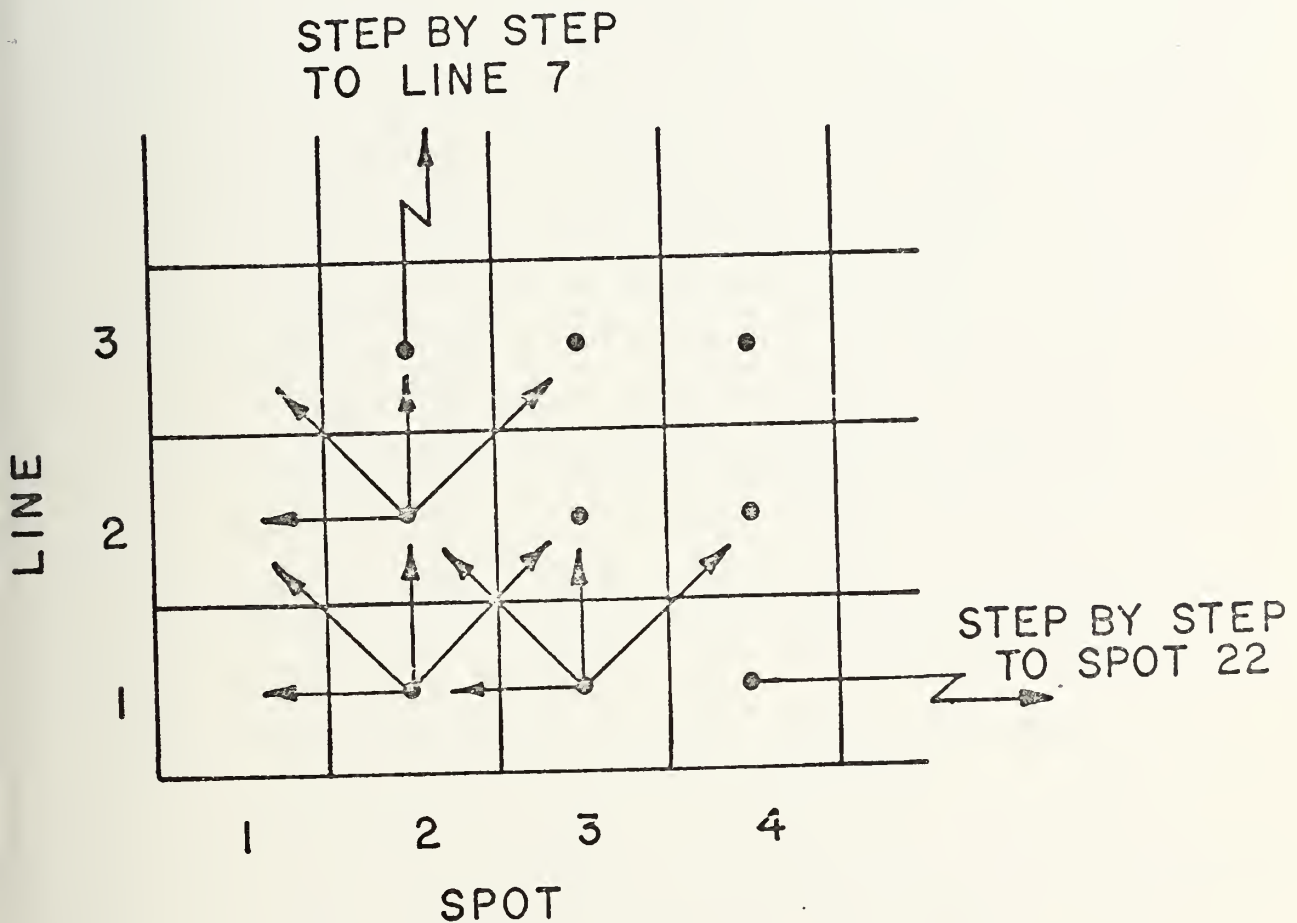


Figure 5. Scanning patterns used by the National Environmental Satellite Service (NESS) for pair comparison in determining VTPR clear-column radiance.

Research on refining the accuracy of determination of clear-column radiances is actively being conducted. This involves both instrumental accuracy improvements as well as the algorithms for the extrapolations of cloud amounts to zero.

III. TRANSMITTANCE MODELS IN THE VTPR CHANNELS

A. ATMOSPHERIC TRANSMITTANCE COMPUTATIONS: GENERAL CONSIDERATIONS

Atmospheric transmittances for the six carbon dioxide spectral intervals used in the retrieval are fundamental and must be computed accurately. The resultant transmittance in any given channel and at any pressure level $P(J)$ in the atmosphere may be expressed as the product of the transmittances due to the carbon dioxide alone $\tau[C(J)]$ and the overlapping transmittances due to the integrated ozone, $OZ(J)$, and water vapor, $U(J)$, from the top of the atmosphere to the level J respectively. Thus

$$\tau(J) = \tau[C(J)] * \tau[U(J)] * \tau[OZ(J)] \quad (3)$$

Here $C(J)$ denotes the total absorber mass of the carbon dioxide from $P(1) = 0.01$ mb to $P(J)$. The symbol $OZ(J)$ denotes the corresponding absorber mass of ozone expressed in NTP standard amounts per square centimeter column above level J , and $U(J)$ is the precipitable water vapor in the same column. As an example of the transmittances produced by the program discussed in this thesis, sample outputs are included following the program listing.

Moran (1974) used only carbon dioxide transmittances acting in the vertical column (i.e., $\tau[U(J)] = \tau[OZ(J)] = 1$, by assumption) and further simplified the computation by selecting

a mid-latitude, standard-atmosphere transmittance model for carbon dioxide in the six listed channels. Moran found that super-adiabatic temperature lapse rates tended to occur between the 1000 mb and 900 mb levels. Consequently he found it necessary to adjust the values of the transmittance profile somewhat arbitrarily in channels 5 and 6, since the transmittance from the surface in these channels tended to be somewhat higher than with the more realistic product transmittances of Eq. 3.

Transmittances in the carbon dioxide channels were based upon the laboratory observations of the carbon dioxide infrared spectrum and resultant calculations by Drayson (1966), made on a line-by-line basis assuming a homogeneous path (for a fixed temperature).

In calculations applied to non-homogeneous vertical paths, Smith (1969), calculates the carbon dioxide transmittances corresponding to the U. S. Standard Atmosphere (1962); and makes improvements on the usual Curtis-Godson modifications [Goody (1964)] applied to path transmittances for varying pressure, temperature, and absorber masses. In addition, modified profiles corresponding to temperature differences from the U.S. Standard Atmosphere by ± 10 , ± 20 , and $\pm 30^\circ\text{K}$ were also computed by Smith, after Drayson's (1966) laboratory calculations. A method for applying temperature corrections to the absorber mass in each non-homogeneous sub-layer was devised so that the effective temperature-modified carbon dioxide transmittances could be adjusted by a variation of

the Curtis-Godson method applied to successive layers, using the laboratory data of Drayson.

The method utilized here for carbon dioxide temperature adjustment along the path will be discussed in greater detail following that for water vapor. This latter method is somewhat more general due to the variable mixing ratio of this constituent in the vertical as well as the greater complexity of the individual line structure in the water vapor infrared spectrum.

B. WATER VAPOR - MIXING RATIO ESTIMATION PROCEDURE

In order to determine the transmissivity due to water vapor in each of the VTPR channels, the precipitable water vapor integrated from $J = 01$ to any arbitrary level must be determined. For this purpose an estimation procedure for determining the mixing ratio, $W(J)$, at each level was used to represent the water vapor profile. The parameter $W(J)$ was used because it was found to be determined from $T(P)$ alone with reasonable skill, using the method of Weinreb and Crosby (1973); and also because it enters directly into the calculation of the water vapor transmittances in the eight VTPR channels.

The calculation of the mixing ratio $W(J)$ may be derived from

$$W(J) = \text{SAT}(T,J) * H(J) \quad (4)$$

$H(J)$ is the relative humidity and is an unknown function of pressure. The use of the water vapor channel ($\nu = 535 \text{ cm}^{-1}$) was not attempted for retrieval in this thesis. Furthermore, $SAT(T,J)$, the saturated mixing ratio is a function of temperature $T(J)$ and pressure $P(J)$ only, and is calculated by the GOFF-GRATCH formula [List 1963]

$$\begin{aligned} \log e_w = & -7.90298(T_s/T - 1) + 5.02808 \log(T_s/T) \\ & - 1.3816 \times 10^{-7} [10^{11.344(1 - T/T_s)} - 1] \\ & + 8.1328 \times 10^{-3} [10^{-3.49149(T_s/T - 1)} - 1] + \log e_{ws} \end{aligned} \quad (5)$$

Here e_w is the saturation vapor pressure over a plane water surface,

T is the temperature in $^{\circ}\text{K}$,

T_s is the steam point temperature $373.16 \text{ }^{\circ}\text{K}$, and

e_{ws} is the saturation vapor pressure of water at the steam point temperature.

The value of $SAT(T,J)$ is then computed using the relationship

$$SAT(T,J) = 0.622 \left(\frac{e_w}{P(J) - e_w} \right) \quad (6)$$

Since no equation directly relates the relative humidity to the temperature profile, the mixing ratio was estimated from the saturated mixing ratios at a specified set of eleven levels (Table 2) by a least-squares formulation based solely upon these eleven saturated mixing ratio predictors after Weinreb and Crosby (1973). The method formulates the mixing

ratio $W(J)$ at the 40 levels $J = 61, 62, \dots, 100$ and is given in the form

$$W(J) = \bar{W}(J) + \sum_{I=1}^{11} CREG(I, J) [SAT(I) - \bar{T}(I)] \quad (7)$$

where $\bar{W}(J)$ is the sample mean mixing ratio at level J over 1100 sample soundings that were used to determine the regression coefficients,

$CREG(I, J)$ is a set of predetermined regression coefficients calculated for each J -level from the 1100 sample soundings,

$SAT(I)$ is the saturation mixing ratio at the level I , where $I = 1, 2, \dots, 11$ is a subset of the 40 J -levels that is found to give the best results (see Table 2), and

$\bar{T}(I)$ is the mean saturation mixing ratio at level I from the 1100 test soundings.

Table 2. Eleven levels used for predictor levels in water vapor retrieval

<u>I</u>	<u>J</u>	<u>P(J) mb</u>
1.	63	209.94
2.	66.	245.37
3.	70	299.01
4.	77	412.26
5.	82	509.93
6.	90	699.03
7.	92	753.17
8.	94	810.25
9.	96	870.35
10.	98	933.57
11.	100	1000.00

Thus the method uses an eleven level saturated mixing ratio profile, $SAT(I)$, and converts it into a 40-level mixing ratio profile, $W(J)$, $J = 61, 62, \dots, 100$. The total 100-level

profile is then converted from the 40-level by using the cubic power-law profile due to Smith (1966)

$$W(J) = W(61) \left[\frac{P(J)}{P(61)} \right]^3 \quad (8)$$

$J < 61$

The mixing ratio is then used in determining the water vapor transmissivity.

C. ADJUSTMENT OF WATER VAPOR MASS IN A NON-HOMOGENEOUS ATMOSPHERE

Assuming that the transmittance by water vapor, $\tau[U(J)]$, in a spectral interval of the VTPR is a known function of the quantity of the precipitable water vapor U , temperature T , and pressure P , an accurate approximation to $\tau[U(J)]$ in the form of a least squares fit polynomial can be calculated. Weinreb and Neuendorfer (1973) proposed such a best-fit model which in effect becomes an analytic function for calculating homogeneous path transmittances. In the Weinreb-Neuendorfer method, an inhomogeneous atmosphere is treated as a sequence of homogeneous layers, each having a constant temperature, pressure, and absorber mass. The transmittance model provides for a homogeneous path as a known function of T , P , and \tilde{U} , where \tilde{U} is the effective water vapor mass. If $\tau(J)$ is the transmittance in the spectral interval of the instrument at level J , then

$$\tau(J) = \tau[P(J), T(J), \tilde{U}(J)] \quad (9)$$

The procedure involved in defining $\tau[(J)]$ at each level as depicted in Fig. 6, uses the functional expression, Eq. 15, for layer 1 without modifying the precipitable water vapor mass, U , from its initially specified value based upon the homogeneous values $P(1)$, $T(1)$, and $U(1)$. This gives rise to the following relationship for layer 1

$$\tau(1) = [P(1), T(1), \tilde{U}(1)] . \quad (10)$$

$$\tilde{U}(1) \equiv U(1)$$

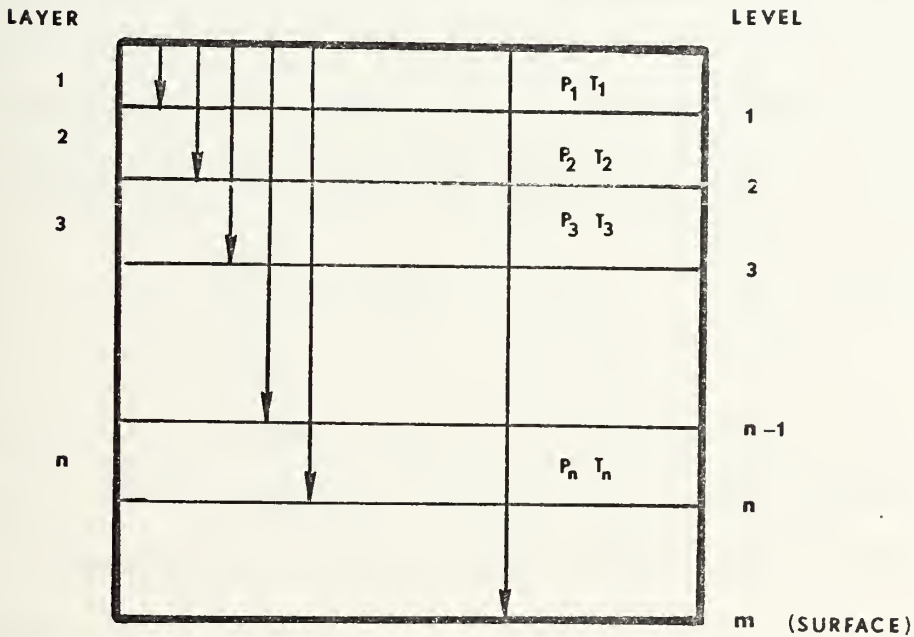


Figure 6. Multi-level atmosphere showing $P(J)$, $T(J)$, and $U(J)$ structures.

In proceeding to level 2, the transmittance through the second layer is affected by the new homogeneous characteristics $P(2)$, $T(2)$, and its water vapor increment ΔU_2 , and is no longer along the $\tau[P(1), T(1), \tilde{U}(1)]$ transmittance curve defined by the

conditions in layer 1 (points A_1 - B_1 in Fig. 7). It is necessary to determine the adjusted value of water vapor mass, denoted V in Fig. 7, with which the radiant transmittance enters the new homogeneous layer 2. This is accomplished by backing up on curve 2 to $\tilde{U} = V$ by solving

$$\tau(1) = \tau[P(2), T(2), V] \quad (11)$$

for V . The solution for V is accomplished by the Newton-Raphson iteration.

This corrected starting water vapor mass, V , with which to enter layer 2, has been deduced using curve 2 in Fig. 7. For the purpose of computing the transmittance at level 2, the new total water vapor mass is then taken as

$$W = V + \Delta U_2 \quad (12)$$

where ΔU_2 is the known increase in precipitable water vapor in layer 2. This moves the transmittance value $\tau[P(2), T(2), W]$ down to point B_2 on curve 2 where the value of $\tau(2)$ is then taken as

$$\tau(2) = \tau[P(2), T(2), \tilde{U}(2) = W] \quad (13)$$

In proceeding downward to level 3 through the next homogeneous layer of characteristics $P(3)$, $T(3)$, ΔU_3 , the corrected amount of water vapor at level 2 is revised from $\tilde{U}(2)$ to V which

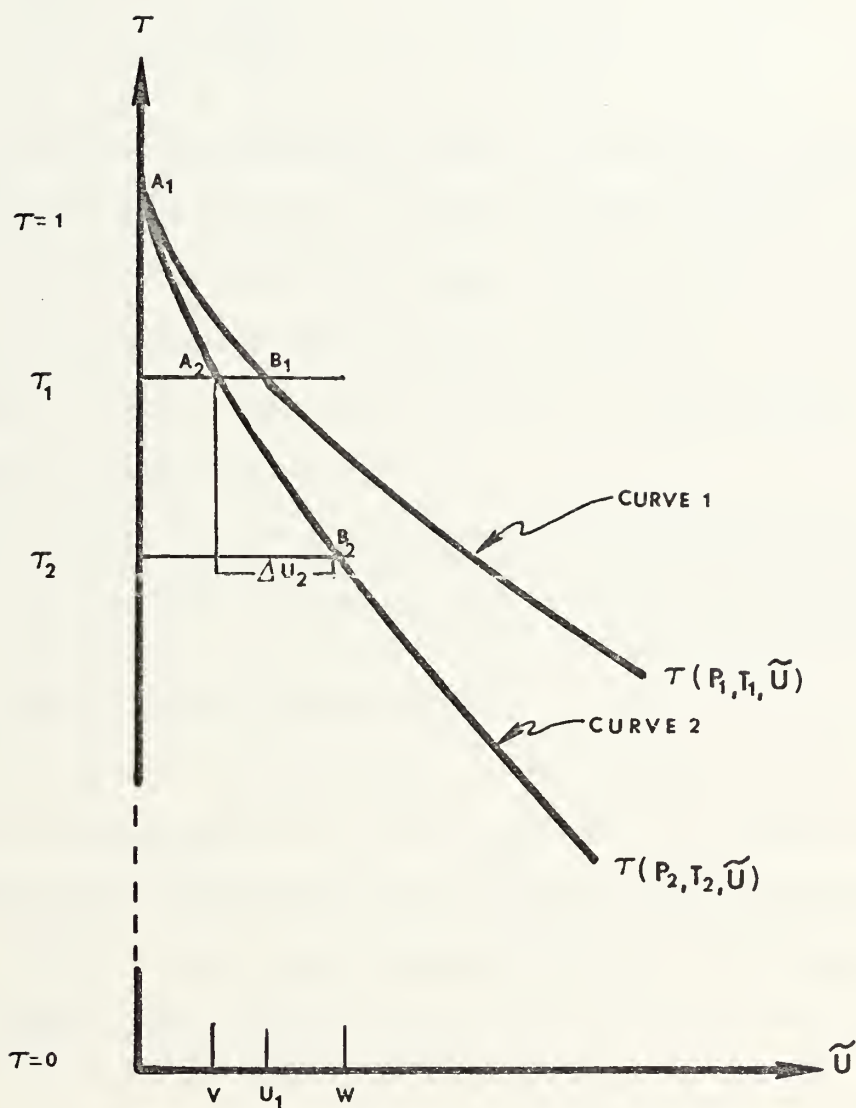


Figure 7. Transmittance curves for atmospheric layers 1 and 2 illustrating modification to effective $U(J)$ in a non-homogeneous atmosphere.

becomes the level 2 starting point of water vapor mass.

Hence the new function

$$\begin{aligned}\tau(3) &= \tau[P(3), T(3), \tilde{U}(3)] \\ \tilde{U}(3) &= V + \Delta U_3\end{aligned}\tag{14}$$

is solved for the new starting mass at the top of level 3. The procedure continues as a series of Newton-Raphson iterations to correct the effective water vapor masses for the radiant transmittance upon succeeding layers. This procedure is followed through each level $J = 2, 3, \dots, 99$ bounding the top of the 98 layers below $J = 2$.

The procedure is shown by Weinreb and Neuendorfer to be exact for a Beer's-Law monochromatic transmittance function.

D. WATER VAPOR TRANSMITTANCE MODEL

The water vapor transmittance calculations use the method of Weinreb and Neuendorfer (1973) applied to a modification of the polynomial representation of water-vapor transmission of Smith (1969). The basic equation for the line transmittance of water vapor implies that

$$\ln\{-\ln \tau [U(J)]\} = \sum_{I=1}^{14} C_I X_I\tag{15}$$

Here

$$\begin{aligned}
 x_1 &= 1 & x_8 &= x_4 x_7 \\
 x_2 &= (0.1) \ln \frac{UT}{273} & x_9 &= x_3 x_4 \\
 x_3 &= \ln(P/1000) & x_{10} &= x_2 x_7 \\
 x_4 &= \ln(T/273) & x_{11} &= x_4 x_7 \\
 x_5 &= x_2 x_3 & x_{12} &= (x_4)^2 \\
 x_6 &= x_2 x_4 & x_{13} &= x_3 x_6 \\
 x_7 &= (x_2)^2 & x_{14} &= x_3 x_7
 \end{aligned}$$

and C_I is a set of coefficients that were predetermined by fitting Eq. 15 by the least-squares method using line-by-line calculations of the transmittances for 130 homogeneous (constant pressure and temperature) paths. From Eq. 15 it follows that

$$\tau[U(J)] = \exp[-\exp(\sum_{I=1}^{14} C_I x_I)] \quad (16)$$

The values of x_3 through x_{14} are directly calculated only if U is known. However, x_2 must be calculated indirectly since U , the water vapor absorber mass, is essentially a sum of scaled values of ΔU between successive J -levels. Newton's method was used to solve for the new value of x_2 , and subsequently other $x_i = x_i x_2$, using the first iteration of

$U_1^{(2)} + \Delta U = U_2^{(1)}$ as the first guess to arrive at the effective $U_2^{(2)}$ at level 2, etc. on to the subsequent J-levels.

Water vapor transmittances in the infrared region have been found to contain a spectral feature not previously explainable by the classical line-spectral approaches. Bignell (1970) found a continuum absorption from the edge of the 20 μm rotational band which overlaps the lines in the water-vapor and carbon-dioxide absorption regions. The continuum absorption coefficient was found to be due to the presence of the water vapor dimer $(\text{H}_2\text{O})_2$. The dimer absorption coefficient in the various spectral regions was found to be proportional to $[T(J)]^{-5}$ (see Eqs. 17 below). Thus, it is necessary to add the dimer correction to Eq. 15 to fully account for the combined transmittances of water vapor in all channels. The dimer contribution at level J to the $\ln[-\ln\tau(J)]$ of Eq. 15 due to water vapor is given by the adjusted dimer mass profile in terms of

$$\text{DIMER}(J) = \text{DIMER}(J-1) + \left[\frac{A(J-1) + A(J)}{2} \right] [P(J) - P(J-1)] \quad (17)$$

$$A(J) = P(J) [W(J)]^2 \left[\frac{303.16}{T(J)} \right]^5$$

The actual transmittance due to the effective dimer mass in each channel is then given by

$$\ln[-\ln \tau(\text{DIMER})] = B(I) * \text{DIMER}(J) \quad (18)$$

where $B(I)$, $I = 1, 2, \dots, 8$ is a set of 8 constant absorption coefficients, the values of which have been given for each channel after Bignell (1970). The combined water-vapor transmittance in each channel then becomes

$$\tau[U(J)] = \exp\{-\exp[DIMER(J)*B(I)]\} \tau(J) \quad (19)$$

where $\tau(J)$ is the value computed using Eq. 16.

The zenith angle correction for water vapor transmittance is included in $DIMER(J)$ and $U(J)$ of Eqs. 9 and 17 by making the following path-corrections for mass:

$$\begin{aligned} DIMER(J) &= DIMER(J)*PATH, \\ U(J) &= U(J)*PATH, \\ PATH &= \sec Z. \end{aligned} \quad (20)$$

Here $\sec Z$ is the secant of the zenith angle from the point representing the center of the box to the radiometer (see Figure 4).

E. CARBON DIOXIDE TRANSMITTANCE MODEL

A polynomial expression for the carbon dioxide transmittance $\tau[C(J)]$ in terms of logarithmic functions similar to Eq. 15 has been shown to be feasible by Smith (1969). However, the absorber mass of carbon dioxide is proportional to pressure, and little dependence upon higher powers of the

$\ln(P/1000)$ term has been found necessary to fit line-by-line computations of transmissivities with increasing pressure in non-homogeneous atmospheres.

However, the carbon dioxide polynomial expansion, similar to Eq. 15 for the water vapor model, has been found to be subject to path correction primarily for the temperature variation along the vertical. The method of Weinreb and Neuendorfer (1973) was shown by Fleming (1974) to be converted into the following form

$$\begin{aligned} \tau[C(J)] = & \tau[C(J-1)] [\alpha(J) + \beta(J) \Delta T(J) + \gamma(J) \Delta T^2(J)] \\ & + \theta_i \{ \tau[C(J-1)] - \tau^*(J-1) \} \end{aligned} \quad (21)$$

where $\tau[C(J)]$ is the transmittance due to carbon dioxide at level J:

$\Delta T(J)$ is the temperature difference between the U. S. Standard Atmosphere (1962) and the average temperature over the layer bounded by the pressure levels J and J-1 ($J = 2, 3, \dots, 100$),

α, β, γ are a set of 3 by 100 transmittance factors that are tuned specifically to the filters of the instrument in use for the data period,

θ_i is a set of six adjustment factors applicable to systematic corrections for temperature variations from the initial standard, and

$\tau^*(J)$ is a correction term approximated after the Newton-Raphson method from

$$\tau^*(J) = \frac{A(J) + B(J) \Delta T(J)}{\Delta T(J-1)} + \frac{D(J) [\Delta T(J)]^2}{[\Delta T(J-1)]^2} \quad (22)$$

where for the initial level $J = 1$, A , B , D are defined as

$$\begin{aligned} A(1) &= \alpha(1) \\ B(1) &= \beta(1) \Delta T(1) \\ D(1) &= \left[\frac{\beta(1) \beta(2)}{\alpha(1)} + \gamma(1) \right] [\Delta T(1)]^2 \end{aligned} \quad (23)$$

and for subsequent layers, $J > 1$, the values of A , B , and D are updated iteratively by

$$\begin{aligned} A^{(1)}(J) &= A^{(2)}(J-1) \\ B^{(1)}(J) &= \frac{B^{(2)}(J-1) \Delta T(J)}{\Delta T(J-1)} \\ D^{(1)}(J) &= \frac{D^{(2)}(J-1) [\Delta T(J)]^2}{[\Delta T(J-1)]^2} \\ D^{(2)}(J) &= \frac{D^{(1)}(J) [\Delta T(J)]^2 \alpha(J)}{[\Delta T(J-1)]^2} + A^{(1)}(J) \gamma(J) [\Delta T(J)]^2 \\ B^{(2)}(J) &= B^{(1)}(J) \alpha(J) + A^{(1)}(J) \beta(J) \Delta T(J) \\ A^{(2)}(J) &= A^{(1)}(J) \alpha(J) \end{aligned} \quad (24)$$

all of which must be computed in the given order.

F. OZONE TRANSMITTANCES

The ozone transmittances $\tau[\text{OZ}(J)]$ are minor contributions appearing in the form of Eq. 3 for each carbon dioxide channel.

They are constant in each channel at a given level, varying, however from level to level. Thus the effect of $\tau[\text{OZ}(\text{J})]$ is expressible in the form of a 6 by 100 array, one member of the array for each carbon dioxide channel at each J-level. The channel values of $\tau[\text{OZ}(\text{J})]$ used here are listed in Appendix B, as extracted from the NESS CLRAD program.

The $\tau[\text{OZ}(\text{J})]$ values in Appendix B have not been path corrected and are based upon globally averaged NTP absorber paths of ozone in the carbon dioxide channels.

G. TRANSMISSIVITY ADJUSTMENT FOR ZENITH ANGLE

When the transmittance in the spectral interval of the VTPR has been calculated, an adjustment must be made to account for the path differences that occur with various zenith angles. The VTPR is designed to measure clear-column radiances from points which subtend a zenith angle of $23^{\circ}47'$ left, 0° , or $23^{\circ}47'$ right of the satellite track. These angles correspond to the center of the three boxes shown in Figure 3. The adjustments to the calculated transmittances must be made for these basic angles and any small deviations from them.

The principle of the correction stems from the fact that if the zenith angle is other than zero degrees, the atmospheric absorbers will have more effect due to the geometry involved (Figure 4) with the longer path, and, therefore, the transmissivity in the layer will be decreased level for level.

The correction for both the carbon dioxide and ozone transmittance at level J is taken from a section of the NESS CLRAD program [McMillin(1974)] and is in the form of

$$\tau(J) = \tau(J)^A \quad (25)$$

$$A = (\text{PATH})^{B(J)} \quad (26)$$

where PATH is the secant of the zenith angle, and B(J) is a polynomial function for carbon dioxide alone. For the ozone path corrected transmittances B(J) \equiv 1 for all atmospheric levels. B(J) is a function of $\ln[P(J)]$ with terms in $\ln[T(J)]$ up to quadratic (and a product of these logarithmic functions), with a set of five predetermined constants for each channel. These constants have been tuned for the particular VTPR instrument in use during the period.

IV. RETRIEVAL OF TEMPERATURE PROFILES

A. INPUT DATA USED FOR TEMPERATURE RETRIEVAL

1. First Guess Temperatures

In addition to the climatological soundings, $T(P)$, from the U. S. Standard Atmosphere Supplements (1966) (see Appendix B), the retrieval program requires a first guess temperature profile in the box center for each VTPR clear-column radiance set. The first guess temperatures are of two basic types depending upon the latitude of the sounding. For tropical latitudes, from the equator to 18 degrees North, radiosonde data is averaged over all latitudes and longitudes to provide a single climatological first guess profile. For the other northern hemisphere retrievals, the first guess profile comes from an application of the National Meteorological Center (NMC) prognostic model for a period of 12 to, at most, 18 hours from the preceding complete analysis. The profile is extrapolated in time and space to the VTPR clear-column sounding location.

The first guess temperatures, as read into the program, give temperatures at the 15 mandatory levels shown by an asterisk (*) in Table 3, from 100 mb to 10 mb. The U. S. Standard Atmosphere Supplement climatology value is adjusted for latitude and month and then fitted to the first guess profile at the 10 mb level. The adjustment, defined as first guess (10 mb) minus standard (10 mb), is then added to all values of the standard

Table 3. 56 level atmosphere with merged climatology and
15 level (*) first guess field for sample sounding.

LEVEL	PRESSURE (mb)	TEMPERATURE (°C)
1	0.01	-87.130
.	.	.
.	.	.
.	.	.
23	1.00	-04.311
.	.	.
.	.	.
.	.	.
34	10.00*	-42.300
35	15.00	-45.300
36	20.00*	-49.925
37	25.00	-53.175
38	30.00*	-56.800
39	40.00	-59.900
40	50.00*	-63.000
41	60.00	-65.600
42	70.00*	-68.200
43	85.00	-69.250
44	90.00	-69.600
45	100.00*	-70.300
46	150.00*	-63.400
47	200.00*	-58.200
48	250.00*	-48.400
49	300.00*	-38.900
50	400.00*	-23.600
51	500.00*	-11.800
52	600.00	-03.500
53	700.00*	4.800
54	850.00*	13.600
55	900.00	16.267
56	1000.00*	21.600

atmosphere, above 10 mb, and the profile is expanded to the 56 levels shown in Table 3.

The 56 level temperature profile is then expanded to the 100 J-levels, where the pressure at level J is given by

$$P(J) = 0.01[1+(J-1)(0.26087836)]^{7/2} \quad (27)$$

where $J = 1, 2, \dots, 100$ and defines the pressure from 0.01 mb to 1000 mb.

2. Other Input Data

The remaining input data required, having given the VTPR first guess sounding, includes the zenith angle, sea surface temperature, and clear-column radiances. This data, along with all of the verifying radiosondes and first guess temperature profiles to 10 mb was kindly provided by NESS in the form of an archival tape.

B. MATHEMATICAL DEVELOPMENT OF THE TEMPERATURE RETRIEVAL

Given a non-scattering atmosphere in thermodynamic equilibrium, the clear-column spectral radiance at the top of the atmosphere in each channel is related to the vertical temperature profile and the absorber mass structure by the RTE, Eq. 1.

The right hand side of Eq. 1 is composed of an earth's surface radiation term, and an atmospheric contribution which is integrated from the surface of the earth (1000 mb) to the top of the atmosphere (0.01 mb).

When the 100 J-levels developed in Eq. 27 are used, Eq. 1 can be rewritten

$$I_i = B_i[T(100)]\tau_i(100) + \int_{J=100}^{J=1} (B_i[T(J)] \frac{d\tau_i(J)}{dJ}) dJ \quad (28)$$

The Planck radiance function used in Eq. 28 at level J and in channel i is

$$B_i[T(J)] = \frac{(C1) * v_i^3}{C2 v_i \exp[\frac{1}{T(J)}] - 1} \quad (29)$$

where v_i is the wave number in channel i,

C1 is the constant 1.9061×10^{-5} erg cm² sec⁻¹ ster⁻¹, and

C2 is the constant 1.43868 cm °K.

In order to reduce the effect of truncation error in the integration function of the RTE, and increase overall stability, the 100-level atmosphere was reduced to a 33-layer atmosphere as shown in Fig. 8. In integrating the RTE over the 100 level atmosphere, Simpson's rule was applied over each sublayer K centered at the fractional J levels of the K-layered atmosphere (Fig. 8). The main virtue of the Simpson quadrature scheme using the weighting factors of 1, 4, 1 over each layer (e.g., J = 01, 02.5, 04), lies in the small discretization error, $(1.5)^5/90$ times the fourth derivative with respect to J of the integrand function of Eq. 28, in substitution of the finite summation for the Riemann integration. The determination of T

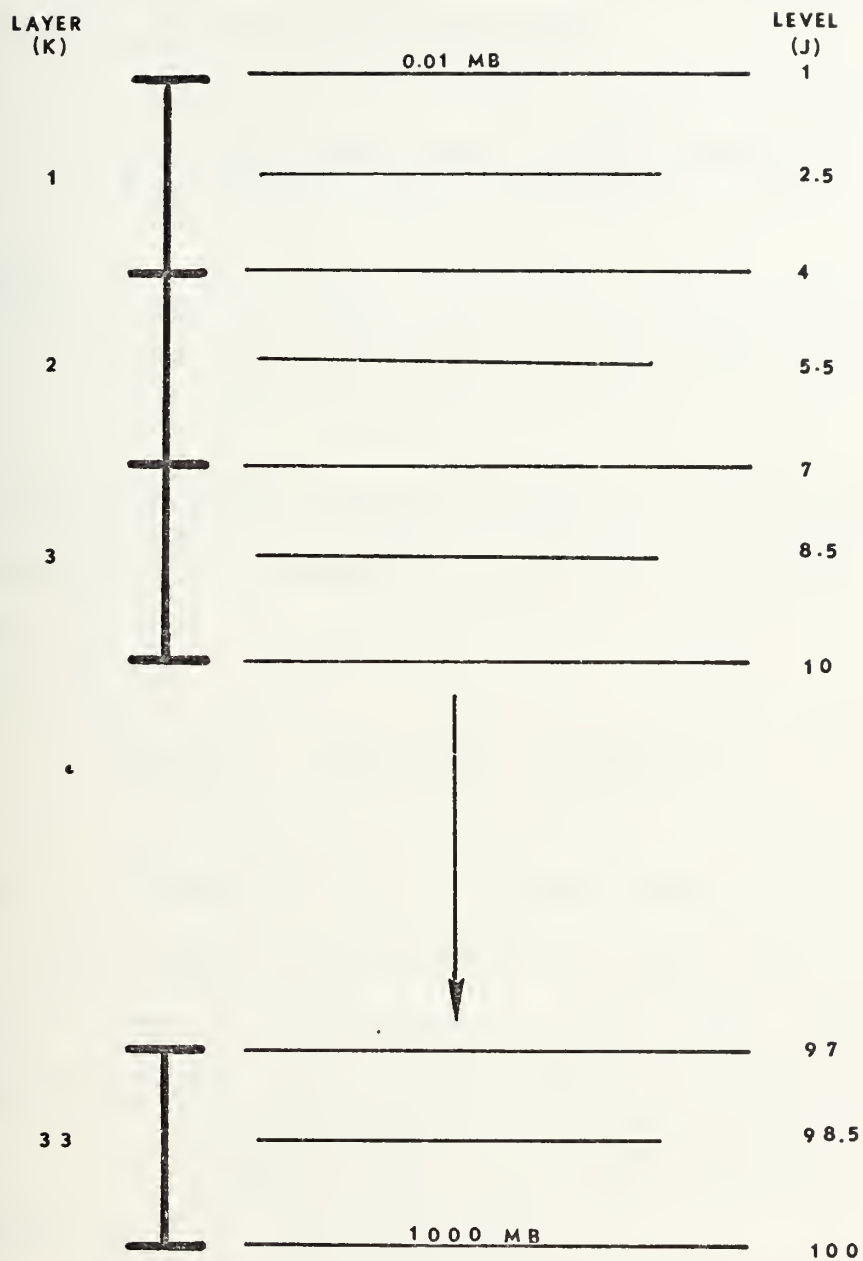


Figure 8. Thirty three K-layer atmosphere model used for the integration of the Radiative Transfer Equation.

at levels $J = 02.5$ etc., is accomplished by interpolation of the $T(P)$ using the $P^{2/7}$ pressure levels, defined by Eq. 27. Therefore, Eq. 28 can be rewritten

$$I_i = B_i [T(100)] \tau_i(100) + \sum_{K=1}^{33} \bar{B}_i(K) \Delta \tau_i(K) , \quad (30)$$

where

$$\bar{B}_i(K) = \frac{1}{6} \{ B_i [T(J_K - 1.5)] + 4B_i [T(K)] + B_i [T(J_K + 1.5)] \} \quad (31)$$

is the layer-mean Planck function for layer K employing Simpson's rule. Moreover $\Delta \tau_i(K)$ now spans three J levels (Fig. 8),

$$\Delta \tau_i(K) = \tau_i(J_K - 1.5) - \tau_i(J_K + 1.5) \quad (32)$$

where J_K is the value of J at the center of layer K .

Using the inversion method of Smith (1970) as modified by Martin (1974), the retrieval of mean layer temperatures is determined from clear-column radiance values as follows:

1. Determine the first guess radiance value in channel i , $I_i^{(1)}$, using Eq. 30.
2. Form the residual by comparing the clear-column radiance with the computed value from Eq. 30, using

$$R_i^{(1)} = I_{i-CLEAR} - I_i^{(1)} \quad (33)$$

3. If the residual is not close to zero the first guess temperature profile $T^{(1)}(P_{J_K})$ must be improved to $T^{(2)}(P_{J_K})$ in accordance with

$$B_i[T^{(2)}(P_{J_K})] = B_i[T^{(1)}(P_{J_K})] + R_i^{(1)} \quad (34)$$

This tends to move the temperature profile closer to the final desired convergent profile. If n steps are required to converge the residual close to zero, the final step is

$$B_i[T^{(n+1)}(P_{J_K})] = B_i[T^{(n)}(P_{J_K})] + R_i^{(n)} \quad (35)$$

where finally

$$\frac{R_i^{(n)}}{I_{i-CLEAR}} \leq 10^{-4} \quad (36)$$

When a convergent Planck function is determined for each channel, i , and at each level, J , the temperature at that level can be determined by solving Eq. 29 for $T(J)$. The value of the Planck function in this case must be a weighted-mean Planck using the six values of $B_i(J)$, $i = 1, 2, \dots, 6$, at each J -level. Figure 9 shows the values of transmittance in each of the six channels with respect to $P^{2/7}$, that is, with respect to the linear J -scale. Figure 10, the first derivative with respect to J of the transmittances in Fig. 9, is the

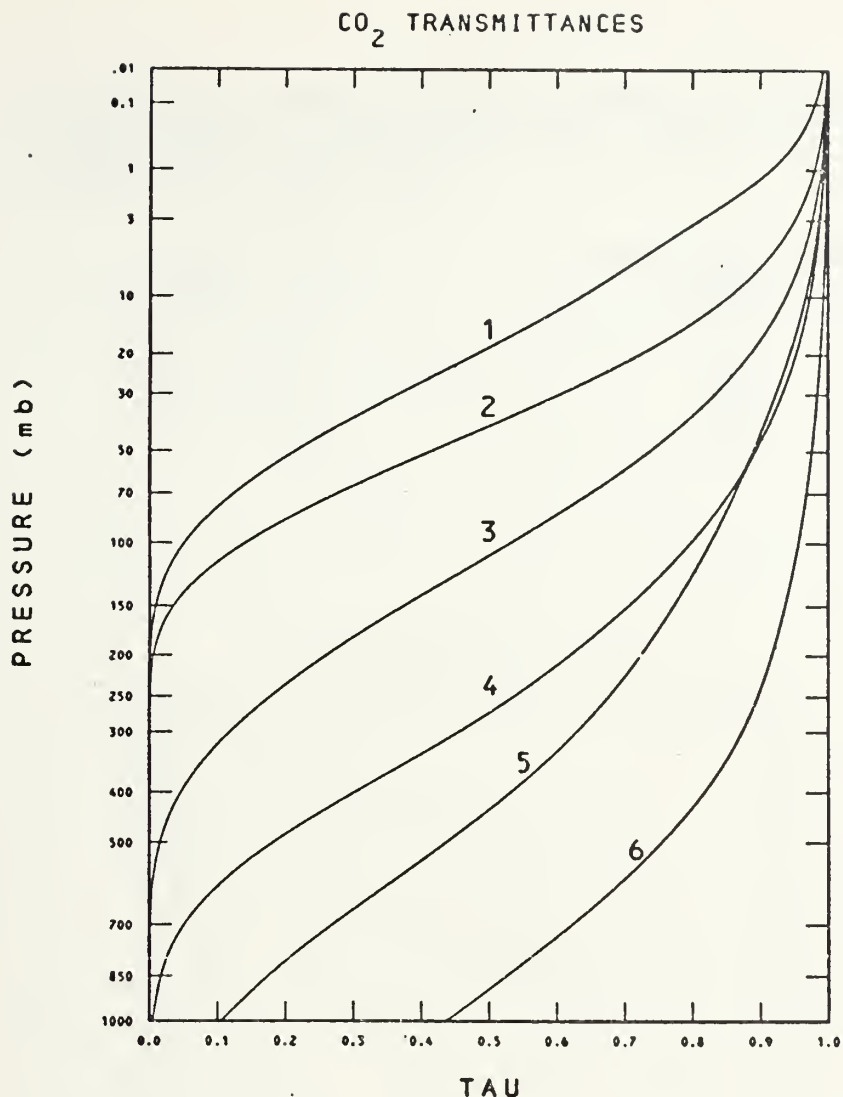


Figure 9. Carbon dioxide transmittances channels 1 through 6, after McMillin et al. (1973).

weighting function used in determining this weighted mean Planck. The usual procedure as used by Smith et al. (1972), involves the use of a constant normalized wave number ($\bar{\nu} = 700 \text{ cm}^{-1}$) in Eq. 37, whereas in this thesis, a normalized wave number, decreasing with decreasing values of pressure was found to give a more accurate result, similar to results of Moran (1974). By using this varying wave number (Table 4), advantage can be taken of the level of maximum contribution of

Table 4. Normalized wave numbers and corresponding pressure levels used in inverting the Planck function for temperature retrieval.

Pressure P(J) mb	Wave Number ($\bar{\nu}$) cm ⁻¹
1000 - 351	720
350 - 96	710
95 - 0.01	690

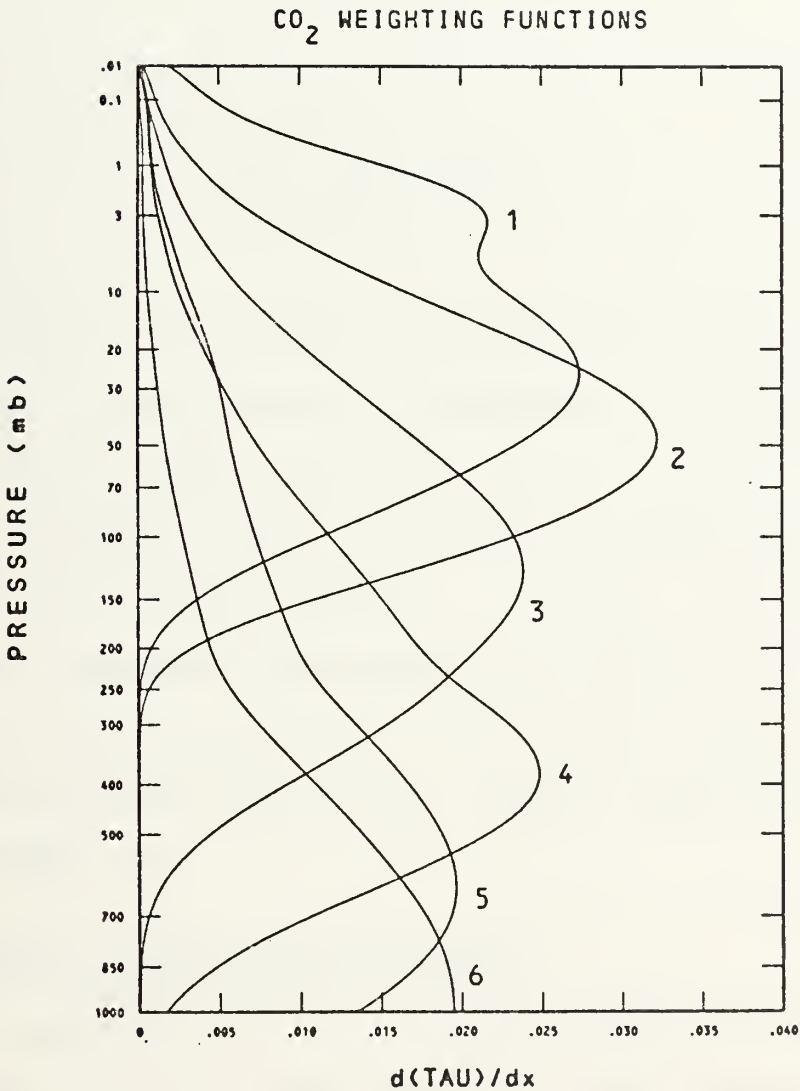


Figure 10. Weighting functions used in determining a weighted mean Planck function.

that channel to the derived equivalent blackbody temperature. The weighted mean Planck function then becomes

$$B^{(n)}[\bar{\nu}, T(J)] = \frac{\sum_{i=1}^6 B_i^{(n)}(J) \Delta\tau_i(J)}{\sum_{i=1}^6 \Delta\tau_i(J)} \quad (37)$$

By using this weighted Planck, the 100 mean temperatures, $\bar{T}(J)$, can be determined by the inversion of Eq. 29

$$\bar{T}(J) = \frac{C_2 \bar{\nu}}{\ln \left[\frac{C_1 \bar{\nu}^3 + B^{(n)}(\bar{\nu}, J)}{B^{(n)}(\bar{\nu}, J)} \right]} \quad (38)$$

In Eqs. 37 and 38, which are accomplished after the iteration procedure in each channel is complete, the values of $\Delta\tau_i(J)$ are centered differences taken over $\Delta J = 2$, but centered on each individual J level. A forward $\Delta\tau_i$ difference is used to initiate the process at level $J = 1$ and a backward difference is used to terminate the weighting process at $J = 100$. In this solution procedure, Eqs. 37, 38, the algorithm used is essentially after Smith et al. (1972), except for the use of the variable $\bar{\nu}$.

C. STEPWISE TEMPERATURE RETRIEVAL

The procedure for retrieving the layer-mean temperatures for layer $J = 1, 2, \dots, 100$, from the clear-column radiances can be summarized as follows (program names refer to the listing at the end of this thesis).

1. Input the necessary data.
 - a. sounding latitude.
 - b. zenith angle.
 - c. 15-level first guess temperatures.
 - d. sea surface temperature.
 - e. clear-column radiances in channels 1 to 6.
2. Expand the 15-level first guess temperature profile to 56 levels and merge it with climatology at the 10 mb level using subroutine UPPER.
3. Expand the 56-level temperature profile to 100 levels using Eq. 27 and subroutine LEVELL.
4. Calculate the atmospheric transmittance due to carbon dioxide in channels 1 through 6 at each level J using subroutine RDTEMP and adjust for the zenith angle by using subroutine MARTAU.
5. Calculate the water vapor content of the atmosphere in the form of a mixing ratio profile, one value at each level J, using function GOFF and Eqs. 7 and 8.
6. Use the mixing ratios to calculate the path corrected atmospheric transmittance due to water vapor in channels 1 through 6 at each level J using subroutine TRANW.
(Note: steps 5 and 6 were performed on the first iteration only, due to the small change in water vapor transmissivity from the first guess to the final temperature profile.)

7. Calculate the total atmospheric transmissivity in each channel and at each level through the product of Eq. 3 which uses path corrected values of transmittance due to carbon dioxide, water vapor, and ozone.

8. For the first iteration, using the 100-level first guess temperatures, the Planck functions must be calculated in each of the 6 channels.

a. Calculate the 100 J-level Planck functions using Eq. 29.

b. Calculate the 33 K-level Planck functions by fitting a fourth order Lagrangian polynomial to the 100 J-level Planck-profile [after Conte and deBoor (1965)].

9. Calculate the $\Delta\tau(J)$ for each channel in the 100 J-level and $\Delta\tau(K)$ for the 33 K-level atmospheres. The $\Delta\tau(K)$ will be used in the discretized form (Eq. 30) of the RTE, in order to reduce the truncation error associated with the finite summation, substituted for the Riemann integration of the integrand function in Eq. 28. This is important while dealing with the $\tau(J)$ values which occur before the temperature profile and its associated transmissivities have converged. The converged $\Delta\tau(J)$ will be used with Eq. 37 in producing the new 100-level temperature profile.

10. Compute the layer-mean Planck values by Eq. 31.

11. Compute the radiance in each channel using Eq. 30 and determine the residual difference between the clear-column radiance and the computed radiance, Eq. 33.

12. If the residual value is not close to zero, another iteration must be performed to improve the accuracy of the retrieved temperature profile.

a. Calculate the new 100-level and 33-level Planck functions by adding the residual to each previous value, Eq. 34.

b. Calculate the new 100-level temperature profile using Eqs. 37 and 38, and go back to step 4. Continue recycling until convergence is achieved (see Eq. 36).

13. If the residual is small enough (Eq. 36 is true), go directly to the calculation of the new 100-level temperature profile, Eqs. 37 and 38.

D. PROGRAM OUTPUT

The program is designed to produce a mean layer temperature profile at 100 levels from 1000 mb to 0.01 mb. For the purpose of testing the accuracy of these retrieved temperatures, additional inputs were needed.

First a set of radiosonde soundings, as close as possible to each retrieval site in latitude, longitude, and real time was read in. While these soundings are not considered to be the exact state of the atmosphere at the retrieval site, they are as close as possible and therefore were used to determine the error in the retrieval program at each level J by using

$$\text{ERROR}(J) = T(J) - AT(J) \quad (39)$$

where $T(J)$ is the retrieved temperature, and

$AT(J)$ is the radiosonde sounding temperature.

Secondly, a set of retrieved temperatures supplied from NESS for each case investigated was read in and compared with the radiosonde temperatures.

The program then output the following for each of the 233 retrievals attempted (see sample output following the program listing):

1. Station number (1,2,...,233)
2. Sounding zenith angle in degrees.
3. Station latitude.
4. The adjustment at 10 mb necessary to fit the first guess temperature profile to the climatological temperatures.
5. The number of iterations necessary for convergence.
6. Table of results, listing for each of the 15 levels:
 - a. Pressure
 - b. Retrieved temperature
 - c. Radiosonde sounding temperature
 - d. Error (retrieved - sounding)
 - e. NESS retrieved temperature
 - f. Error (NESS retrieved - sounding)

In order to easily compare the accuracy of the retrieval with the radiosonde data and also to compare the error of this method with that of NESS, histograms were drawn and statistical data were obtained. The errors were compared level for level on an overall basis (globally averaged) and also on a latitude-band basis for the latitude ranges shown in Table 5.

Table 5. Latitude bands used for error analysis of the VTPR retrieved temperatures.

<u>LATITUDE BAND</u>	<u>BAND WIDTH</u>
1	$0 \leq \text{LAT} < 20\text{N}$
2	$20\text{N} \leq \text{LAT} < 40\text{N}$
3	$40\text{N} \leq \text{LAT} < 60\text{N}$
4	$60\text{N} \leq \text{LAT}$

V. RESULTS OF THE VTPR TEMPERATURE RETRIEVAL

In general, the errors (retrieved temperature - radiosonde temperature) were less than 5 °K when averaged over the latitude-bands shown in Table 5. The errors also compared favorably with the results of the NESS VTPR retrieval in all 15 atmospheric levels and the four latitude bands. In calculating the errors, the assumption that the radiosondes matched the VTPR retrieval sites exactly in time and space was made. The difference, though small (averaging ± 0.6 degrees in latitude, ± 0.7 degrees in longitude, and ± 1.87 hours in time), coupled with the small data base of 233 retrievals, could have had some effect on the results and should be of some consideration.

A. GLOBAL RESULTS

The global mean results obtained here are summarized in Table 6 along with the averaged results from the NESS retrievals. The frequency distributions of the global error analysis at each of 15 key atmospheric levels are shown as a function of the error classes encountered (See Appendix A-1 to A-15). These frequency distributions, in the form of histograms, are included as a visual aid in analyzing the deviation of the error from the mean. They show that even though the range of errors can extend over as much as 20 °K, the probability of a relatively large error is much less than the probability of the small errors in the vicinity of the mean.

Table 6. Retrieved temperature error analysis on a global basis.

PRESSURE (mb)	RETRIEVAL		NESS		NO. OF SAMPLES
	MEAN ERROR (°K)	RMS ERROR	MEAN ERROR (°K)	RMS ERROR	
10	-0.55	4.00	-0.75	4.51	59
20	0.57	3.25	-0.11	2.72	112
30	-0.06	3.20	-0.17	3.12	142
50	0.37	3.20	-0.17	3.12	142
70	0.75	4.39	0.91	5.12	179
100	-0.45	3.89	-2.30	5.12	179
150	-0.30	2.58	-1.51	2.73	208
200	-0.66	3.33	-1.04	3.29	215
250	0.15	3.22	0.41	3.33	206
300	-0.58	2.82	0.24	2.70	223
400	-0.18	2.79	-0.09	2.07	226
500	-0.67	3.09	-0.32	2.13	227
700	-0.99	3.29	-0.86	2.81	226
850	-0.08	3.26	-0.31	3.55	227
1000	-0.24	1.77	0.26	3.89	196

B. LATITUDE BAND RESULTS

Because of space limitations, frequency distributions were not included for the latitude band results. However, Table 7 furnishes a summary of the latitude band analysis of errors including their root mean square errors along with the corresponding NESS results.

Table 7. Retrieved temperature error analysis on a latitude band basis (including the corresponding NESS results in parentheses). For each level in each latitude band the listings are:
 mean error in °K
 root mean square error
 sample size

PRESSURE (mb)	LATITUDE BANDS IN DEGREES NORTH				
	0 - 19.9	20 - 39.9	40 - 59.9	>60	
10	-2.10(-3.54) 4.00(5.16) 13	-0.62(1.54) 4.87(5.54) 18	0.58(0.91) 3.78(3.66) 21	-0.91(2.47) 2.05(4.37) 7	
20	-1.22(-2.43) 2.73(3.32) 18	1.54(0.11) 3.26(2.50) 36	1.29(1.02) 3.37(2.48) 44	-1.88(-1.25) 3.60(3.47) 14	
30	0.95(0.15) 2.73(3.32) 22	1.28(1.77) 3.26(2.50) 45	-0.34(-5.46) 3.37(6.48) 56	-1.88(-1.25) 4.61(4.94) 19	
50	4.48(4.50) 5.59(5.81) 23	1.56(2.99) 3.46(4.18) 60	-0.75(-0.89) 2.85(2.96) 73	-3.53(-4.03) 4.23(6.10) 23	
70	1.00(8.48) 3.49(9.09) 23	1.64(3.14) 3.49(4.34) 60	-0.89(-1.30) 3.02(3.40) 73	-3.55(-5.43) 4.25(5.99) 23	

Table 7 (Continued)

LATITUDE BANDS IN DEGREES NORTH

PRESSURE (mb)	0 - 19.9	20 - 39.9	40 - 59.9	>60
100	2.93(1.08) 4.87(3.32) 27	-0.66(0.54) 2.96(3.13) 64	-1.80(-4.03) 3.52(5.02) 86	-4.62(-7.41) 5.38(7.86) 24
150	1.09(-0.30) 3.01(1.84) 29	0.73(-1.24) 2.75(2.92) 66	-1.21(-2.13) 2.27(2.92) 89	-1.38(-1.47) 2.64(2.42) 24
200	-0.09(-1.12) 2.12(2.09) 31	-0.81(-2.46) 3.77(3.39) 69	-0.82(-0.47) 3.49(3.38) 91	-0.33(1.00) 2.69(2.43) 24
250	-0.12(-0.51) 2.10(1.73) 29	-0.42(-1.18) 3.19(3.15) 66	0.46(1.37) 3.47(3.59) 88	0.96(2.43) 3.69(4.36) 23
300	0.07(-1.11) 2.43(2.13) 32	0.35(-0.83) 2.68(2.82) 71	-0.24(1.21) 2.83(2.71) 94	0.15(1.32) 2.98(3.08) 26

Table 7 (Continued)

LATITUDE BANDS IN DEGREES NORTH

PRESSURE (mb)	0 - 19.9	20 - 39.9	40 - 59.9	>60
400	-0.44(-0.50) 1.53(1.33) 33	-0.09(-0.12) 2.58(2.14) 73	-0.43(0.04) 3.19(2.32) 94	0.77(-0.01) 3.15(1.70) 26
500	-0.07(0.80) 1.71(1.56) 33	-0.79(-0.30) 2.68(2.17) 73	-1.06(-0.54) 3.44(2.22) 95	0.34(-0.92) 4.15(2.98) 26
700	-0.91(0.64) 1.95(1.92) 34	-1.19(-0.42) 2.64(2.53) 70	-1.33(-1.47) 3.87(3.36) 97	0.70(-1.88) 4.09(3.04) 26
850	0.57(2.27) 2.44(3.10) 34	0.20(0.94) 2.64(2.94) 70	-0.45(-1.18) 3.86(3.35) 97	-0.30(-3.81) 4.19(5.69) 26
1000	0.57(1.71) 1.11(2.91) 33	-0.36(1.08) 2.19(3.25) 64	-0.55(-0.69) 1.65(3.74) 80	0.11(-3.68) 1.76(7.26) 19

VI. CONCLUSIONS

The first objective of this thesis was to incorporate the state-of-the-art methods [as used by Fritz et al. (1972)] in calculating atmospheric transmittances, into the retrieval scheme. The method involved here for calculating the effects of water vapor, ozone, and carbon dioxide transmittance proved to be satisfactory. This, coupled with the inclusion of a 33 level integration scheme and the use of a variable wave number, as opposed to the constant $\bar{\nu} = 700 \text{ cm}^{-1}$, combined to give results comparable to those of NESS.

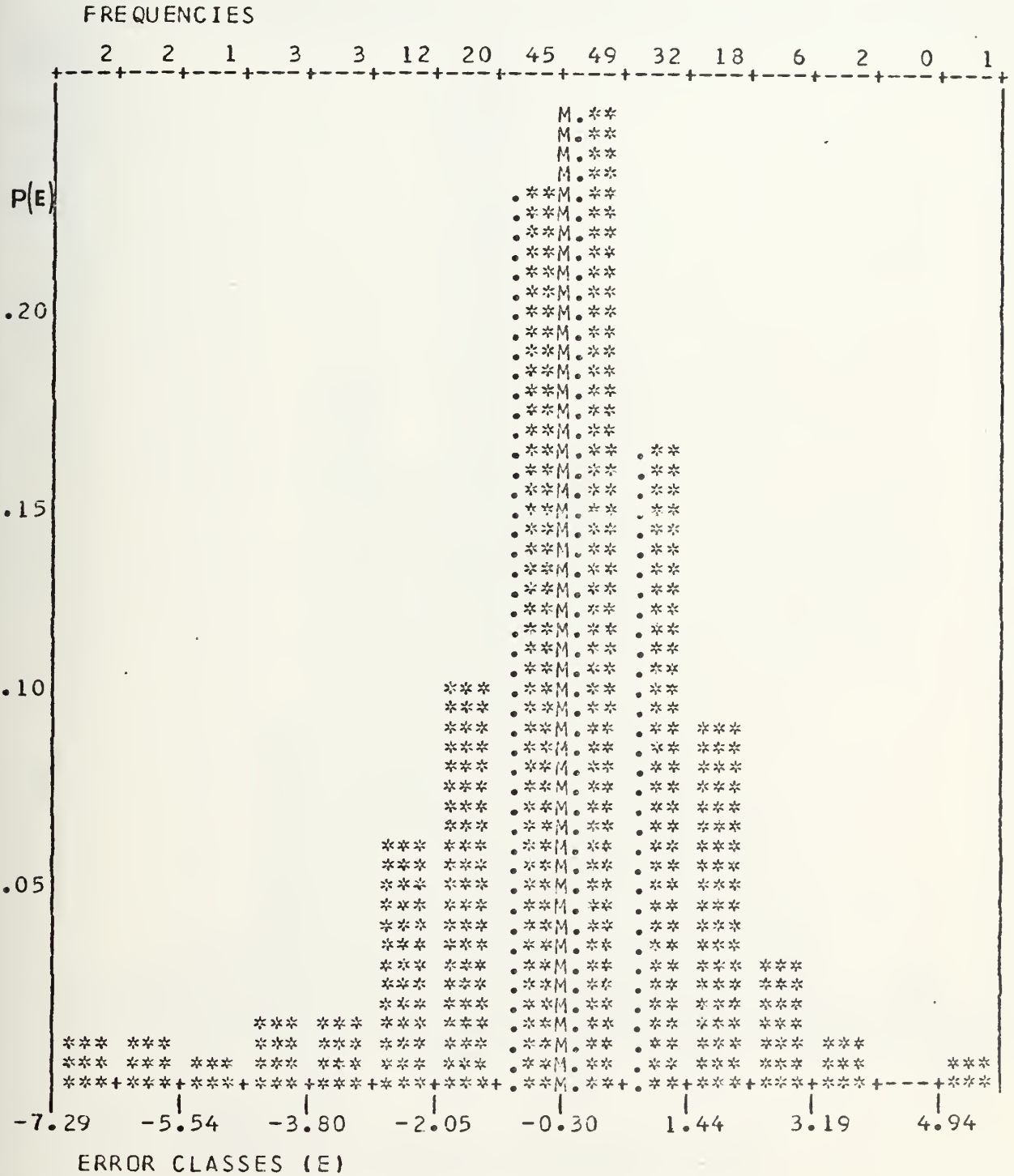
The temperature profile convergence occurred after an average of 5 iterations. While this is an improvement over the Moran (1974) model, as would be expected with the more sophisticated procedures incorporated, the number of iterations required would possibly be reduced further through the use of a more accurate first guess temperature profile. Gelman et al. (1972) used a regression technique for estimating the first guess temperatures above 10 mb, as opposed to merging with the standard atmosphere climatology as used here. Since this regression technique of Gelman produces a more accurate first guess temperature profile, it would reduce the number of iterations required for convergence even further. However this program was not available locally for inclusion in this thesis.

The second objective, that of evaluation through comparison with matching radiosondes, showed that the retrieval system produced errors that were comparable to NESS retrievals, or better, especially in the area of the tropopause. The small data base of 233 soundings is not considered large enough to evaluate the accuracy of the retrieval system beyond that, and more experimentation with a larger sample, and inclusion of the Gelman regression technique is required.

It is concluded that this thesis has demonstrated a consistent and accurate means of temperature profile retrieval from VTPR clear-column radiance data.

APPENDIX A-1

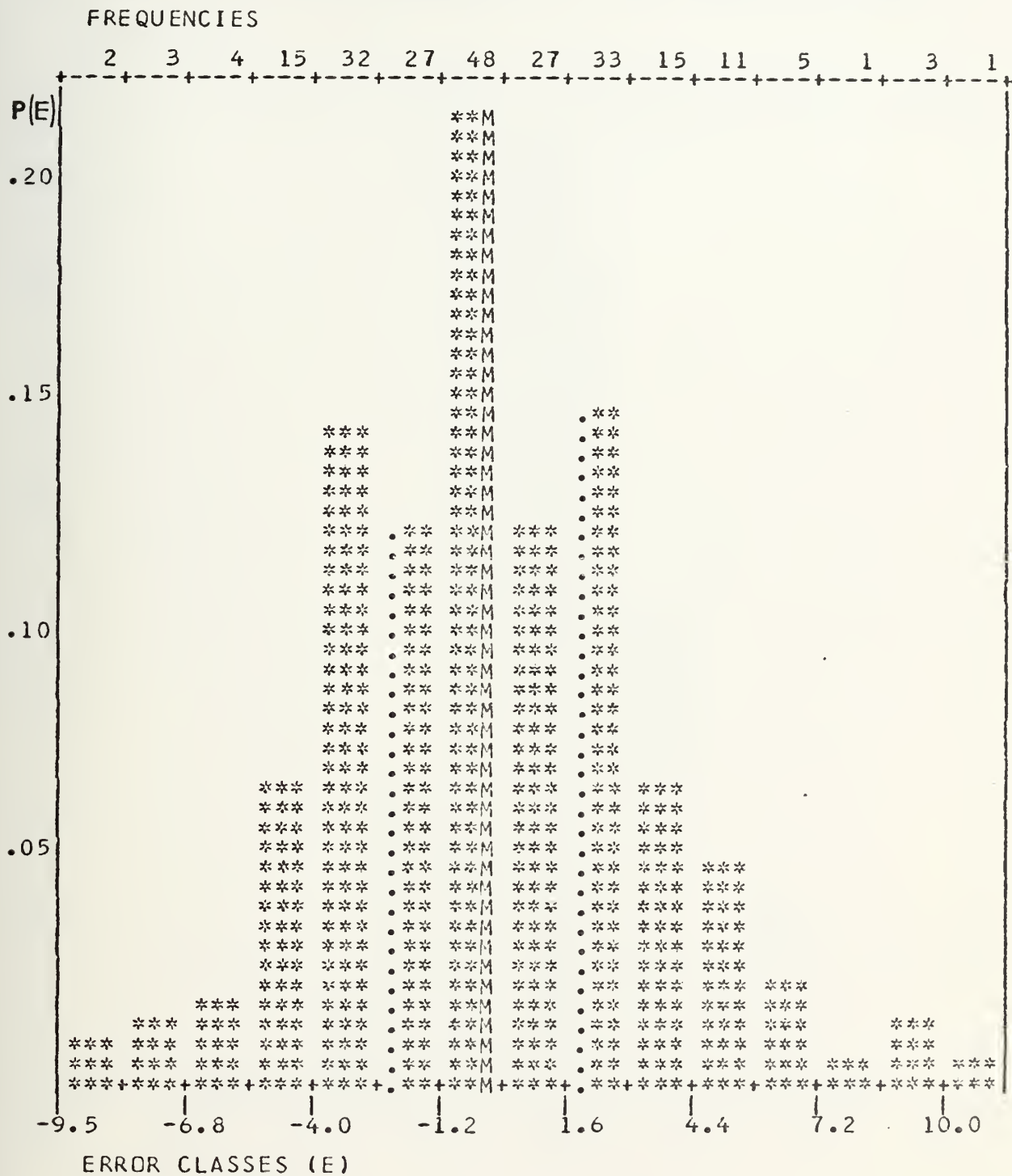
Histogram of the globally averaged errors showing probability distribution $[P(E)]$ of the occurrence of the errors, the actual error frequencies in the error class E (marked along the top), the Mean (M), and the Quartiles (\cdot), for sample size 196.



1000 MB HISTOGRAM FOR GLOBALLY AVERAGED ERRORS

APPENDIX A-2

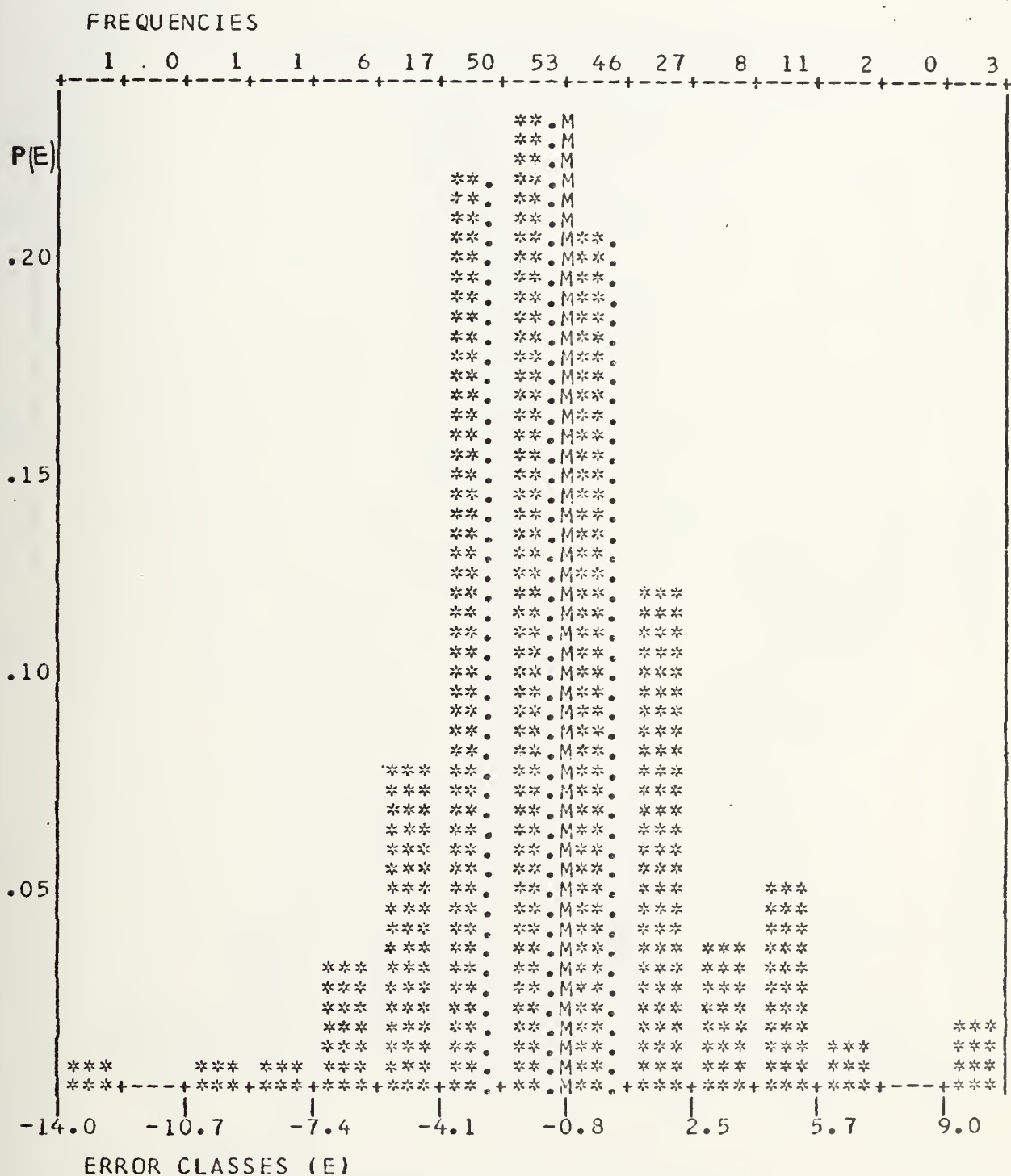
Histogram of the globally averaged errors showing probability distribution $[P(E)]$ of the occurrence of the errors, the actual error frequencies in the error class E (marked along the top), the Mean (M), and the Quartiles (\cdot), for sample size 227.



850 MB HISTOGRAM FOR GLOBALLY AVERAGED ERRORS

APPENDIX A-3

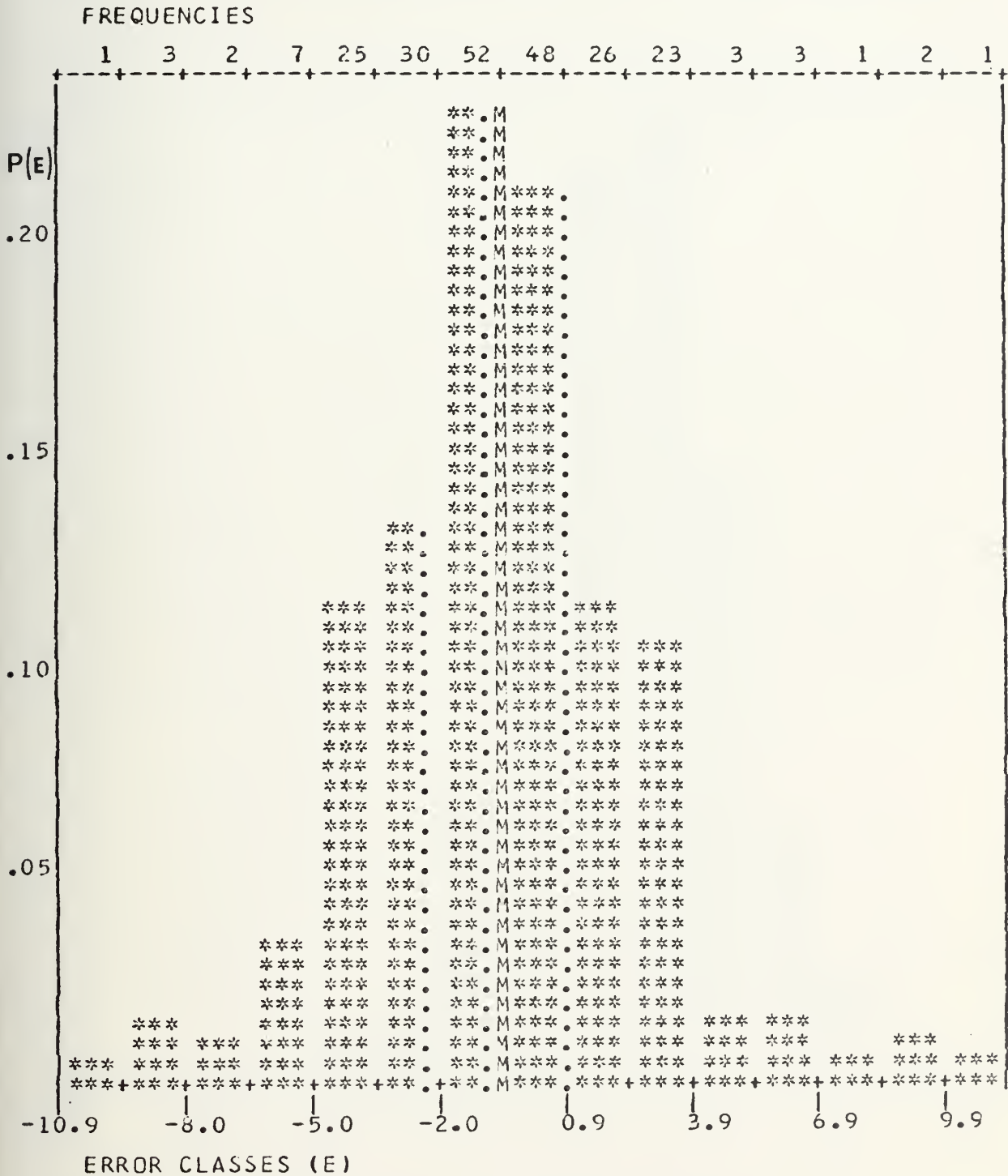
Histogram of the globally averaged errors showing probability distribution $[P(E)]$ of the occurrence of the errors, the actual error frequencies in the error class E (marked along the top), the Mean (M), and the Quartiles (\cdot), for sample size 226.



700 MB HISTOGRAM FOR GLOBALLY AVERAGED ERRORS

APPENDIX A-4

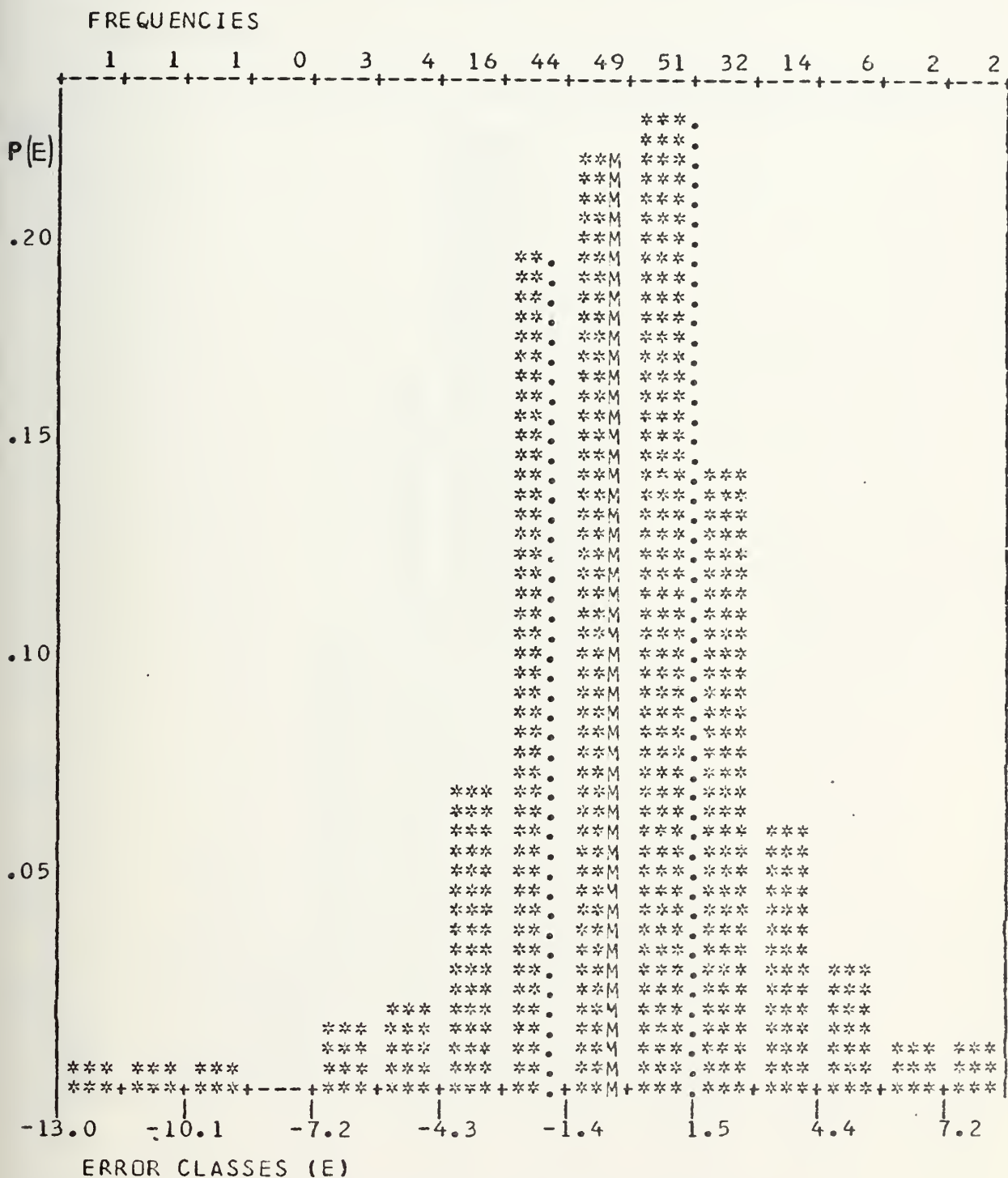
Histogram of the globally averaged errors showing probability distribution $P(E)$ of the occurrence of the errors, the actual error frequencies in the error class E (marked along the top), the Mean (M), and the Quartiles (\cdot), for sample size 227.



500 MB HISTOGRAM FOR GLOBALLY AVERAGED ERRORS

APPENDIX A-5

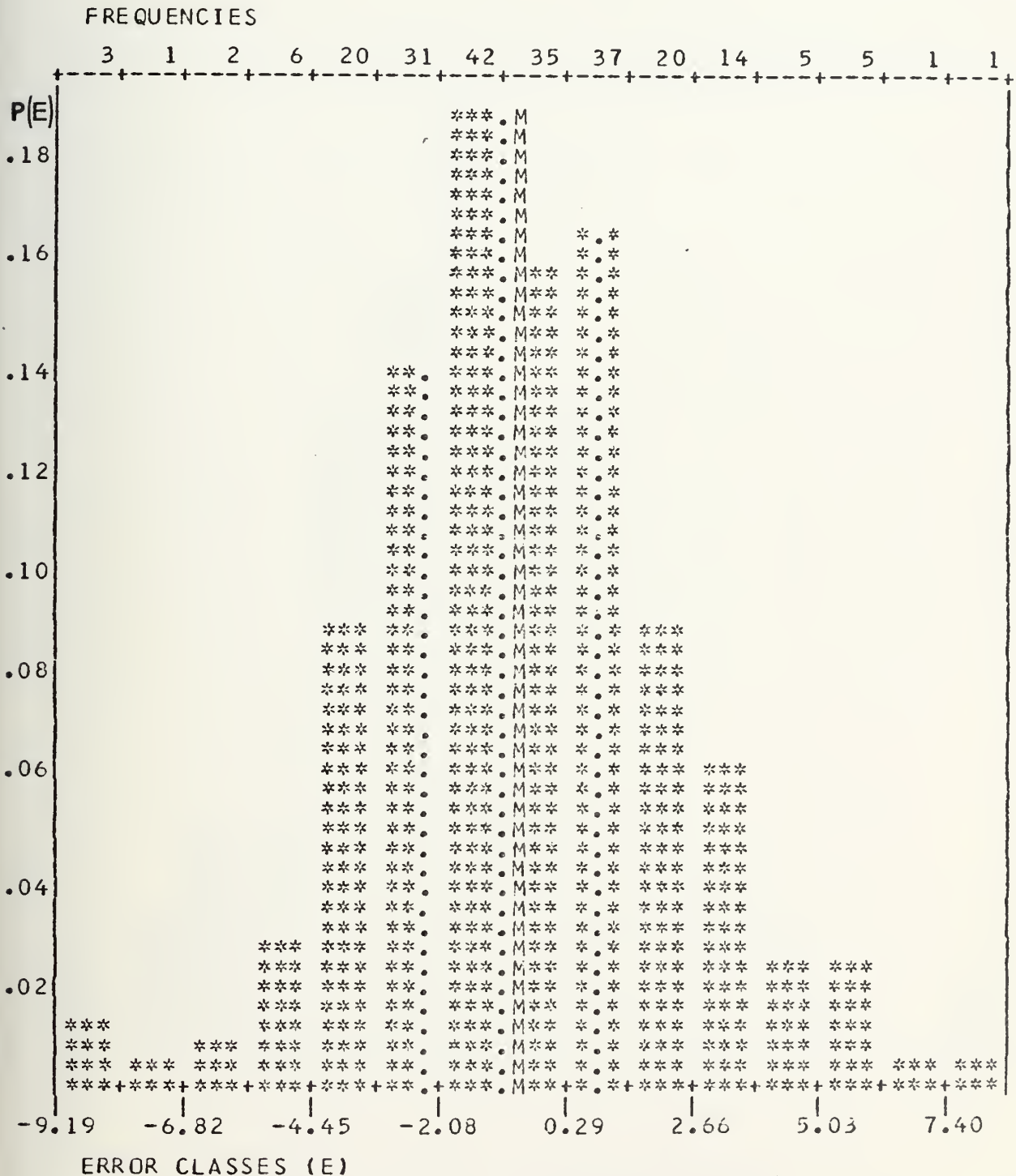
Histogram of the globally averaged errors showing probability distribution $[P(E)]$ of the occurrence of the errors, the actual error frequencies in the error class E (marked along the top), the Mean (M), and the Quartiles (\cdot), for sample size 226.



400 MB HISTOGRAM FOR GLOBALLY AVERAGED ERRORS

APPENDIX A-6

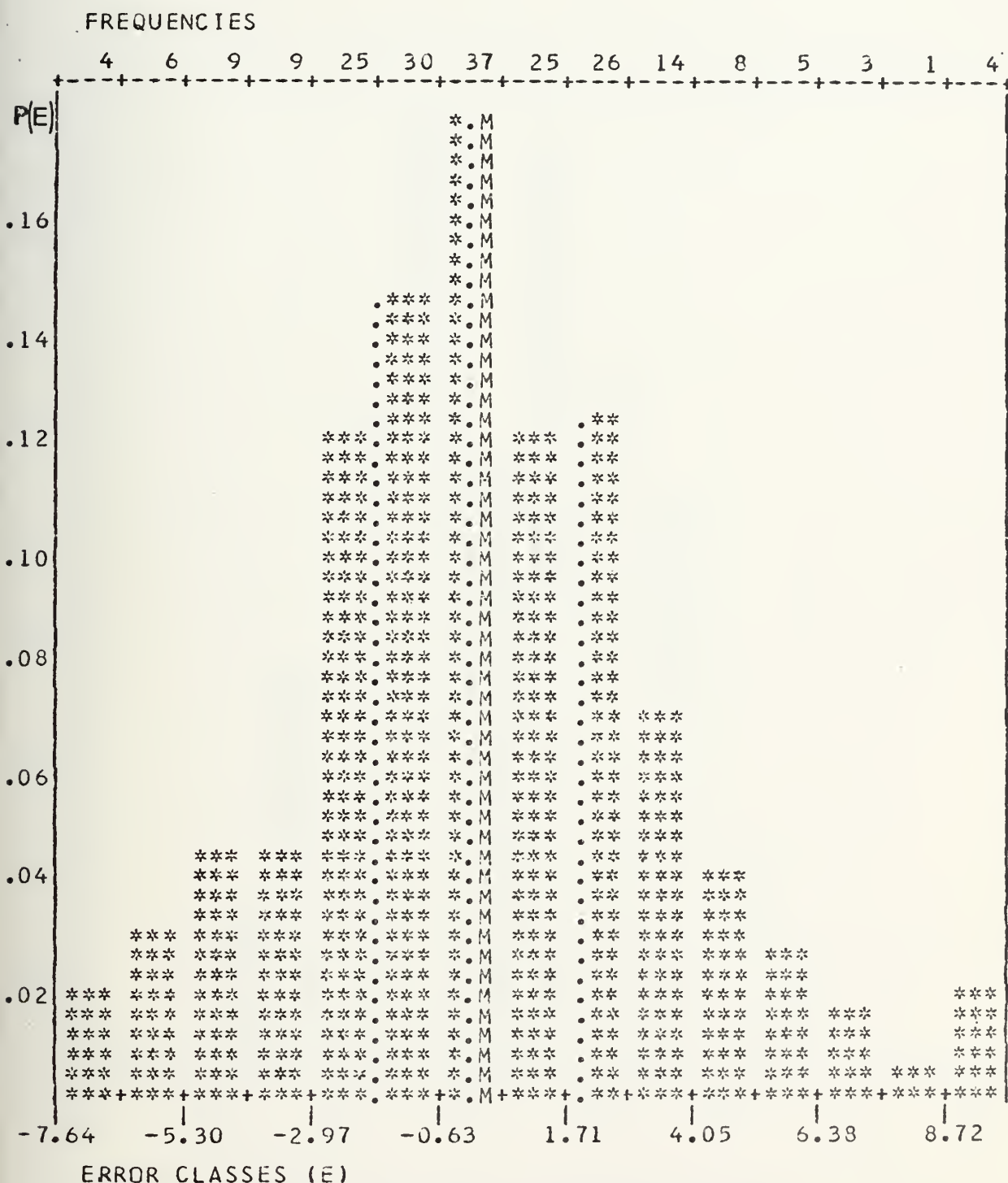
Histogram of the globally averaged errors showing probability distribution $[P(E)]$ of the occurrence of the errors, the actual error frequencies in the error class E (marked along the top), the Mean (M), and the Quartiles (\cdot), for sample size 223.



300 MB HISTOGRAM FOR GLOBALLY AVERAGED ERRORS

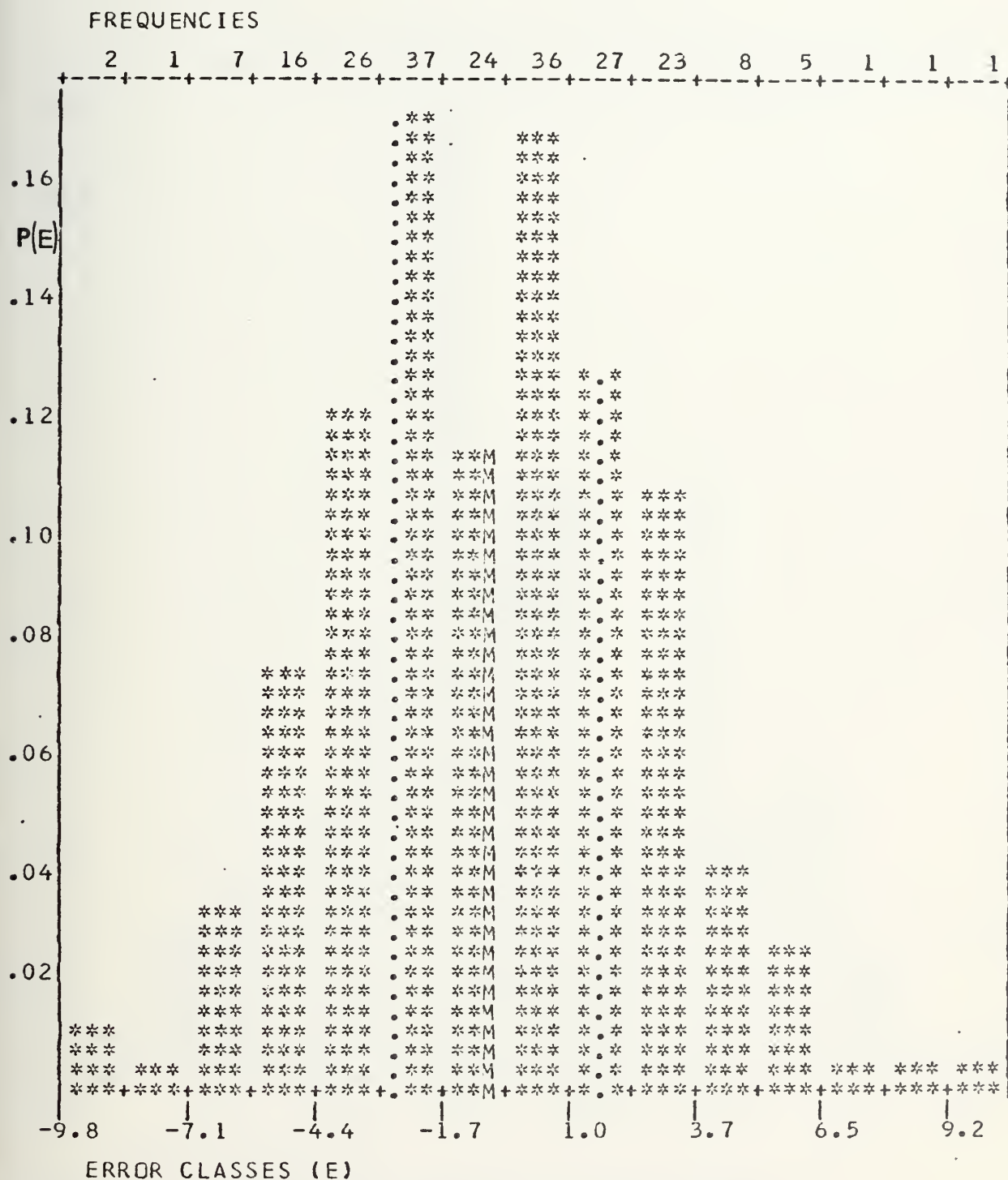
APPENDIX A-7

Histogram of the globally averaged errors showing probability distribution $P(E)$ of the occurrence of the errors, the actual error frequencies in the error class E (marked along the top), the Mean (M), and the Quartiles (\cdot), for sample size 206.



APPENDIX A-8

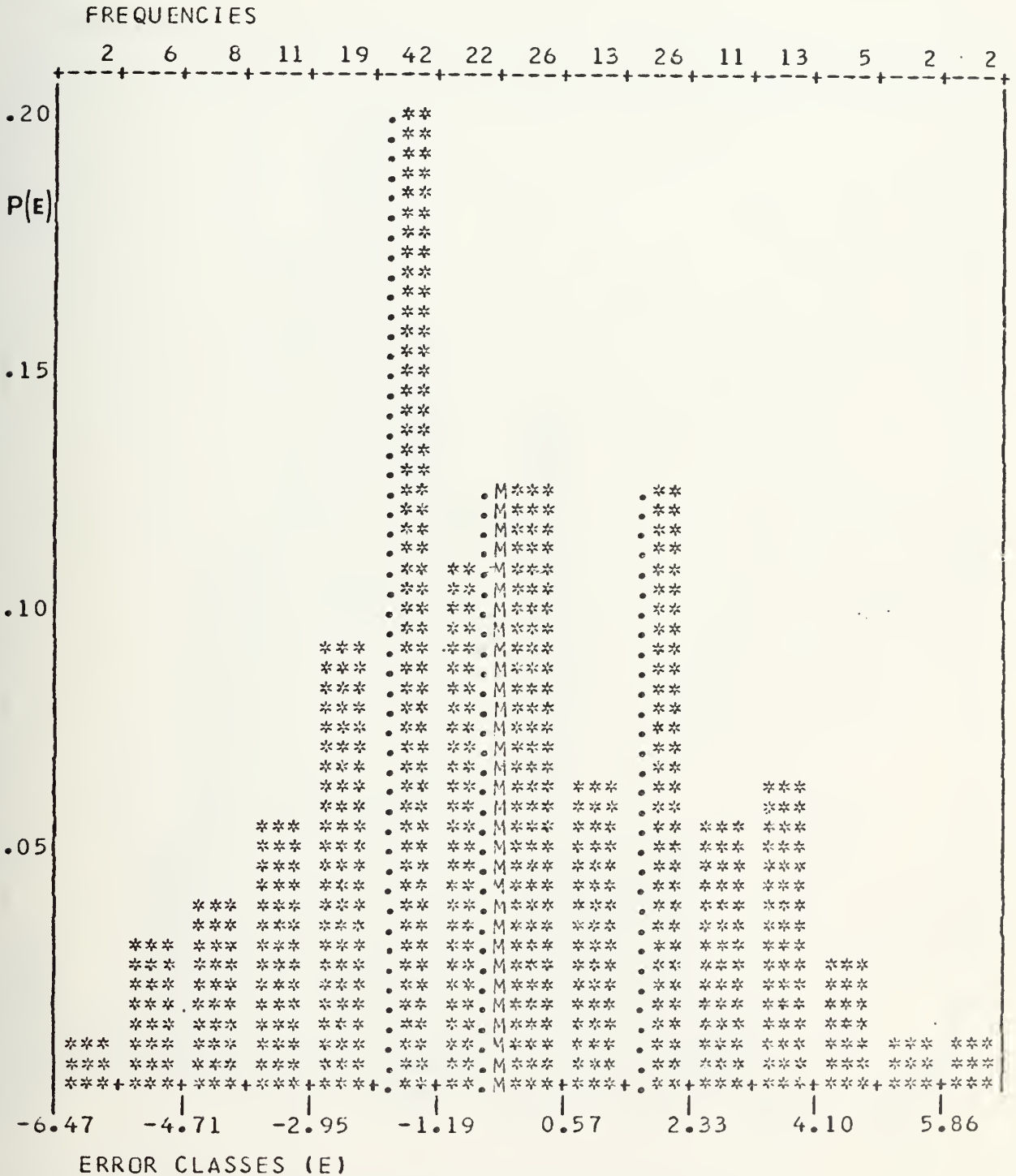
Histogram of the globally averaged errors showing probability distribution $[P(E)]$ of the occurrence of the errors, the actual error frequencies in the error class E (marked along the top), the Mean (M), and the Quartiles (\cdot), for sample size 215.



200 MB HISTOGRAM FOR GLOBALLY AVERAGED ERRORS

APPENDIX A-9

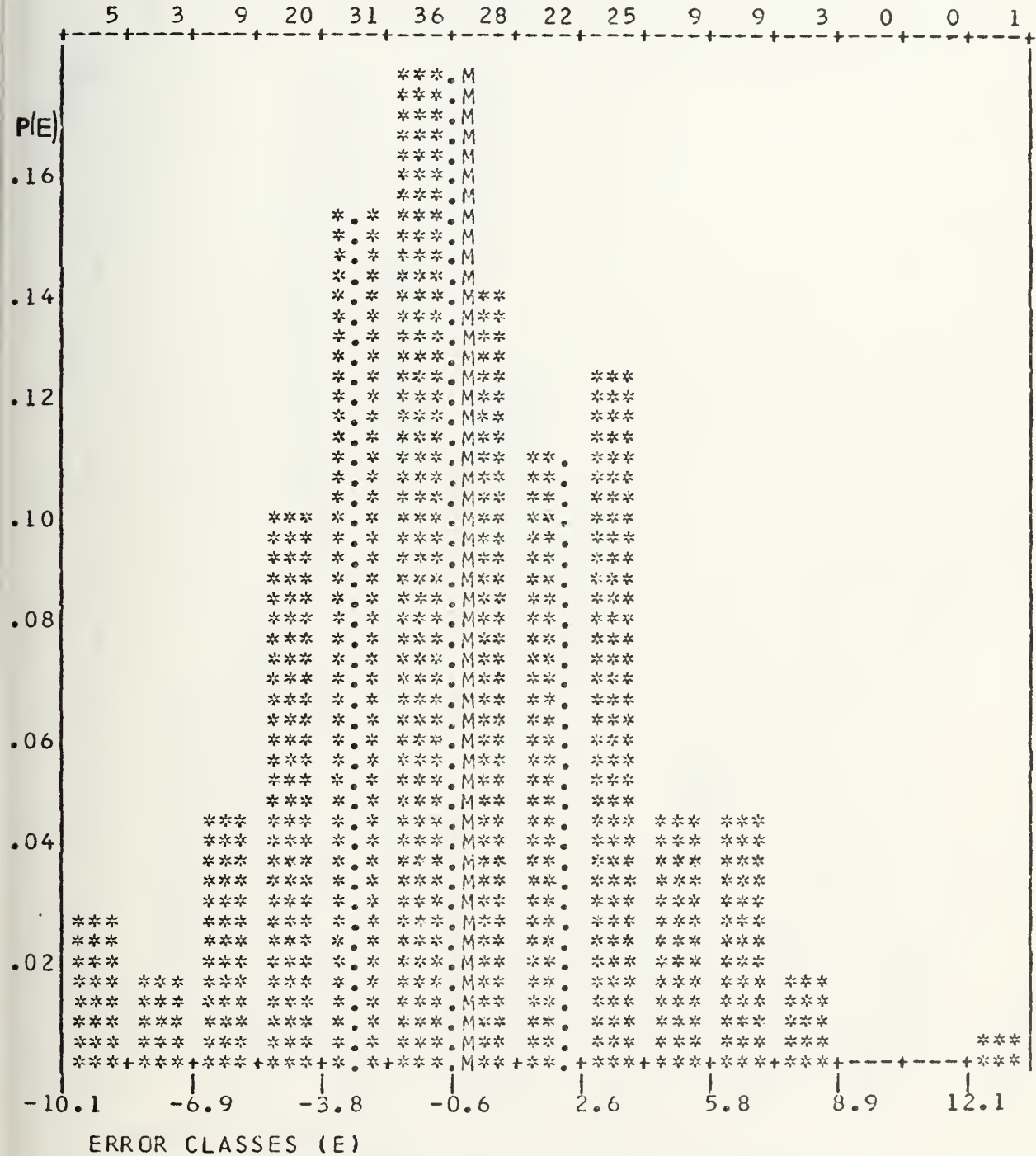
Histogram of the globally averaged errors showing probability distribution $P(E)$ of the occurrence of the errors, the actual error frequencies in the error class E (marked along the top), the Mean (M), and the Quartiles (\cdot), for sample size 208.



APPENDIX A-10

Histogram of the globally averaged errors showing probability distribution $P(E)$ of the occurrence of the errors, the actual error frequencies in the error class E (marked along the top), the Mean (M), and the Quartiles (\cdot), for sample size 179.

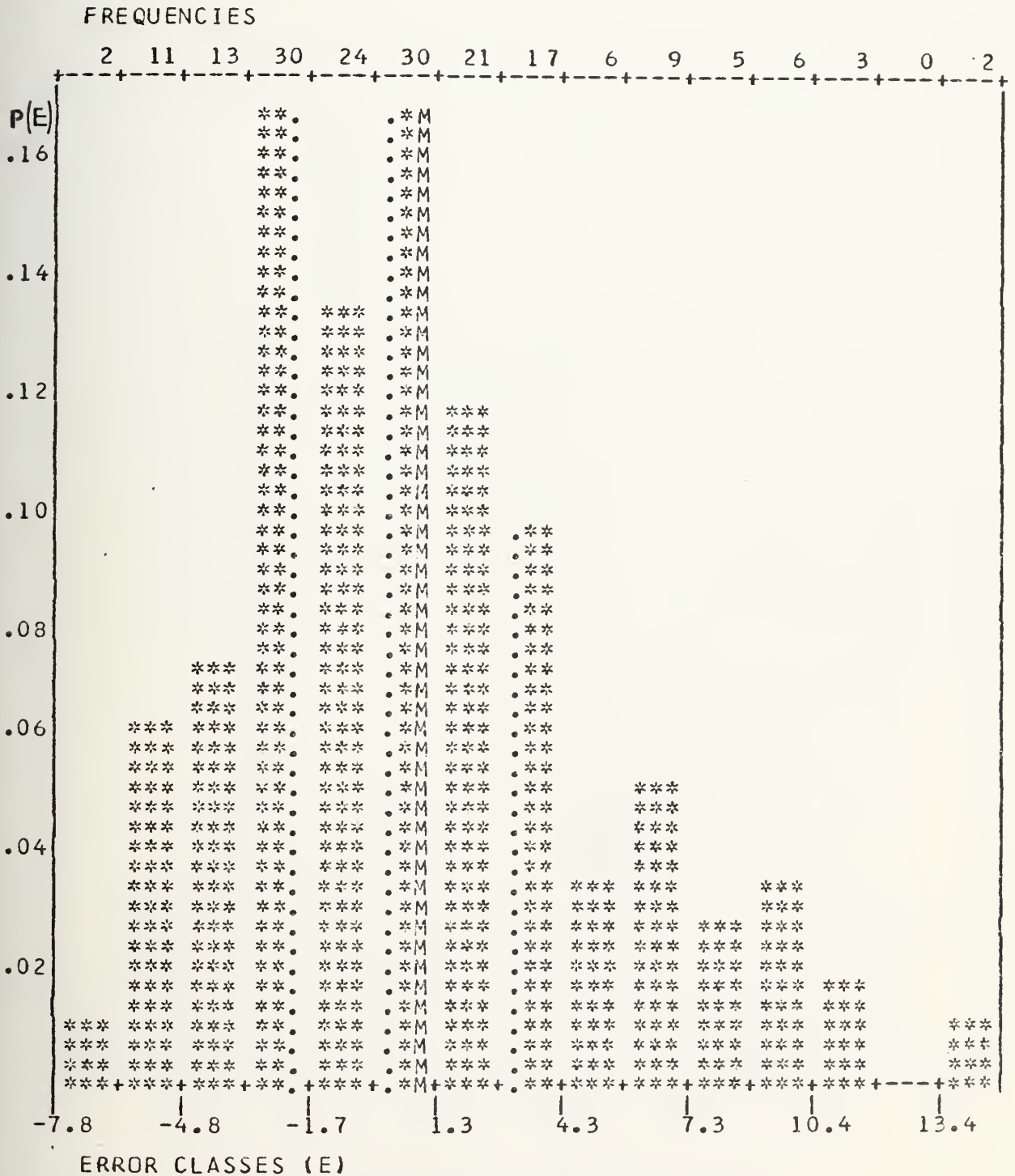
FREQUENCIES



100 MB HISTOGRAM FOR GLOBALLY AVERAGED ERRORS

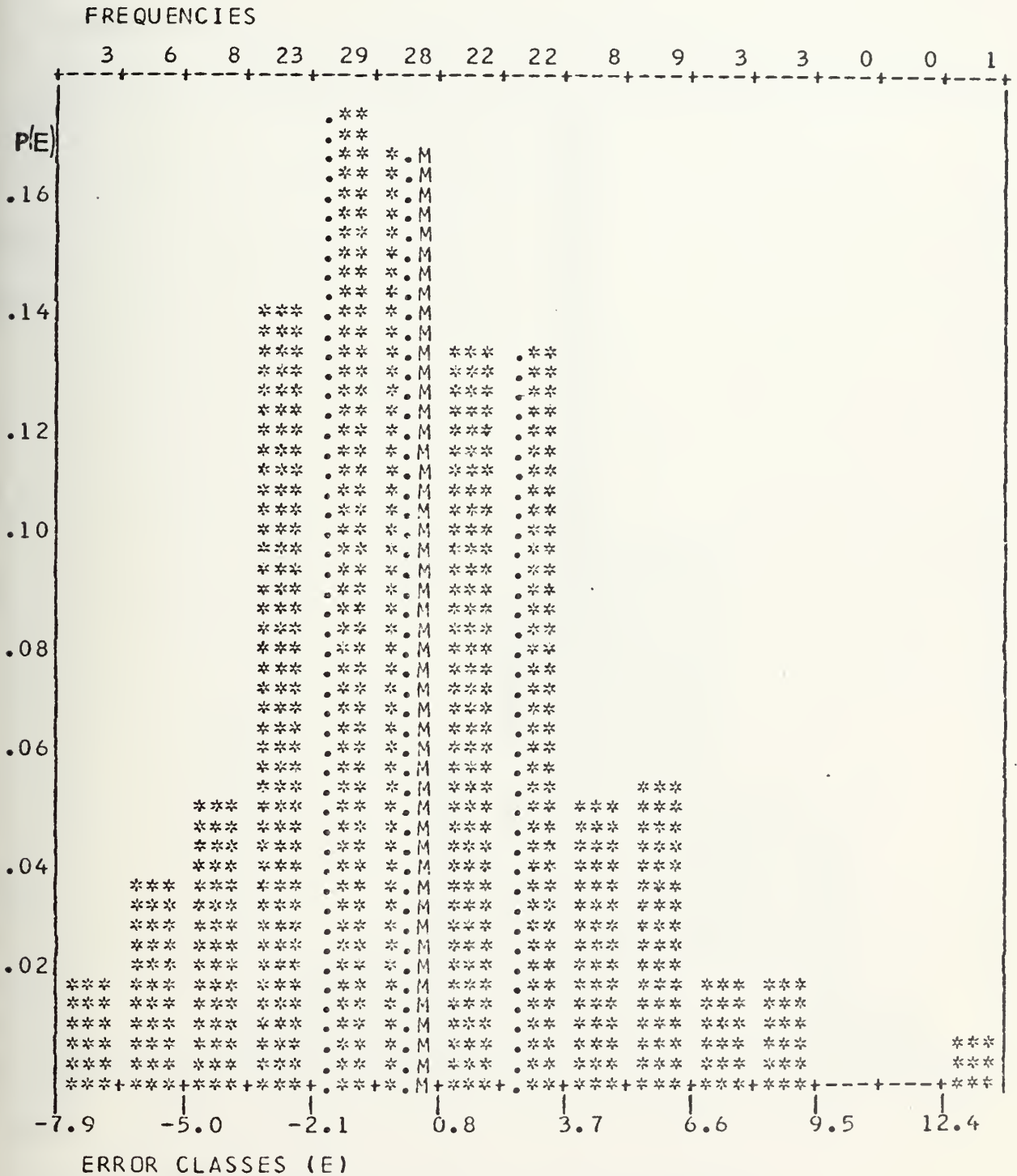
APPENDIX A-11

Histogram of the globally averaged errors showing probability distribution $P(E)$ of the occurrence of the errors, the actual error frequencies in the error class E (marked along the top), the Mean (M), and the Quartiles (\cdot), for sample size 179.



APPENDIX A-12

Histogram of the globally averaged errors showing probability distribution $[P(E)]$ of the occurrence of the errors, the actual error frequencies in the error class E (marked along the top), the Mean (M), and the Quartiles (\cdot), for sample size 142.

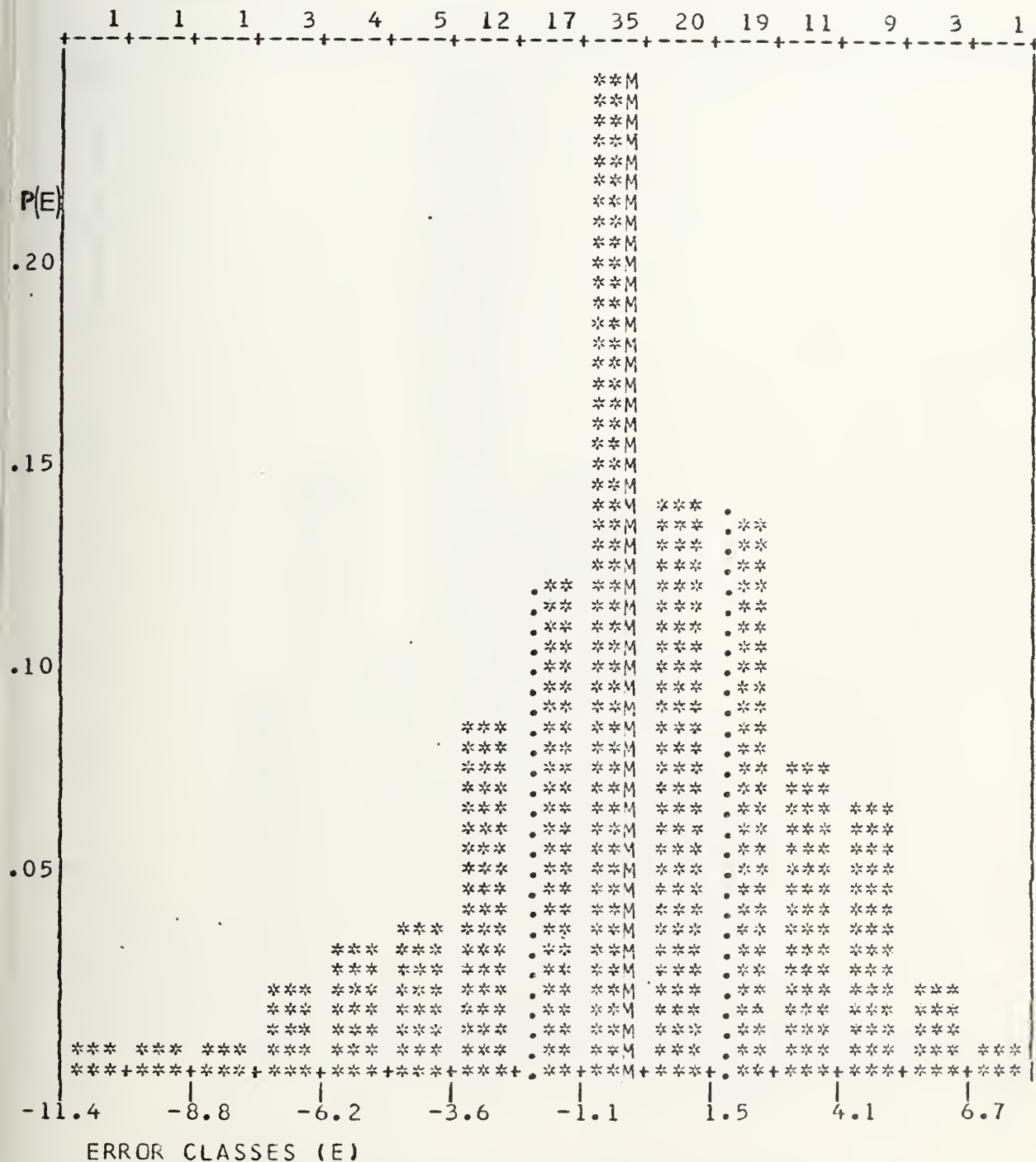


50 MB HISTOGRAM FOR GLOBALLY AVERAGED ERRORS

APPENDIX A-13

Histogram of the globally averaged errors showing probability distribution $P(E)$ of the occurrence of the errors, the actual error frequencies in the error class E (marked along the top), the Mean (M), and the Quartiles (\cdot), for sample size 142.

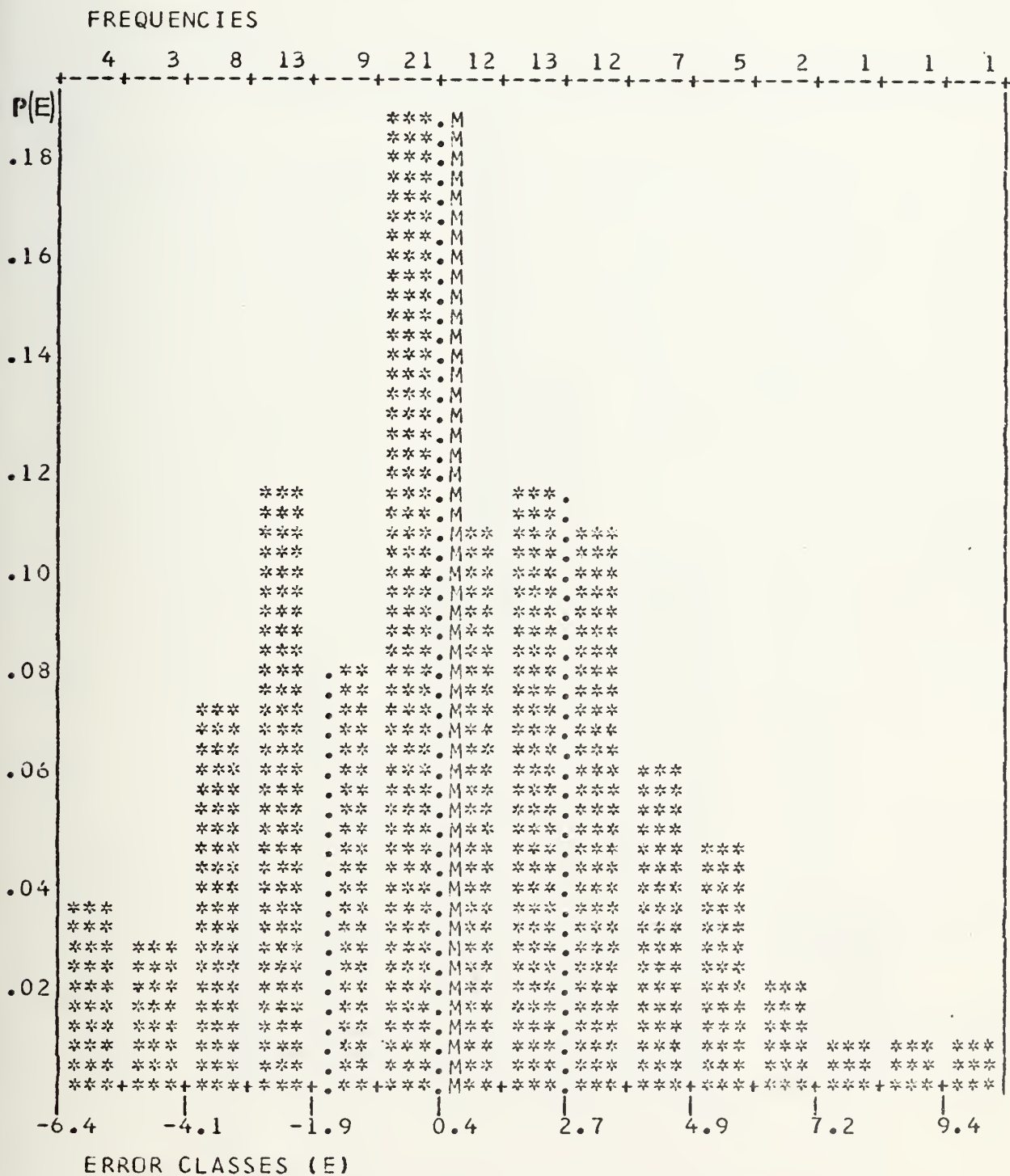
FREQUENCIES



30 MB HISTOGRAM FOR GLOBALLY AVERAGED ERRORS

APPENDIX A-14

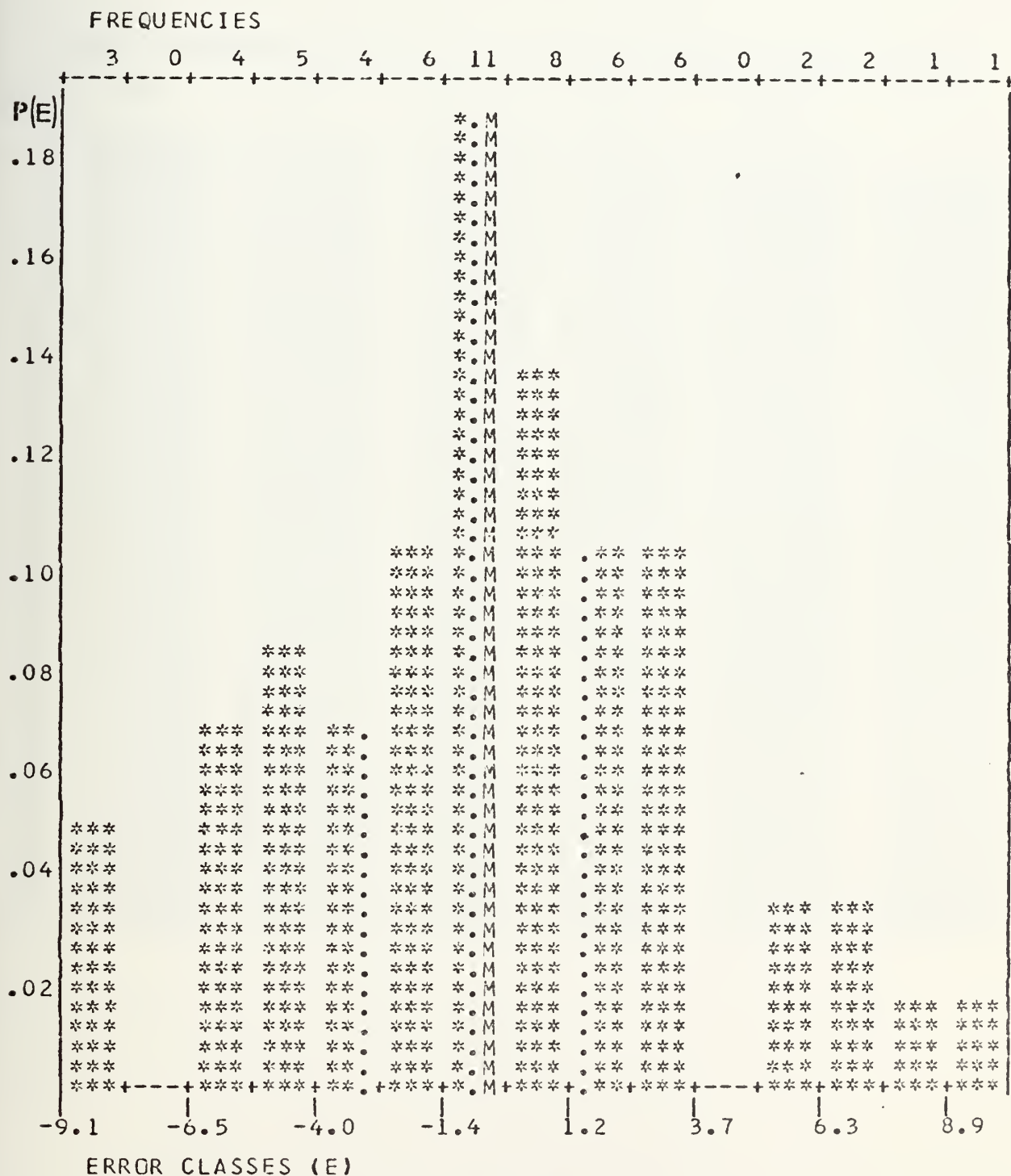
Histogram of the globally averaged errors showing probability distribution $[P(E)]$ of the occurrence of the errors, the actual error frequencies in the error class E (marked along the top), the Mean (M), and the Quartiles (\cdot), for sample size 112.



20 MB HISTOGRAM FOR GLOBALLY AVERAGED ERRORS

•

Histogram of the globally averaged errors showing probability distribution $[P(E)]$ of the occurrence of the errors, the actual error frequencies in the error class E (marked along the top), the Mean (M), and the Quartiles (\cdot), for sample size 59.



10 MB HISTOGRAM FOR GLOBALLY AVERAGED ERRORS

APPENDIX B

OZONE TRANSMITTANCES FOR THE SIX VTPR CLEAR-COLUMN CHANNELS

LEVEL	CHAN 1	CHAN 2	CHAN 3	CHAN 4	CHAN 5	CHAN 6
1	0.999992	0.999987	0.999986	0.999987	0.999991	0.999992
2	0.999982	0.999974	0.999972	0.999968	0.999974	0.999985
3	0.999966	0.999953	0.999949	0.999940	0.999949	0.999971
4	0.999941	0.999917	0.999914	0.999900	0.999912	0.999943
5	0.999906	0.999865	0.999866	0.999844	0.999857	0.999914
6	0.999859	0.999795	0.999804	0.999771	0.999780	0.999869
7	0.999797	0.999703	0.999725	0.999679	0.999679	0.999810
8	0.999717	0.999586	0.999626	0.999565	0.999551	0.999734
9	0.999618	0.999440	0.999504	0.999425	0.999392	0.999640
10	0.999497	0.999263	0.999358	0.999253	0.999198	0.999525
11	0.999352	0.999051	0.999183	0.999059	0.998967	0.999385
12	0.999182	0.998802	0.998979	0.998826	0.998694	0.999223
13	0.998982	0.998510	0.998742	0.998554	0.998375	0.999032
14	0.998748	0.998172	0.998466	0.998239	0.998006	0.998810
15	0.998476	0.997781	0.998148	0.997874	0.997579	0.998553
16	0.998162	0.997333	0.997783	0.997453	0.997092	0.998258
17	0.997801	0.996823	0.997365	0.996973	0.996537	0.997922
18	0.997392	0.996249	0.996892	0.996429	0.995914	0.997543
19	0.996937	0.995611	0.996361	0.995823	0.995224	0.997121
20	0.996440	0.994915	0.995773	0.995156	0.994470	0.996657
21	0.995905	0.994163	0.995124	0.994430	0.993656	0.996152
22	0.995331	0.993353	0.994415	0.993643	0.992781	0.995506
23	0.994703	0.992469	0.993645	0.992783	0.991827	0.995012
24	0.993998	0.991490	0.992312	0.991334	0.990771	0.994364
25	0.993196	0.990395	0.991916	0.990779	0.989591	0.993655
26	0.992294	0.989178	0.990952	0.989614	0.988283	0.992883
27	0.991320	0.987867	0.989911	0.988352	0.986872	0.992050
28	0.990306	0.986489	0.988731	0.987012	0.985391	0.991162
29	0.989287	0.985076	0.987552	0.985610	0.983869	0.990224
30	0.988294	0.983657	0.986212	0.984165	0.982333	0.989240
31	0.987361	0.982262	0.984751	0.982693	0.980829	0.988214
32	0.986509	0.980911	0.983165	0.981209	0.979362	0.987153
33	0.985736	0.979606	0.981446	0.979717	0.977941	0.986062
34	0.985037	0.978345	0.979671	0.978222	0.976565	0.984945
35	0.984405	0.977129	0.977793	0.976728	0.975231	0.983810
36	0.983835	0.975954	0.975849	0.975240	0.973939	0.982662
37	0.983323	0.974821	0.973853	0.973761	0.972689	0.981507
38	0.982861	0.973728	0.971821	0.972295	0.971479	0.980350
39	0.982445	0.972674	0.969768	0.970848	0.970309	0.979197
40	0.982069	0.971658	0.967708	0.969423	0.969177	0.978054

41	0.981727	0.970676	0.965657	0.958025	0.868082	0.975925
42	0.981414	0.969733	0.963631	0.956657	0.957024	0.975820
43	0.981124	0.968822	0.961643	0.955325	0.956001	0.974742
44	0.980852	0.967945	0.959710	0.954032	0.955013	0.973695
45	0.980592	0.967099	0.957846	0.952782	0.964059	0.972688
46	0.980338	0.966284	0.956067	0.961580	0.963137	0.971725
47	0.980086	0.965498	0.954388	0.950430	0.962247	0.970813
48	0.979828	0.964740	0.952823	0.959336	0.961388	0.969956
49	0.979561	0.964010	0.951389	0.958303	0.960558	0.969150
50	0.979277	0.963305	0.950100	0.957335	0.959758	0.968433
51	0.978972	0.962625	0.948970	0.956436	0.958985	0.967777
52	0.978647	0.961970	0.947998	0.955605	0.958241	0.967195
53	0.978307	0.961342	0.947171	0.954841	0.957528	0.966679
54	0.977957	0.960744	0.946474	0.954140	0.956848	0.966226
55	0.977603	0.960175	0.945893	0.953500	0.956203	0.965828
56	0.977250	0.959640	0.945414	0.952917	0.955595	0.965482
57	0.976905	0.959139	0.945022	0.952389	0.955027	0.965182
58	0.976572	0.958674	0.944704	0.951912	0.954500	0.964922
59	0.976256	0.958247	0.944446	0.951485	0.954016	0.964697
60	0.975965	0.957860	0.944232	0.951103	0.953578	0.964502
61	0.975702	0.957514	0.944050	0.950764	0.953188	0.964331
62	0.975474	0.957212	0.943884	0.950466	0.952848	0.964180
63	0.975285	0.956955	0.943772	0.950204	0.952559	0.964042
64	0.975131	0.956738	0.943562	0.949976	0.952316	0.963915
65	0.975008	0.956555	0.943406	0.949775	0.952113	0.963802
66	0.974908	0.956400	0.943253	0.949599	0.951942	0.963696
67	0.974828	0.956266	0.943105	0.949443	0.951795	0.963599
68	0.974760	0.956153	0.942962	0.949302	0.951670	0.963509
69	0.974700	0.956049	0.942827	0.949173	0.951556	0.963425
70	0.974642	0.955949	0.942699	0.949049	0.951447	0.963346
71	0.974581	0.955849	0.942579	0.948929	0.951337	0.963270
72	0.974517	0.955748	0.942467	0.948811	0.951226	0.963197
73	0.974450	0.955646	0.942362	0.948693	0.951113	0.963125
74	0.974380	0.955543	0.942263	0.948578	0.950999	0.963058
75	0.974310	0.955440	0.942169	0.948463	0.950884	0.962991
76	0.974238	0.955335	0.942079	0.948350	0.950767	0.962925
77	0.974165	0.955230	0.941992	0.948237	0.950650	0.962860
78	0.974093	0.955124	0.941908	0.948125	0.950532	0.962795
79	0.974022	0.955019	0.941824	0.948014	0.950413	0.962732
80	0.973953	0.954913	0.941741	0.947903	0.950294	0.962667

81	0.973885	0.954807	0.941657	0.947792	0.950174	0.962602
82	0.973820	0.954701	0.941572	0.947680	0.950055	0.962535
83	0.973758	0.954595	0.941485	0.947569	0.949935	0.962468
84	0.973698	0.954488	0.941395	0.947456	0.949814	0.962398
85	0.973638	0.954380	0.941303	0.947343	0.949691	0.962327
86	0.973577	0.954269	0.941209	0.947227	0.949566	0.962253
87	0.973515	0.954156	0.941112	0.947110	0.949438	0.962177
88	0.973451	0.954039	0.941012	0.946990	0.949306	0.962098
89	0.973383	0.953917	0.940910	0.946867	0.949170	0.962017
90	0.973311	0.953790	0.940804	0.946741	0.949029	0.961932
91	0.973233	0.953658	0.940696	0.946611	0.948881	0.961844
92	0.973150	0.953520	0.940584	0.946478	0.948729	0.961753
93	0.973063	0.953377	0.940470	0.946342	0.948572	0.961660
94	0.972972	0.953231	0.940354	0.946203	0.948411	0.961564
95	0.972878	0.953080	0.940236	0.946062	0.948246	0.961465
96	0.972781	0.952927	0.940116	0.945919	0.948079	0.961367
97	0.972681	0.952772	0.939995	0.945774	0.947909	0.961265
98	0.972580	0.952614	0.939873	0.945628	0.947737	0.961164
99	0.972478	0.952456	0.939751	0.945482	0.947564	0.961064
100	0.972376	0.952297	0.939628	0.945335	0.947391	0.960958

APPENDIX C

U. S. STANDARD ATMOSPHERE SUPPLEMENTS

LEVEL	15N	ANN	30N	JUL	30N	JAN	45N	JUL	60N	JUL	60N	JAN	75N	JUL	75N	JAN
1	184.50		191.40	174.20	194.50	194.50	215.30	171.00	233.00	178.00	233.00	178.00	223.00	178.00	223.00	178.00
2	190.90		197.50	180.00	203.10	203.10	219.10	182.10	238.00	185.10	241.00	185.10	238.00	185.10	241.00	185.10
3	196.20		206.70	186.00	209.50	209.50	222.50	187.80	241.00	190.80	245.00	190.80	245.00	190.80	245.00	190.80
4	200.90		210.90	191.50	214.50	214.50	228.50	192.70	245.00	195.40	248.00	195.40	248.00	195.40	248.00	195.40
5	204.80		215.00	196.20	219.00	219.00	231.30	199.40	248.00	203.70	251.00	203.70	251.00	203.70	251.00	203.70
6	215.60		220.00	205.00	224.00	224.00	234.40	206.90	251.00	211.40	255.00	211.40	255.00	211.40	255.00	211.40
7	219.60		224.20	215.20	228.20	228.20	236.40	211.40	255.00	215.40	259.00	215.40	259.00	215.40	259.00	215.40
8	223.60		227.10	219.10	231.10	231.10	239.40	215.40	259.00	219.40	263.00	219.40	263.00	219.40	263.00	219.40
9	226.60		231.20	222.60	235.20	235.20	243.00	222.50	263.00	222.50	267.00	222.50	267.00	222.50	267.00	222.50
10	232.00		234.40	230.00	247.00	247.00	247.00	227.00	267.00	227.00	271.00	227.00	271.00	227.00	271.00	227.00
11	248.90		250.00	245.10	255.10	255.10	255.10	250.00	271.00	250.00	275.00	250.00	275.00	250.00	275.00	250.00
12	254.90		254.40	251.90	257.40	257.40	257.40	255.10	275.00	255.10	279.00	255.10	279.00	255.10	279.00	255.10
13	261.80		261.40	259.40	265.40	265.40	265.40	263.00	279.00	263.00	283.00	263.00	283.00	263.00	283.00	263.00
14	267.80		265.80	268.40	269.80	269.80	269.80	266.90	283.00	266.90	287.00	266.90	287.00	266.90	287.00	266.90
15	270.20		269.20	275.70	275.70	275.70	275.70	272.50	287.00	272.50	291.00	272.50	291.00	272.50	291.00	272.50
16	270.20		269.20	275.70	275.70	275.70	275.70	272.50	291.00	272.50	295.00	272.50	295.00	272.50	295.00	272.50
17	270.20		269.20	275.70	275.70	275.70	275.70	272.50	295.00	272.50	299.00	272.50	299.00	272.50	299.00	272.50
18	270.20		269.20	275.70	275.70	275.70	275.70	272.50	299.00	272.50	303.00	272.50	303.00	272.50	303.00	272.50
19	270.20		269.20	275.70	275.70	275.70	275.70	272.50	303.00	272.50	307.00	272.50	307.00	272.50	307.00	272.50
20	270.20		269.20	275.70	275.70	275.70	275.70	272.50	307.00	272.50	311.00	272.50	311.00	272.50	311.00	272.50
21	270.20		269.20	275.70	275.70	275.70	275.70	272.50	311.00	272.50	315.00	272.50	315.00	272.50	315.00	272.50
22	270.20		269.20	275.70	275.70	275.70	275.70	272.50	315.00	272.50	319.00	272.50	319.00	272.50	319.00	272.50
23	270.20		269.20	275.70	275.70	275.70	275.70	272.50	319.00	272.50	323.00	272.50	323.00	272.50	323.00	272.50
24	270.20		269.20	275.70	275.70	275.70	275.70	272.50	323.00	272.50	327.00	272.50	327.00	272.50	327.00	272.50
25	270.20		269.20	275.70	275.70	275.70	275.70	272.50	327.00	272.50	331.00	272.50	331.00	272.50	331.00	272.50
26	270.20		269.20	275.70	275.70	275.70	275.70	272.50	331.00	272.50	335.00	272.50	335.00	272.50	335.00	272.50
27	270.20		269.20	275.70	275.70	275.70	275.70	272.50	335.00	272.50	339.00	272.50	339.00	272.50	339.00	272.50
28	270.20		269.20	275.70	275.70	275.70	275.70	272.50	339.00	272.50	343.00	272.50	343.00	272.50	343.00	272.50
29	270.20		269.20	275.70	275.70	275.70	275.70	272.50	343.00	272.50	347.00	272.50	347.00	272.50	347.00	272.50
30	270.20		269.20	275.70	275.70	275.70	275.70	272.50	347.00	272.50	351.00	272.50	351.00	272.50	351.00	272.50
31	270.20		269.20	275.70	275.70	275.70	275.70	272.50	351.00	272.50	355.00	272.50	355.00	272.50	355.00	272.50
32	270.20		269.20	275.70	275.70	275.70	275.70	272.50	355.00	272.50	359.00	272.50	359.00	272.50	359.00	272.50
33	270.20		269.20	275.70	275.70	275.70	275.70	272.50	359.00	272.50	363.00	272.50	363.00	272.50	363.00	272.50
34	270.20		269.20	275.70	275.70	275.70	275.70	272.50	363.00	272.50	367.00	272.50	367.00	272.50	367.00	272.50
35	270.20		269.20	275.70	275.70	275.70	275.70	272.50	367.00	272.50	371.00	272.50	371.00	272.50	371.00	272.50
36	270.20		269.20	275.70	275.70	275.70	275.70	272.50	371.00	272.50	375.00	272.50	375.00	272.50	375.00	272.50
37	270.20		269.20	275.70	275.70	275.70	275.70	272.50	375.00	272.50	379.00	272.50	379.00	272.50	379.00	272.50
38	270.20		269.20	275.70	275.70	275.70	275.70	272.50	379.00	272.50	383.00	272.50	383.00	272.50	383.00	272.50
39	270.20		269.20	275.70	275.70	275.70	275.70	272.50	383.00	272.50	387.00	272.50	387.00	272.50	387.00	272.50
40	270.20		269.20	275.70	275.70	275.70	275.70	272.50	387.00	272.50	391.00	272.50	391.00	272.50	391.00	272.50

41
42
43
44
45
46
47
48
49
50
51
52
53
54
55
56

204.30
200.20
197.20
195.50
195.10
209.40
220.40
230.60
239.00
254.90
264.10
273.60
282.70
293.40
300.10

211.40
209.20
205.40
203.70
204.50
208.20
221.00
231.40
240.40
255.30
266.80
274.20
282.30
293.30
300.60

206.20
204.30
203.20
203.30
205.50
216.80
224.00
233.00
243.80
256.20
266.20
274.60
282.00
286.30

219.80
217.50
216.50
215.70
215.30
221.30
229.30
238.10
253.00
262.40
272.00
281.30
289.50
293.80

215.50
215.10
215.30
216.60
216.90
217.80
218.60
219.50
223.70
237.30
245.00
251.90
261.70
266.60
271.60

225.20
225.20
225.20
225.20
225.20
225.20
225.70
230.40
234.50
255.90
264.50
270.80
281.90
286.20

214.90
215.20
215.40
215.80
217.20
217.20
217.50
218.10
219.60
233.20
243.80
253.10
259.00
257.30

230.30
230.20
230.20
230.20
230.20
230.40
228.00
227.10
229.70
241.00
252.00
261.50
268.60
275.80
278.40

220.80
209.10
210.10
210.10
212.50
213.40
214.60
215.70
223.50
234.10
241.70
251.80
251.40

TEST AND EVALUATION
OF A VTIPR RETRIEVAL SYSTEM
FROM CLEAR-COLUMN NOAA 2 RADIANCES

LCDR HARRY M. DYCK JR.
NAVAL POSTGRADUATE SCHOOL
MARCH 1975

COMMON/WORK/VTIPR(2,100),A1(100,6),A2(100,6),A3(100,6),TAU(100,6)	5	MAIN
COMMON/FIRST/STATM(10,56),FG(2,56)	10	MAIN
COMMON/SCND/TSTD(100),A(6)	15	MAIN
COMMON/THRD/D1(6),D4(6),D5(6),D10(6),D12(6)	20	MAIN
COMMON/FOUR/DIM(100),TAUW(100,8),CW(8,14),U(100),AA(14),PATH,NP,	25	MAIN
1W(100)	30	MAIN
DIMENSION REPORT(2,15),PREF(56)	35	MAIN
DIMENSION CREC(40,11),TBAR(11),WBAR(40),WS(11)	40	MAIN
DIMENSION LEVEL(11),SAT(11)	45	MAIN
DIMENSION B(33,6),BB(100,6),BMEAN(33,6),RADIOT(6)	50	MAIN
DIMENSION CHAN(6),RADOBS(6),DTAUW(33,6),T(15),T33(33)	55	MAIN
DIMENSION DDTAUW(100,6)	60	MAIN
DIMENSION AT(15)	65	MAIN
DIMENSION TERROR(4,235)	70	MAIN
DIMENSION ERROR(4,15,233)	75	MAIN
DIMENSION TTROR(235)	80	MAIN
DIMENSION VT(15),VERROR(4,15,233),TVRDR(4,234),TVOR(235)	85	MAIN
DIMENSION QZTAU(100,6)	90	MAIN
DIMENSION AVCHAN(100)	95	MAIN

87


```

C      READ (5,425) (REPORT(1,K),K=1,15)
C
C      DO 120 I=2,10
C      READ (5,435) (STATM(I,J),J=1,14)
C      READ (5,435) (STATM(I,J),J=15,28)
C      READ (5,435) (STATM(I,J),J=29,42)
C      READ (5,435) (STATM(I,J),J=43,56)
C      120 CONTINUE
C
C      DO 125 I=1,12
C      J = I*8
C      K = J-7
C      READ (5,450) (TSTD(N),N=K,J)
C      125 CONTINUE
C
C      READ (5,450) (TSTD(N),N=97,100)
C      READ (5,450) (A(N),N=1,6)
C
C      DO 145 I=1,6
C
C      DO 130 L=1,10
C      KK = 10*L
C      K = KK-9
C      READ (5,445) (A1(N,I),N=K,KK)
C      130 CONTINUE
C
C      DO 135 L=1,17
C      KK = 6*L
C      K = KK-5
C      IF (L.EQ.17) KK = 100
C      READ (5,455) (A2(N,I),N=K,KK)
C      135 CONTINUE
C
C      DO 140 L=1,17
C      KK = 6*L
C      K = KK-5
C      IF (L.EQ.17) KK = 100
C      READ (5,455) (A3(N,I),N=K,KK)
C      140 CONTINUE
C
C

```

```

MAIN 345
MAIN 350
MAIN 355
MAIN 360
MAIN 365
MAIN 370
MAIN 375
MAIN 380
MAIN 385
MAIN 390
MAIN 405
MAIN 410
MAIN 415
MAIN 420
MAIN 425
MAIN 430
MAIN 435
MAIN 440
MAIN 445
MAIN 450
MAIN 455
MAIN 460
MAIN 465
MAIN 470
MAIN 475
MAIN 480
MAIN 485
MAIN 490
MAIN 495
MAIN 500
MAIN 505
MAIN 520
MAIN 525
MAIN 530
MAIN 535
MAIN 540
MAIN 545
MAIN 550
MAIN 555
MAIN 570
MAIN 575
MAIN 580
MAIN 585
MAIN 590
MAIN 595
MAIN 600
MAIN 605
MAIN 610

```


90


```

C      CALL UPPER (ALAT)
C      EXPAND 56 LEVEL TO 100 LEVEL ATMOSPHERE
C
C      DO 180 I=1,100
C      AB = FLOAT(I)
C      AAB = (1.+(.26087836*(AB-1.0)))*3.50
C      VTPR(1,I) = AAB*.01
C      VTPR(2,I) = 99.9
C      CONTINUE
C      VTPR(1,100) = 1000.000
C
C      DO 185 I=34,56
C      IF (FG(2,I).LT.99.8) GO TO 185
C      CALL LEVELL (FG(1,I),TT)
C      FG(2,I) = TT
C      CONTINUE
C
C      DO 190 I=1,100
C      CALL LEVELL (VTPR(1,I),TT)
C      VTPR(2,I) = TT
C      CONTINUE
C
C      CONVERT TEMPERATURES TO KELVIN
C
C      DO 195 I=1,100
C      VTPR(2,I) = VTPR(2,I)+273.16
C      CONTINUE
C
C      SET A COUNTER - IFLAG - TO COUNT THE NJMBER OF ITERATIONS USED
C      TO CONVERGE
C
C      IFLAG = 0
C      VTPR(2,100) = TSFC
C
C      CALCULATE THE TRANSMITTANCE DUE TO CO2
C
C      CALL RDTEMP (PATH)
C
C      IF THE ZENITH ANGLE IS GREATER THAN ZERO THAN THE VALUES OF TAU

```

```

MAIN1130
MAIN1135
MAIN1140
MAIN1145
MAIN1150
MAIN1155
MAIN1160
MAIN1165
MAIN1170
MAIN1175
MAIN1180
MAIN1185
MAIN1190
MAIN1200
MAIN1205
MAIN1210
MAIN1215
MAIN1220
MAIN1225
MAIN1230
MAIN1235
MAIN1240
MAIN1245
MAIN1250
MAIN1255
MAIN1260
MAIN1265
MAIN1270
MAIN1275
MAIN1280
MAIN1290
MAIN1295
MAIN1300
MAIN1310
MAIN1315
MAIN1320
MAIN1325
MAIN1330
MAIN1340
MAIN1345
MAIN1350
MAIN1355
MAIN1360
MAIN1365
MAIN1370
MAIN1375
MAIN1380
MAIN1385
MAIN1390
MAIN1395

```



```

C C      MUST BE CORRECTED.
C C      CALL MARTAU (PATH)
C C      IF (IFLAG-GE.1) GO TO 230
C C      DETERMINE THE WATER VAPOR CONTENT OF THE ATMOSPHERE
C C      KK = 1
C C
C C      DO 205 I=63,100
C C      IF (I.NE.LEVEL(KK)) GO TO 205
C C      SAT(KK) = GOFF(VTPR(2,I),VTPR(1,I))
C C      KK = KK+1
C C      205 CONTINUE
C C
C C      FORM W FIRST GUESS =WBAR+CREG*(SAT-TBAR)
C C
C C      DO 215 M=1,40
C C      W(M) = WBAR(M)
C C
C C      DO 210 L=1,11
C C      W(M) = W(M)+CREG(M,L)*(SAT(L)-TBAR(L))
C C      210 CONTINUE
C C
C C      215 CONTINUE
C C
C C      DO 220 M=61,100
C C      W(M) = W(M-61+1)
C C      IF (W(M).LT.0.00) W(M)=0.00
C C      220 CONTINUE
C C
C C      DO 225 M=1,61
C C      W(M) = W(61)*(VTPR(1,M)/VTPR(2,61))**3
C C      IF (W(M).LT.0.00) W(M)=0.00
C C      225 CONTINUE
C C
C C

```

```

MAIN1400
MAIN1405
MAIN1410
MAIN1415
MAIN1420
MAIN1425
MAIN1430
MAIN1435
MAIN1440
MAIN1445
MAIN1450
MAIN1455
MAIN1460
MAIN1465
MAIN1470
MAIN1475
MAIN1480
MAIN1485
MAIN1490
MAIN1495
MAIN1500
MAIN1505
MAIN1510
MAIN1515
MAIN1520
MAIN1525
MAIN1530
MAIN1535
MAIN1540
MAIN1545
MAIN1550
MAIN1555
MAIN1560
MAIN1575
MAIN1580
MAIN1585
MAIN1590
MAIN1595
MAIN1600
MAIN1605
MAIN1610
MAIN1615
MAIN1620
MAIN1625
MAIN1630
MAIN1635
MAIN1640
MAIN1645

```



```

C C      CALCULATE THE TRANSMITTANCE DUE TO WATER VAPOR
C C      230 CALL TRANW (TOTWV,1,8)
C C
C C      DO 240 I=1,100
C C
C C      DO 235 J=1,6
C C
C C      TOTAL TRANSMITTANCE IS THE PRODUCT OF CO2*WATER*OZONE
C C      TAUW(I,J) = TAU(I,J)*TAUW(I,J)*OZTAU(I,J)**PATH
C C      235 CONTINUE
C C
C C      240 CONTINUE
C C
C C      IF (IFLAG.GT.1) GO TO 265
C C      VTPR(2,100) = TSFC
C C      COMPUTE PLANK VALUES AT 100 LEVELS
C C
C C      DO 250 I=1,6
C C
C C      DO 245 J=1,100
C C      BB(J,I) = (C1*CHAN(I)**3)/(EXP(C2*CHAN(I))/VTPR(2,J))-1.)
C C      245 CONTINUE
C C
C C      250 CONTINUE
C C
C C      COMPUTE 33 LEVEL PLANK FUNCTION BY USING A 4TH ORDER LAGRANGIAN
C C
C C      DO 260 I=1,6
C C      K = 1
C C
C C      DO 255 J=4,100,3
C C      X = ((J-1)+(J-2))/2.

```



```

      B(K,I) = BB(J,I)*(X-(J-1))*(X-(J-2))*(X-(J-3))/((J-(J-1))*(J-(J-1))*(J-(J-2))
      1)*(J-(J-3)))+BB(J-1,I)*(X-J)*(X-(J-2))*(X-(J-3))/((J-(J-1))*(J-(J-1))*(J-(J-2))
      2-(J-2))*(J-1)-(J-3))+BB(J-2,I)*(X-J)*(X-(J-1))*(X-(J-3))/((J-(J-1))*(J-(J-1))*(J-(J-2))
      3-J)*(J-2)-(J-1))*(J-2)-(J-3))+BB(J-3,I)*(X-J)*(X-(J-1))*(X-(J-2))
      4)/((J-(J-3)-J)*(J-3)-(J-1))*(J-3)-(J-2))
      K = K+1
255 CONTINUE
CC
260 CONTINUE
CC
      COMPUTE DELTA TAUW FOR 100 LEVELS
CC
265 DO 275 I=1,6
      DDTAUW(1,I) = ABS(TAUW(1,I)-TAUW(2,I))*2
      DDTAUW(100,I) = ABS(TAUW(99,I)-TAUW(100,I))*2
      CC
270 DO 270 J=2,99
      DDTAUW(J,I) = ABS(TAUW(J+1,I)-TAUW(J-1,I))
      CONTINUE
      CC
275 CONTINUE
      CC
      COMPUTE DELTA TAUW FOR THE 33 LEVELS
      CC
      DO 285 I=1,6
      K = 1
      CC
      DO 280 J=4,100,3
      DTAUW(K,I) = TAUW(J-3,I)-TAUW(J,I)
      K = K+1
      CONTINUE
      CC
280 CONTINUE
      CC
285 CONTINUE
      CC

```



```

C      COMPUTE MEAN LAYER PLANCK VALUES
C
C      DO 295 I=1,6
C      K = 1
C
C      DO 290 J=4,100,3
C      BMEAN(K,I) = (BB(J,I)+4.*B(K,I)+BB(J-3,I))/6.
C      K = K+1
C      290 CONTINUE
C
C      295 CONTINUE
C      IFLAG = IFLAG+1
C
C      COMPUTE FIRST GUESS RADIANCE
C
C      DO 315 I=1,6
C      IF (TAUW(100,I).LT.1.E-07) GO TO 300
C      RADSFCE = BB(100,I)*TAUW(100,I)
C      GO TO 305
C      300 RADSFCE = 0.0
C      305 RADATM = 0.0
C
C      DO 310 K=1,33
C      IF (DTAUW(K,I).LT.1.E-07) GO TO 310
C      RAD = BMEAN(K,I)*DTAUW(K,I)
C      RADATM = RADATM+RAD
C      310 CONTINUE
C
C      RADTOT(I) = RADATM+RADSFCE
C      315 CONTINUE
C      KOUNT = 0
C
C      DO 330 I=1,6
C      RESID = RADOBS(I)-RADTOT(I)
C
C      330 CONTINUE

```



```

C      EPS = ABS(RESID/RADOBS(I))
C      TEST FOR CONVERGENCE OF THE COMPUTED AND OBSERVED RADIANCES
C
C      IF (EPS.LT.1.E-04) GO TO 330
C      KOUNT = KOUNT+1
C
C      DO 320 K=1,33
C      B(K,I) = B(K,I)+RESID
C      CONTINUE
C      320
C
C      COMPUTE NEW PLANCKS FOR NEXT ITERATION
C
C      DO 325 J=1,100
C      BB(J,I) = BB(J,I)+RESID
C      CONTINUE
C      325
C
C      330 CONTINUE
C
C      DO 340 J=1,100
C      SUMDT = 0.0
C      SUMBDT = 0.0
C
C      DO 335 I=1,6
C      SUMBDT = SUMBDT+(BB(J,I)*DDTAUW(J,I))
C      SUMDT = SUMDT+DDTAUW(J,I)
C      CONTINUE
C      335
C
C      BREF = SUMBDT/SUMDT
C      VTPR(2,J) = (C2*710.0)/ALOG((C1*710.0**3+BREF)/BREF)
C      CONTINUE
C      340
C
C      IF (KOUNT.GT.0) GO TO 200
C      WRITE (6,505) IFLAG
C
C      REDUCE THE 100 LEVEL TEMPERATURE PROFILE TO 15 LEVELS WITH A
C      FOURTH ORDER LAGRANGIAN

```



```

DO 355 K=2,15
  III = 0
C
C
DO 350 J=24,96
  IF (REPORT(I,K).LE.VTPR(1,J)) GO TO 345
  GO TO 350
  IF (III.GE.1) GO TO 350
  Y = VTPR(1,J)-REPORT(1,K)
  Z = VTPR(1,J)-VTPR(1,J-1)
  X = FLOAT(J)-(Y/Z)
  T(K) = VTPR(2,J-2)*(X-(J-1))*(X-J)*(X-(J+1))/(X-(J-2)-(J+1))*(X-(J-1))*(X-(J-2))
  1-J)*(X-(J-2)-(J+1))+VTPR(2,J-1)*(X-(J-2))*(X-(J-1))/(X-(J-2)-(J+1))*(X-(J-1))*(X-(J-2))
  2J-2)*(X-(J-1)-J)*(X-(J-1)-(J+1))+VTPR(2,J)*(X-(J-2))*(X-(J-1))/(X-(J-2)-(J+1))*(X-(J-1))*(X-(J-2))
  3+1)/(X-(J-2))*(X-(J-1)-(J+1))+VTPR(2,J+1)*(X-(J-2))*(X-(J-1))/(X-(J-2)-(J+1))*(X-(J-1))*(X-(J-2))
  4)*(X-J)/(X-(J+1)-(J-2))*(X-(J-1)-(J+1))*(X-(J-1)-(J+1))
  III = 1
  350 CONTINUE
C
C
355 CONTINUE
C
C
T(1) = VTPR(2,100)
WRITE (6,515)
SET COUNTER I FOR LATITUDE BAND
C
C
IF (ALAT.GT.60.0) I=4
IF (ALAT.LE.60.0) I=3
IF (ALAT.LE.40.0) I=2
IF (ALAT.LE.20.0) I=1
C
DO 360 K=1,15
  IF (AT(K).GT.99.8) GO TO 360
  ERROR(I,K,LOOP) = T(K)-(AT(K)+273.16)
  VERROR(I,K,LOOP) = VT(K)-AT(K)
  T(K)=T(K)-273.16
  WRITE (6,510) K,REPORT(1,K),T(K),AT(K),ERROR(I,K,LOOP),VT(K),VERROR(I,K,LOOP)
  1R(I,K,LOOP)
  360 CONTINUE
C
365 CONTINUE
C
370 CONTINUE
  LOOP = LOOP-1
C
DO 390 I=1,4

```

```

MAIN2610
MAIN2615
MAIN2620
MAIN2625
MAIN2630
MAIN2635
MAIN2640
MAIN2645
MAIN2650
MAIN2655
MAIN2660
MAIN2665
MAIN2670
MAIN2675
MAIN2680
MAIN2685
MAIN2690
MAIN2695
MAIN2700
MAIN2705
MAIN2710
MAIN2715
MAIN2720
MAIN2725
MAIN2730
MAIN2735
MAIN2740
MAIN2745
MAIN2750
MAIN2755
MAIN2760
MAIN2765
MAIN2770
MAIN2775
MAIN2780
MAIN2785
MAIN2790
MAIN2793
MAIN2795
MAIN2800
MAIN2805
MAIN2810
MAIN2815
MAIN2820
MAIN2825
MAIN2830
MAIN2835
MAIN2840

```



```

C
DO 385 K=1,15
N = 0
DO 375 KLOOP=1,LLOOP
IF (ERROR(I,K,KLOOP).EQ.0.0) GO TO 375
N = N+1
ERROR(I,N) = ERROR(I,K,KLOOP)
TVROR(I,N) = VERROR(I,K,KLOOP)
375 CONTINUE
C
DO 380 II=1,N
TROR(II) = TROR(I,II)
TVROR(II) = TVROR(I,II)
380 CONTINUE
C
DRAW HISTOGRAMS OF THE ERRORS
CALL HISTG (TROR,N,NBAR)
WRITE (6,415) REPORT(1,K)
CALL HISTG (TVROR,N,NBAR)
WRITE (6,410) REPORT(1,K),I
385 CONTINUE
C
390 CONTINUE
C
STOP
C
395 FORMAT (10F7.6)
400 FORMAT (F10.3)
405 FORMAT ('0',//)//)
410 FORMAT ('0',//) ***** HISTOGRAM FOR PRESSURE LEVEL ',F6.0,2X,'AND
1 TITUDE BAND',I5,2X,'AND USING NESS VTPR *****')
415 FORMAT ('0',F6.0,'MB HISTOGRAM FOR GLOBALLY AVERAGED ERRORS')
420 FORMAT ('0',STATION NUMBER
425 FORMAT (15F4.0)
430 FORMAT (15F5.1)
435 FORMAT (14F5.1)
440 FORMAT (9F8.3)
445 FORMAT (10F8.7)
450 FORMAT (8F7.3)
455 FORMAT (1P6E13.6)
460 FORMAT (6(F7.4,3X))
465 FORMAT (F8.5)
470 FORMAT (7E11.4)

```

```

MAIN2845
MAIN2850
MAIN2855
MAIN2860
MAIN2865
MAIN2870
MAIN2875
MAIN2880
MAIN2885
MAIN2890
MAIN2895
MAIN2900
MAIN2905
MAIN2910
MAIN2915
MAIN2920
MAIN2925
MAIN2930
MAIN2935
MAIN2940
MAIN2945
MAIN2950
MAIN2955
MAIN2960
MAIN2965
MAIN2970
MAIN2975
MAIN2980
MAIN2985
MAIN2990
MAIN2995
MAIN3000
MAIN3005
MAIN3010
MAIN3015
MAIN3020
MAIN3025
MAIN3035
MAIN3040
MAIN3045
MAIN3050
MAIN3055
MAIN3060
MAIN3065
MAIN3070
MAIN3075
MAIN3080
MAIN3085

```



```

475 FORMAT (11I3)
480 FORMAT (8E10.4)
485 FORMAT (7F8.5)
490 FORMAT (9F5.1)
495 FORMAT (9F9.5)
500 FORMAT (' ', 'ZENITH ANGLE = ', F4.1)
505 FORMAT ('0', 'THE TEMPERATURE PROFILE CONVERGED AFTER', I4, ' ITERATIONS')
      IICNS = IICNS + 1
510 FORMAT (' ', I4, '2X', 6(F10.3, 2X))
515 FORMAT ('0', 'I10', 'PRESSURE', T23, 'TEMP.', T35, 'SOUNDING', T48, 'ERROR',
      T60, 'NESS', T72, 'NESS-ERROR', //)
      END

```

```

MAIN3090
MAIN3095
MAIN3100
MAIN3105
MAIN3110
MAIN3115
MAIN3120
MAIN3125
MAIN3130
MAIN3135
MAIN3140
MAIN3145

```


[illegible]

[illegible]

102


```

C
C      DO 130 I=1,6
C
C      DO 130 K=1,100
C      TAU(K,I) = CHOP(TAU(K,I),0.0,1.0)
C      130 CONTINUE
C      RETURN
C      END

```

```

RDTIP 245
RDTIP 250
RDTIP 255
RDTIP 260
RDTIP 265
RDTIP 270
RDTIP 275
RDTIP 280
RDTIP 285
RDTIP 290

```



```

      FUNCTION GOFF( T,PP)
      CCCCCCCCCCCCCCCCCCCCCCCCCCCCCCCCCCCCCCCCCCCCCCCCCCCCCC
      C      GOFF RETURNS SATURATED MIXING RATIO GIVEN TEMP AND PRESS
      C      CCCCCCCCCCCCCCCCCCCCCCCCCCCCCCCCCCCCCCCCCCCCCCCCCCCC
      C      TS = 373.16
      C      AA = -7.90298*(TS/T-1.)
      C      BB = 5.02808*ALOG10(TS/T)
      C      CC = 11.344*(1.-(T/TS))
      C      DD = (-1.3816E-07)*(10**C-1)
      C      ESUBS = 1013.246*10**(AA+BB+CC+DD)
      C      FROM SAT VAPOR PRESSURE GET SAT MIXING RATIO
      C      GOFF = 621.98*ESUBS/(PP-ESUBS)
      C      RETURN
      C      END

```



```

255 AA(9) = AA(3)*AA(4)
260 AA(12) = AA(4)**2
265 COF3 = CW(I,10)
270 COF2 = CW(I,7)+CW(I,8)*AA(4)+CW(I,14)*AA(3)
275 COF1 = CW(I,2)+CW(I,5)*AA(3)+CW(I,6)*AA(4)+CW(I,11)*AA(12)+CW(I,13)
280 1)*AA(9)
285 COFO = CW(I,1)+CW(I,3)*AA(3)+CW(I,4)*AA(4)+CW(I,9)*AA(9)+CW(I,12)*
290 1AA(12)
295 IFLAG = IFLAG+1
300
305 FIRST TIME U IS NON-ZERO, COMPUTE TAUW DIRECTLY FROM POLY EXPANSION
310
315 IF (IFLAG.NE.1) GO TO 115
320 D = U(K)
325 GO TO 125
330
335 FROM WW(K-1) COMPUTE UPSTART THEN ADD DELTA U
340
345 NEWTONS METHOD TO SOLVE FOR AA(2). 1ST GUESS IS LAST VALUE OF AA
350
355 115 A22 = AA(2)**2
360 A23 = AA(2)**3
365 F = COFO+COF1*AA(2)+COF2*A22+COF3*A23
370 F = F-WW
375 F1 = COF1+2.0*COF2*AA(2)+3.0*COF3*A22
380 IF (F1.EQ.0.0) GO TO 120
385 AA(2) = AA(2)-F/F1
390
395 NOW HAVE AA(2). DERIVE U-START AND ADD DELTA-U
400
405 D = EXP(10.*AA(2)-AA(4))+U(K)-U(K-1)
410 AA(2) = 0.1*(ALOG(D)+AA(4))
415 A22 = AA(2)**2
420 A23 = AA(2)**3
425
430 WW IS LOG(-LOG(TAUW))
435
440 WW = COFO+COF1*AA(2)+COF2*A22+COF3*A23
445 XARG = DIM(K)*BIGNEL(1)+EXP(WW)
450 TRAN = EXP(-XARG)
455 TAUW(K,1) = CHOP(TRAN,0.0,1.0)
460
465 130 CONTINUE
470
475 C 135 CONTINUE
480
485 RETURN
END

```



```

FUNCTION CHOP(X,Y,Z)
IF (X-Y) 105,105,110
105 RETURN
110 IF (X-Z) 120,115,115
115 CHOP = Z
120 RETURN X
END

```

```

CHOP 5
CHOP 10
CHOP 15
CHOP 20
CHOP 25
CHOP 30
CHOP 35
CHOP 40
CHOP 45
CHOP 50

```


CARBON DIOXIDE TRANSMITTANCES FOR THE SIX VTPR CHANNELS

LEVEL	CHAN 1	CHAN 2	CHAN 3	CHAN 4	CHAN 5	CHAN 6
1	0.991131	0.999653	0.999886	0.999912	0.999936	0.999993
2	0.988616	0.999418	0.999733	0.999799	0.999842	0.999935
3	0.985314	0.999092	0.999537	0.999575	0.999653	0.999962
4	0.980754	0.998608	0.999259	0.999173	0.999308	0.999909
5	0.975299	0.997973	0.998884	0.998641	0.998848	0.999315
6	0.969083	0.997204	0.998390	0.998053	0.998348	0.999674
7	0.961684	0.996247	0.997750	0.997415	0.997822	0.999485
8	0.952678	0.995045	0.996952	0.996738	0.997281	0.999253
9	0.941640	0.993540	0.995971	0.995022	0.996731	0.998991
10	0.928429	0.991679	0.994789	0.995254	0.996155	0.998697
11	0.913059	0.989418	0.993404	0.994433	0.995537	0.998400
12	0.895530	0.986719	0.991792	0.993556	0.994859	0.998101
13	0.875965	0.983537	0.989937	0.992624	0.994112	0.997802
14	0.854614	0.979809	0.987813	0.991627	0.993282	0.997503
15	0.831837	0.975464	0.985379	0.990533	0.992342	0.997193
16	0.808120	0.970429	0.982596	0.989324	0.991280	0.996865
17	0.783978	0.964630	0.979426	0.987985	0.990083	0.996519
18	0.759806	0.957987	0.975819	0.986496	0.988739	0.996145
19	0.735895	0.950424	0.971736	0.984847	0.987244	0.995739
20	0.712363	0.941861	0.967135	0.983030	0.985595	0.995301
21	0.689153	0.932223	0.961984	0.981041	0.983792	0.994823
22	0.666067	0.921432	0.956255	0.978881	0.981841	0.994319
23	0.642842	0.909414	0.949899	0.975531	0.979731	0.993767
24	0.619215	0.896098	0.942897	0.973993	0.977470	0.993178
25	0.594999	0.881417	0.935216	0.971258	0.975059	0.992543
26	0.570067	0.865308	0.926777	0.968284	0.972473	0.991863
27	0.544428	0.847723	0.917538	0.965057	0.969713	0.991121
28	0.518133	0.828618	0.907477	0.961575	0.966787	0.990321
29	0.491282	0.807966	0.896576	0.957833	0.963705	0.989465
30	0.463997	0.785753	0.884823	0.953848	0.960479	0.988555
31	0.436414	0.761986	0.872210	0.949607	0.957125	0.987592
32	0.408677	0.736687	0.858738	0.945123	0.953658	0.986582
33	0.380939	0.709907	0.844414	0.940408	0.950097	0.985527
34	0.353356	0.681707	0.829254	0.935474	0.946459	0.984435
35	0.326084	0.652176	0.813267	0.930328	0.942757	0.983308
36	0.299286	0.621431	0.796393	0.924929	0.938977	0.982136
37	0.273120	0.589637	0.778590	0.919237	0.935107	0.980904
38	0.247735	0.556957	0.759887	0.913260	0.931157	0.979613
39	0.223274	0.523557	0.740321	0.907008	0.927138	0.978282
40	0.199827	0.489605	0.720067	0.900580	0.923095	0.976925

41	0.177535	0.455338	0.699027	0.893880	0.918984	0.975520
42	0.156501	0.420970	0.677231	0.886900	0.914800	0.974066
43	0.136779	0.386711	0.654787	0.879668	0.910554	0.972570
44	0.118460	0.352818	0.631511	0.872096	0.906201	0.971004
45	0.101568	0.319468	0.607929	0.864268	0.901789	0.969402
46	0.086144	0.286895	0.583764	0.856180	0.897299	0.967754
47	0.072217	0.255350	0.559096	0.847746	0.892698	0.966037
48	0.059791	0.225062	0.533982	0.838940	0.887974	0.964244
49	0.048830	0.196242	0.508515	0.829770	0.883125	0.962375
50	0.039287	0.169099	0.482838	0.820248	0.878152	0.960436
51	0.031120	0.143870	0.456970	0.810294	0.873021	0.958401
52	0.024258	0.120747	0.430848	0.799742	0.857663	0.956221
53	0.018584	0.099830	0.404528	0.788502	0.862036	0.953867
54	0.013970	0.081190	0.378156	0.776550	0.856124	0.951329
55	0.010292	0.064897	0.351884	0.763863	0.849909	0.948596
56	0.007424	0.050927	0.325859	0.750427	0.843377	0.945657
57	0.005227	0.039151	0.300236	0.736235	0.835517	0.942506
58	0.003538	0.029433	0.275213	0.721332	0.829334	0.939146
59	0.002388	0.021629	0.250973	0.705756	0.821833	0.935582
60	0.001541	0.015515	0.227612	0.689479	0.813392	0.931796
61	0.000968	0.010838	0.205211	0.672462	0.805783	0.927765
62	0.000591	0.007353	0.183853	0.654664	0.797179	0.923464
63	0.000341	0.004810	0.163611	0.636031	0.788142	0.918861
64	0.000180	0.003047	0.144515	0.616461	0.778612	0.913897
65	0.000082	0.001886	0.126588	0.595843	0.768520	0.908503
66	0.000020	0.001156	0.109856	0.574072	0.757798	0.902609
67	0.000000	0.000691	0.094406	0.551202	0.746438	0.896197
68	0.0	0.000395	0.080334	0.527442	0.734486	0.889290
69	0.0	0.000221	0.067655	0.502886	0.721936	0.881867
70	0.0	0.000123	0.056346	0.477534	0.708741	0.873871
71	0.0	0.000060	0.046403	0.451509	0.694903	0.865288
72	0.0	0.000019	0.037766	0.425025	0.680453	0.856134
73	0.0	0.000000	0.030335	0.398223	0.665387	0.846389
74	0.0	0.0	0.023984	0.371034	0.649593	0.835938
75	0.0	0.0	0.018661	0.343825	0.633165	0.824852
76	0.0	0.0	0.014292	0.315940	0.616200	0.813206
77	0.0	0.0	0.010759	0.290388	0.598623	0.800919
78	0.0	0.0	0.007967	0.264438	0.580505	0.788043
79	0.0	0.0	0.005844	0.239271	0.561878	0.774598
80	0.0	0.0	0.004220	0.215037	0.542755	0.760583

81	0.0	0.0	0.002995	0.191890	0.523149	0.745995
82	0.0	0.0	0.002071	0.170036	0.503112	0.730874
83	0.0	0.0	0.001380	0.149654	0.482760	0.715302
84	0.0	0.0	0.000885	0.130787	0.462181	0.699323
85	0.0	0.0	0.000548	0.113420	0.441413	0.682954
86	0.0	0.0	0.000334	0.097547	0.420495	0.666182
87	0.0	0.0	0.000208	0.083170	0.399466	0.649015
88	0.0	0.0	0.000132	0.070295	0.378367	0.631455
89	0.0	0.0	0.0	0.058915	0.357233	0.613499
90	0.0	0.0	0.0	0.048942	0.336122	0.595161
91	0.0	0.0	0.0	0.040301	0.315182	0.576550
92	0.0	0.0	0.0	0.032900	0.294559	0.557781
93	0.0	0.0	0.0	0.026612	0.274311	0.538879
94	0.0	0.0	0.0	0.021319	0.254492	0.519862
95	0.0	0.0	0.0	0.016910	0.235156	0.500744
96	0.0	0.0	0.0	0.013286	0.216375	0.481554
97	0.0	0.0	0.0	0.010351	0.198231	0.462330
98	0.0	0.0	0.0	0.008008	0.180793	0.443100
99	0.0	0.0	0.0	0.005171	0.164126	0.423879
100	0.0	0.0	0.0	0.004732	0.148023	0.404273

WATER VAPOR TRANSMITTANCES FOR THE SIX VTPR CHANNELS

[illegible]

41	0.999996	1.000000	0.999999	0.999999	1.000000	1.000000
42	0.999993	1.000000	0.999999	0.999999	1.000000	1.000000
43	0.999990	0.999999	0.999998	0.999998	1.000000	1.000000
44	0.999985	0.999999	0.999997	0.999997	1.000000	1.000000
45	0.999978	0.999999	0.999996	0.999995	1.000000	1.000000
46	0.999968	0.999998	0.999993	0.999993	1.000000	0.999999
47	0.999955	0.999997	0.999991	0.999990	0.999999	0.999999
48	0.999938	0.999996	0.999987	0.999985	0.999999	0.999999
49	0.999915	0.999994	0.999981	0.999979	0.999998	0.999998
50	0.999884	0.999991	0.999973	0.999970	0.999997	0.999997
51	0.999845	0.999987	0.999963	0.999959	0.999996	0.999996
52	0.999794	0.999982	0.999949	0.999943	0.999995	0.999994
53	0.999728	0.999975	0.999929	0.999921	0.999992	0.999991
54	0.999645	0.999965	0.999902	0.999891	0.999988	0.999986
55	0.999540	0.999951	0.999865	0.999852	0.999983	0.999980
56	0.999409	0.999933	0.999816	0.999799	0.999976	0.999971
57	0.999246	0.999909	0.999750	0.999730	0.999966	0.999958
58	0.999046	0.999877	0.999663	0.999640	0.999952	0.999940
59	0.998802	0.999835	0.999550	0.999525	0.999934	0.999915
60	0.998508	0.999782	0.999406	0.999380	0.999910	0.999884
61	0.998154	0.999714	0.999221	0.999196	0.999878	0.999841
62	0.997638	0.999609	0.998936	0.998915	0.999827	0.999772
63	0.996922	0.999451	0.998507	0.998501	0.999749	0.999662
64	0.996058	0.999246	0.997946	0.997970	0.999644	0.999511
65	0.995036	0.998985	0.997228	0.997302	0.999507	0.999308
66	0.993836	0.998659	0.996322	0.996477	0.999331	0.999040
67	0.992429	0.998254	0.995187	0.995462	0.999107	0.998691
68	0.990770	0.997752	0.993765	0.994211	0.998823	0.998236
69	0.988810	0.997129	0.991987	0.992674	0.998464	0.997545
70	0.986513	0.996367	0.989793	0.990807	0.998014	0.996891
71	0.983706	0.995397	0.986988	0.988452	0.997429	0.995893
72	0.980191	0.994134	0.983340	0.985424	0.996650	0.994548
73	0.975928	0.992542	0.978758	0.981663	0.995646	0.992799
74	0.970894	0.990595	0.973175	0.977128	0.994392	0.990596
75	0.965046	0.988257	0.966507	0.971763	0.992855	0.987877
76	0.958313	0.985478	0.958637	0.965490	0.990997	0.984569
77	0.950473	0.982140	0.949299	0.958100	0.988726	0.980522
78	0.941307	0.978111	0.938244	0.949395	0.985944	0.975585
79	0.930816	0.973349	0.925471	0.939377	0.982611	0.969708
80	0.919023	0.967821	0.911009	0.928071	0.978699	0.962857

81	0.905727	0.961377	0.894622	0.915290	0.974090	0.954860
82	0.890766	0.953864	0.876160	0.900897	0.968669	0.945573
83	0.873758	0.944969	0.855273	0.884572	0.962200	0.934722
84	0.854578	0.934496	0.831906	0.855226	0.954532	0.922169
85	0.833367	0.922399	0.806297	0.846008	0.945618	0.907931
86	0.810018	0.908478	0.778395	0.823828	0.935296	0.891857
87	0.783846	0.892089	0.747524	0.799060	0.923055	0.873369
88	0.754456	0.872718	0.713374	0.771343	0.908470	0.852050
89	0.721769	0.850020	0.676024	0.740611	0.891226	0.827689
90	0.685355	0.823326	0.635195	0.706457	0.870735	0.799774
91	0.644398	0.791447	0.590386	0.658154	0.845954	0.767476
92	0.596892	0.751831	0.540043	0.623868	0.814646	0.728876
93	0.541886	0.702560	0.483718	0.572615	0.774898	0.682605
94	0.480873	0.643995	0.423278	0.515535	0.726492	0.629166
95	0.416116	0.577550	0.361101	0.454401	0.669975	0.569725
96	0.349820	0.504901	0.299315	0.390912	0.606039	0.505494
97	0.283816	0.427585	0.239564	0.326423	0.535146	0.437412
98	0.219603	0.346967	0.183059	0.261954	0.457417	0.366077
99	0.160078	0.266685	0.132022	0.199974	0.375108	0.293774
100	0.110715	0.195466	0.090253	0.145974	0.296695	0.226899

TOTAL ATMOSPHERIC TRANSMITTANCE (PATH-CORRECTED)

LEVEL	CHAN 1	CHAN 2	CHAN 3	CHAN 4	CHAN 5	CHAN 6
1	0.991123	0.999640	0.999872	0.999899	0.999927	0.999985
2	0.988599	0.999392	0.999705	0.999767	0.999816	0.999970
3	0.985280	0.999045	0.999485	0.999515	0.999602	0.999933
4	0.980696	0.998526	0.999173	0.999073	0.999220	0.999857
5	0.975207	0.997838	0.998750	0.998485	0.998706	0.999729
6	0.968946	0.996999	0.998194	0.997825	0.998129	0.999543
7	0.961489	0.995951	0.997475	0.997095	0.997501	0.999295
8	0.952409	0.994633	0.996579	0.996305	0.996834	0.998992
9	0.941280	0.992984	0.995477	0.995449	0.996125	0.998631
10	0.927962	0.990948	0.994151	0.994515	0.995356	0.998223
11	0.912467	0.988479	0.992592	0.993497	0.994508	0.997787
12	0.894798	0.985537	0.990779	0.992390	0.993560	0.997325
13	0.875073	0.982071	0.988691	0.991189	0.992497	0.996836
14	0.853544	0.978018	0.986298	0.989880	0.991301	0.996315
15	0.830569	0.973299	0.983554	0.988427	0.989940	0.995750
16	0.806635	0.967841	0.980417	0.986804	0.988397	0.995130
17	0.782254	0.961565	0.976845	0.984995	0.986654	0.994448
18	0.757824	0.954394	0.972786	0.982973	0.984699	0.993697
19	0.733641	0.946252	0.968199	0.980733	0.982529	0.992873
20	0.709827	0.937072	0.963047	0.978268	0.980144	0.991973
21	0.686330	0.926781	0.957293	0.975577	0.977551	0.991000
22	0.662957	0.915307	0.950914	0.972658	0.974753	0.989950
23	0.639437	0.902565	0.943862	0.969483	0.971724	0.988810
24	0.615498	0.888472	0.936119	0.966039	0.968449	0.987580
25	0.590951	0.872951	0.927656	0.962301	0.964909	0.986250
26	0.565674	0.855943	0.918391	0.958227	0.961078	0.984804
27	0.539702	0.837437	0.908280	0.953816	0.956982	0.983241
28	0.513110	0.817422	0.897295	0.949086	0.952663	0.981568
29	0.486019	0.795908	0.885415	0.944054	0.948159	0.979792
30	0.458565	0.772911	0.872623	0.938743	0.943515	0.977917
31	0.430898	0.748469	0.858910	0.933172	0.938775	0.975952
32	0.403163	0.722624	0.844280	0.927363	0.933976	0.973906
33	0.375505	0.695429	0.828747	0.921333	0.929138	0.971791
34	0.348059	0.666944	0.812395	0.915100	0.924278	0.969614
35	0.320999	0.637259	0.795206	0.908677	0.919405	0.967383
36	0.294448	0.606487	0.777159	0.902027	0.914505	0.965107
37	0.268565	0.574790	0.758231	0.895116	0.909567	0.962764
38	0.243488	0.542324	0.738474	0.887957	0.904598	0.960368
39	0.219354	0.509250	0.717938	0.880566	0.899609	0.957930
40	0.196243	0.475728	0.696814	0.873041	0.894641	0.955485

41	0.174290	0.441985	0.675019	0.865296	0.797749	0.953010
42	0.153591	0.408228	0.652599	0.857326	0.884633	0.950512
43	0.134196	0.374654	0.629669	0.849163	0.879594	0.948003
44	0.116190	0.341508	0.606161	0.840715	0.874495	0.945461
45	0.099594	0.308956	0.582299	0.832097	0.869376	0.942924
46	0.084448	0.277221	0.558113	0.823279	0.864220	0.940389
47	0.070776	0.246539	0.533589	0.814191	0.858994	0.937840
48	0.058581	0.217125	0.508783	0.804812	0.853685	0.935272
49	0.047828	0.189178	0.483785	0.795153	0.848290	0.932694
50	0.038468	0.162892	0.458732	0.785227	0.842810	0.930114
51	0.030461	0.138491	0.433634	0.774961	0.837210	0.927513
52	0.023735	0.116153	0.408421	0.764193	0.831424	0.924845
53	0.018176	0.095968	0.383130	0.752833	0.825415	0.922074
54	0.013657	0.078000	0.357879	0.740855	0.819169	0.919185
55	0.010057	0.062309	0.332799	0.728234	0.812670	0.916160
56	0.007251	0.048868	0.308014	0.714949	0.805906	0.912987
57	0.005102	0.037548	0.283658	0.700992	0.798868	0.909650
58	0.003500	0.028213	0.259906	0.686396	0.791560	0.906147
59	0.002329	0.020723	0.236923	0.671196	0.783989	0.902477
60	0.001502	0.014858	0.214790	0.655358	0.776134	0.898614
61	0.000943	0.010375	0.193578	0.638837	0.767968	0.894529
62	0.000575	0.007036	0.173351	0.621560	0.759458	0.890181
63	0.000332	0.004601	0.154180	0.603452	0.750562	0.885520
64	0.000175	0.002913	0.136078	0.584433	0.741219	0.880483
65	0.000080	0.001803	0.119093	0.564389	0.731356	0.875010
66	0.000019	0.001104	0.103241	0.543216	0.720896	0.869005
67	0.000000	0.000659	0.088606	0.520958	0.709821	0.862442
68	0.0	0.000376	0.075280	0.497802	0.698165	0.855326
69	0.0	0.000210	0.063276	0.473828	0.685906	0.847611
70	0.0	0.000117	0.052575	0.449036	0.672989	0.839222
71	0.0	0.000057	0.043169	0.423501	0.659386	0.830082
72	0.0	0.000019	0.035000	0.397390	0.645095	0.820129
73	0.0	0.000000	0.027979	0.370863	0.630102	0.809309
74	0.0	0.0	0.021993	0.343904	0.614297	0.797485
75	0.0	0.0	0.016993	0.315897	0.597764	0.784694
76	0.0	0.0	0.012907	0.290197	0.580587	0.770972
77	0.0	0.0	0.009621	0.263819	0.562664	0.756151
78	0.0	0.0	0.007040	0.239032	0.544031	0.740200
79	0.0	0.0	0.005094	0.213081	0.524729	0.723140
80	0.0	0.0	0.003621	0.189172	0.504789	0.704991

81	0.0	0.0	0.002523	0.166465	0.484202	0.685681
82	0.0	0.0	0.001709	0.145170	0.463007	0.665203
83	0.0	0.0	0.001112	0.125439	0.441255	0.643513
84	0.0	0.0	0.000693	0.107338	0.419025	0.620648
85	0.0	0.0	0.000416	0.090901	0.396407	0.596714
86	0.0	0.0	0.000245	0.076121	0.373451	0.571711
87	0.0	0.0	0.000146	0.062943	0.350085	0.545390
88	0.0	0.0	0.000089	0.051347	0.326309	0.517638
89	0.0	0.0	0.0	0.041315	0.302192	0.488498
90	0.0	0.0	0.0	0.032734	0.277755	0.457873
91	0.0	0.0	0.0	0.025489	0.252999	0.425604
92	0.0	0.0	0.0	0.019426	0.227658	0.391003
93	0.0	0.0	0.0	0.014421	0.201631	0.353738
94	0.0	0.0	0.0	0.010399	0.175348	0.314507
95	0.0	0.0	0.0	0.007269	0.149394	0.274293
96	0.0	0.0	0.0	0.004913	0.124323	0.234018
97	0.0	0.0	0.0	0.003195	0.100556	0.194395
98	0.0	0.0	0.0	0.001984	0.078375	0.155909
99	0.0	0.0	0.0	0.001167	0.058336	0.119676
100	0.0	0.0	0.0	0.000653	0.041607	0.088149

STATION NUMBER = 1
 ZENITH ANGLE = 0.5
 STATION LATITUDE = 28.50
 STANDARD ATMOSPHERE TEMPERATURE ADJUSTMENT = -1.35
 THE TEMPERATURE PROFILE CONVERGED AFTER 5 ITERATIONS

	PRESSURE	TEMP.	SOUNDING	ERROR	NESS	NESS-ERROR
1	1000.000	19.040	17.800	1.240	19.500	1.700
2	850.000	9.258	8.200	1.058	12.200	4.000
3	700.000	0.673	2.400	-1.727	4.500	1.800
4	500.000	-15.343	-11.900	-3.442	-12.800	-0.600
5	400.000	-26.558	-23.700	-2.858	-40.000	-1.100
6	300.000	-41.024	-37.800	-3.224	-49.200	-1.200
7	250.000	-59.096	-50.500	-8.596	-58.200	-1.300
8	200.000	-63.405	-59.100	-4.305	-63.200	-1.400
9	150.000	-69.225	-67.300	-1.925	-69.300	-2.600
10	100.000	-66.877	-62.500	0.625	-63.300	-1.200
11	70.000	-61.774	-55.200	0.115	-56.900	-1.600
12	50.000	-55.185	-51.300	3.413	-50.900	0.400
13	30.000	-47.887	-36.500	-3.974	-42.000	-5.500
14	20.000	-40.474				
15	10.000					

LIST OF REFERENCES

1. Bignell, K. J., "The Water-Vapour Infra-Red Continuum," Quarterly Journal of the Royal Meteorological Society, Vol. 96, p. 390-403, 1970.
2. Chahine, M. T., "Remote Sounding of Cloudy Atmospheres, I The Single Cloud Layer," Journal of the Atmospheric Sciences, Vol. 31, No. 1, p. 233-243, 1974.
3. Committee on Extension to the Standard Atmosphere, U. S. Standard Atmosphere Supplements, U. S. Government Printing Office, Washington, D. C., 1966.
4. Committee on Extension to the Standard Atmosphere, U. S. Standard Atmosphere Supplements, U. S. Government Printing Office, Washington, D. C., 1962.
5. Conte, S. D. and de Boor, C., Elementary Numerical Analysis, 2d. Ed., p. 191-194, McGraw Hill, 1965.
6. Drayson, S. R., "Atmospheric Transmission in the CO₂ Bands Between 12 μ and 18 μ ," Applied Optics, Vol. 5, p. 385-391, 1966.
7. Fleming, H. E., unpublished notes on carbon dioxide transmittance supplied by personal communication, 1974.
8. Fritz, S., Wark, D. Q., Fleming, H. E., Smith, W. L., Jacobowitz, H., Hilleary, D. T., Alishouse, J. C., "Temperature Sounding from Satellites," NOAA Technical Report NESS 59, p. 1-47, Washington D. C., 1972.
9. Gelman, M. E., Miller, A. J., Woolf, H. M., "Regression Technique for Determining Temperature Profiles in the Upper Atmosphere from Satellite-Measured Radiances," Monthly Weather Review, Vol. 100, No. 7, p. 542-547, 1972.
10. Goody, R. M., Atmospheric Radiation I Theoretical Basis, p. 236-242, Oxford, 1964.
11. Jastrow, R. and Halem, M., "Accuracy and Coverage of Temperature Data Derived From the IR Radiometer on the NOAA 2 Satellite," Journal of the Atmospheric Sciences, Vol. 30, No. 6, p. 958-964, 1973.
12. Kaplan, L. D., "Interference of Atmospheric Structure from Remote Radiation Measurements," Journal of the Optical Society of America, Vol. 49, No. 10, p. 1004-1007, 1959.

13. Martin, F. L., NOAA-VTPR Data Observations and Pressure-Temperature Sounding (T(P)) Retrievals, paper presented at the U. S. Naval Postgraduate School as a text in part for a course in Satellite Meteorology, 1974.
14. McMillin, L. M., Wark, D. Q., Siomkajlo, J. M., Abel, P. G., Weowetski, A., Lauritson, L. A., Pritchard, J. A., Crosby, D. S., Woolf, H. M., Luebbe, R. C., Weinreb, M. P., Fleming, H. E., Bittner, F. E., Hayden, C. M., "Satellite Infrared Soundings from NOAA Spacecraft," NOAA Technical Report NESS 65, p. 1-112, Washington, D. C. 1973.
15. McMillin, L. M., unpublished notes on the CLRAD program explaining the NESS procedures for zenith angle corrections supplied by personal communication, 1974.
16. Moran, D. R., Iterative Retrieval and Statistical Specifications of Atmospheric Thickness from VTPR Clear-Column Radiance Data, M. S. Thesis, Naval Postgraduate School, Monterey, California, 1974.
17. Smith, W. L., "Note on the Relationship Between Total Precipitable Water and Surface Dew Point," Journal of Applied Meteorology, Vol. 5, No. 4, p. 726-727, 1966.
18. Smith, W. L., "A Polynomial Representation of Carbon Dioxide and Water Vapor Transmission," ESSA Technical Report NESC 47, p. 1-20, Washington, D. C., 1969.
19. Smith, W. L., "Iterative Solution of the Radiative Transfer Equation for the Temperature and Absorbing Gas Profile of an Atmosphere," Applied Optics, Vol. 9, No. 9, p. 1993-1999, 1970.
20. Smith, W. L., "Computing Temperature Profiles Under Cloudy Sky Conditions," Monthly Weather Review, Vol. 98, No. 8, p. 588-589, 1970.
21. Smith, W. L., "Calculation of Clear-Column Radiances Using Airborne Infrared Temperature Profile Radiometer Measurements Over Partly Cloudy Areas," NOAA Technical Memorandum NESS 28, p. 1-12, Washington, D. C., 1971.
22. Smith, W. L., "Satellite Techniques for Observing the Temperature Structure of the Atmosphere," Bulletin of the American Meteorological Society, Vol. 53, No. 11, p. 1074-1082, 1972.
23. Smith, W. L., Woolf, H. M., Fleming, H. E., "Retrieval of Atmospheric Temperature Profiles from Satellite Measurements for Dynamical Forecasting," Journal of Applied Meteorology, Vol. 11, No. 1, p. 113-122, 1972.

24. Smith, W. L., Woolf, H. M., Abel, P. G., Hayden, C. M., Chalfant, M., Grady, N., "NIMBUS 5 Sounder Data Processing System," NOAA Technical Memorandum NESS 57, p. 1-8, Washington, D. C., 1974.
25. Weinreb, M. P., and Neuendorfer, A. C., "Method to Apply Homogeneous-Path Transmittance Models to Inhomogeneous Atmospheres," Journal of Atmospheric Sciences, Vol. 30, No. 4, p. 662-666, 1973.
26. Weinreb, M. P., and Crosby, D. S., Estimation of Atmospheric Moisture Profiles from Satellite Measurements by a Combination of Linear and Non-Linear Methods, paper presented at the Third Conference on Probability and Statistics in Atmospheric Science, Boulder, Colorado, 1973.

INITIAL DISTRIBUTION LIST

	No. Copies
1. Defense Documentation Center Cameron Station Alexandria, Virginia 22314	2
2. Library, Code 0212 Naval Postgraduate School Monterey, California 93940	2
3. Professor Frank L. Martin, Code 51Mr Department of Meteorology Naval Postgraduate School Monterey, California 93940	5
4. LCDR Harry M. Dyck Jr. USS Cochrane (DDG-21) FPO San Francisco, California 96610	2
5. Department of Meteorology, Code 51 Naval Postgraduate School Monterey, California 93940	3
6. Naval Weather Service Command Naval Weather Service Headquarters Washington Navy Yard Washington, D.C. 20390	1
7. Naval Oceanographic Office Library, Code 3330 Washington, D.C. 20373	1
8. Environmental Prediction Research Facility ATTN: Mr. Roland Nagle Monterey, California 93940	1
9. Dr. L.M. McMillin, Routing Code S11222 NOAA-NESS Federal Office Building No. 4 Suitland, Maryland 20233	1
10. Dr. M.E. Weinreb, Routing Code S321 NOAA-NESS Federal Office Building No. 4 Suitland, Maryland 20233	1

11. Fleet Numerical Weather Central
ATTN: W.R. Lambertson, LCDR, USN
Monterey, California 93940

1

Thesis

D957

Dyck

c.1

Test and evaluation
of a VTPR retrieval
system from clear-
column NOAA 2 radiances.

158734

Thesis

D957

Dyck

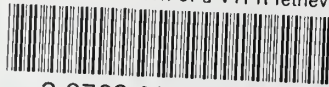
c.1

Test and evaluation
of a VTPR retrieval
system from clear-
column NOAA 2 radiances.

158734

thesD957

Test and evaluation of a VTPR retrieval



3 2768 001 89630 1

DUDLEY KNOX LIBRARY